Hub Location Problems with Profit Considerations

by

Gita Taherkhani

A thesis
presented to the University of Waterloo
in fulfillment of the
thesis requirement for the degree of
Doctor of Philosophy
in
Management Sciences

Waterloo, Ontario, Canada, 2019

Examining Committee Membership

The following served on the Examining Committee for this thesis. The decision of the Examining Committee is by majority vote.

External Examiner	Jean-François Cordeau Professor, Department of Logistics and Operations Management, HEC Montréal
Supervisor	Sibel Alumur Alev Assistant Professor, Department of Management Sciences, University of Waterloo
Internal Member	James Bookbinder Professor, Department of Management Sciences, University of Waterloo
Internal Member	Samir Elhedhli Professor, Department of Management Sciences, University of Waterloo
Internal-External Member	Kumaraswamy Ponnambalam Professor, Department of Systems Design Engineering, University of Waterloo

Author's Declaration

This thesis consists of material all of which I authored or co-authored: see Statement of Contributions included in the thesis. This is a true copy of the thesis, including any required final revisions, as accepted by my examiners.

I understand that my thesis may be made electronically available to the public.

Statement of Contributions

I am the sole author of Chapters 1, 2, and 6.

Chapters 3, 4, and 5 are part of articles (Gita Taherkhani and Sibel Alumur Alev [94]), (Gita Taherkhani, Sibel Alumur Alev, and Seyed Mojtaba Hosseini [95]), and (Gita Taherkhani, Sibel Alumur Alev, and Seyed Mojtaba Hosseini [96]). All authors participated in writing of the articles.

Abstract

This thesis studies profit maximizing hub location problems. These problems seek to find the optimal number and locations of hubs, allocations of demand nodes to these hubs, and routes of flows through the network to serve a given set of demands between origin-destination pairs while maximizing total profit. Taking revenue into consideration, it is assumed that a portion of the demand can remain unserved when it is not profitable to be served. Potential applications of these problems arise in the design of airline passenger and freight transportation networks, truckload and less-than-truckload transportation, and express shipment and postal delivery.

Firstly, mathematical formulations for different versions of profit maximizing hub location problems are developed. Alternative allocation strategies are modeled including multiple allocation, single allocation, and r-allocation, as well as allowing for the possibility of direct connections between non-hub nodes. Extensive computational analyses are performed to compare the resulting hub networks under different models, and also to evaluate the solution potential of the proposed models on commercial solvers with emphasis on the effect of the choice of parameters.

Secondly, revenue management decisions are incorporated into the profit maximizing hub location problems by considering capacities of hubs. In this setting, the demand of commodities are segmented into different classes and there is available capacity at hubs which is to be allocated to these different demand segments. The decision maker needs to determine the proportion of each class of demand to serve between origin-destination pairs based on the profit to be obtained from satisfying this demand. A strong mixed-integer programming formulation of the problem is presented and Benders-based algorithms are proposed to optimally solve large-scale instances of the problem. A new methodology is developed to strengthen the Benders optimality cuts by decomposing the subproblem in a two-phase fashion. The algorithms are enhanced by the integration of improved variable fixing techniques. Computational results show that large-scale instances with up to 500 nodes and 750,000 commodities of different demand segments can be solved to optimality,

and that the proposed algorithms generate cuts that provide significant speedups compared to using Pareto-optimal cuts.

As precise information on demand may not be known in advance, demand uncertainty is then incorporated into the profit maximizing hub location problems with capacity allocation, and a two-stage stochastic program is developed. The first stage decision is the locations of hubs, while the assignment of demand nodes to hubs, optimal routes of flows, and capacity allocation decisions are made in the second stage. A Monte-Carlo simulation-based algorithm is developed that integrates a sample average approximation scheme with the proposed Benders decomposition algorithm. Novel acceleration techniques are presented to improve the convergence of the algorithm. The efficiency and robustness of the algorithm are evaluated through extensive computational experiments. Instances with up to 75 nodes and 16,875 commodities are optimally solved, which is the largest set of instances that have been solved exactly to date for any type of stochastic hub location problems.

Lastly, robust-stochastic models are developed in which two different types of uncertainty including stochastic demand and uncertain revenue are simultaneously incorporated into the capacitated problem. To embed uncertain revenues into the problem, robust optimization techniques are employed and two particular cases are investigated: interval uncertainty with a max-min criterion and discrete scenarios with a min-max regret objective. Mixed integer programming formulations for each of these cases are presented and Benders-based algorithms coupled with sample average approximation scheme are developed. Inspired by the repetitive nature of sample average approximation scheme, general techniques for accelerating the algorithms are proposed and instances involving up to 75 nodes and 16,875 commodities are solved to optimality. The effects of uncertainty on optimal hub network designs are investigated and the quality of the solutions obtained from different modeling approaches are compared under various parameter settings. Computational results justify the need for embedding both sources of uncertainty in decision making to provide robust solutions.

Acknowledgements

First and foremost, I would like to express my sincere gratitude to Prof. Sibel Alumur Alev. She has not only provided me her professional expertise, valuable guidance and the financial support I needed to complete my Ph.D. studies, but also been a real friend and a true mentor. I feel extremely fortunate to have worked with her. I learned a lot from her, and I am very grateful to have her as my supervisor.

I would like to thank the members of my dissertation committee: Professor James Bookbinder, Professor Samir Elhedhli, Professor Jean-François Cordeau, and Professor Kumaraswamy Ponnambalam. I am grateful for their time and effort spent in reading the thesis, and providing their comments and helpful suggestions.

I was lucky to make wonderful friends in Waterloo, of whom some have become a shoulder to lean on. My thanks to them all.

Lastly and most importantly, I could not have come this far without the continued support of my parents Farzaneh and Hooshang Taherkhani and my lovely sister Diba. Thank you for your unconditional love, care, and patience.

Dedication

My lovely parents, it is to you that I dedicate this thesis.

Table of Contents

List of Acronyms

AP Australian Post

BD Benders Decomposition

CAB Civil Aeronautics Board

DS Dual Subproblem

HLP Hub Location Problem

KP Knapsack Problem

LB Lower Bound

LP Linear Program

MIP Mixed Integer Program

MILP Mixed Integer Linear Program

MP Master Problem

MWC Maximum Weight Cover

MWM Maximum Weighted Matching

OR Operations Research

PS Primal Subproblem

PO Pareto Optimal

RSM Robust-Stochastic Model

SAA Sample Average Approximation

UB Upper Bound

List of Tables

List of Figures

Chapter 1

Introduction

Hubs are special facilities that serve as switching, sorting, connecting, and consolidation points in many-to-many distribution networks. In hub networks, demands between origin-destination (O-D) pairs are routed through hubs instead of using direct connections. Exploiting hub facilities results in establishing fewer links in the network, compared with establishing fully interconnected networks to serve O-D pairs. The aim of using hubs is to reduce the costs of establishing a network connecting many origins and destinations, and also to consolidate flows at hubs to exploit economies of scale. Figure 1.1 demonstrates the differences between a fully interconnected network and a hub network. Circles in this figure represent demand nodes, whereas squares denote the hub facilities.

A hub location problem (HLP) is a network design problem consisting generally of two main decisions: the locations of hubs and the allocations of demand nodes to these hubs. The optimal routes of flow on the hub network to satisfy the demand between O-D pairs is also to be determined. Routing traffic flows through hubs allows to take advantage of economies of scale and thus decreases the transportation cost of the flows via hub links. Economies of scale means that the costs decrease as the scale of the operations increase. The reader may refer to the reviews on hub location by Campbell et al. [30], Alumur and Kara [5], Campbell and O'Kelly [33], and Contreras [34].

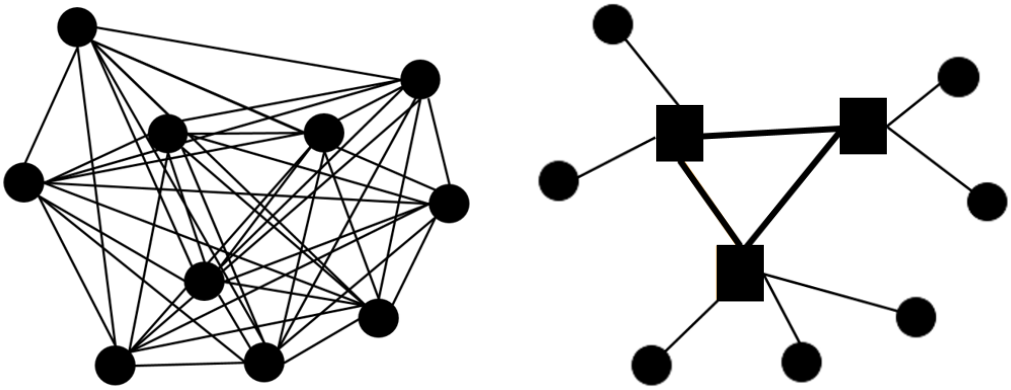

(a) Fully interconnected network (b) A hub network with 3 hubs

Figure 1.1: Serving the demand between 10 nodes.

Hub location problems have widespread applications in transportation as well as telecommunications. Application areas of HLPs in transportation include air passenger transportation, freight transportation, express shipments, postal delivery, truckload and less-than-truckload transportation, and rapid transit systems. In transportation applications, demand is specified as flows of commodities such as passengers, mail, and goods to be transported in vehicles between O-D pairs. Depending on the geographic scope, the type of vehicles moved on physical networks can change; for example, trucks are commonly used on roads, trains in railways, airplane through air, and vessels through water. Hub facilities are transportation terminals or sorting centers where the volume of transportation is high, hence economies of scale on transportation costs can be achieved.

Applications of HLPs in telecommunications include a wide variety of distributed data networks in areas such as computer communication, telephone networks, video teleconferences, and distributed computer processing. In this area, demand is for transmission of information (such as data, voice, video, etc.) through a variety of physical links (such as fiber optic links and co-axial cables) or through the air (such as satellite channel and microwave links). Hub facilities are generally electronic devices such as switches, concentrators, and routers. (Campbell et al. [30] and Contreras [34])

Hub location problems can be classified based on the design of the access network which represents the allocations of demand nodes to hubs. There are two basic allocation strategies in the literature: single allocation and multiple allocation. In single allocation, each node must be allocated to exactly one hub (Figure 1.1b). In multiple allocation, on the other hand, there is no limit on the maximum number of hubs that a node can be allocated to. Additionally, Yaman [101] introduced the r-allocation strategy, where each node can be allocated to at most r hubs.

Most of the classical hub location models consider common major assumptions. First, the hub-level network is assumed to be complete and distances satisfy triangle inequality. Second, there is economies of scale for the transportation cost of the flows via hub links, incorporated by a discount factor. Third assumption ensures that all demand flows between origin and destination nodes are served. Lastly, direct transportation between a pair of demand nodes (without using any hubs) is not allowed.

From the objective function perspective, most of the studies within hub location problems focus on minimization objectives. The common feature of these problems is that all demand between O-D pairs should be satisfied (as stated in the third assumption) with the aim of minimizing total network cost. In such a case, no value is associated with the served demand which implicitly implies that the total revenue covers total cost. However, from a profit point of view, it may be more advantageous not to serve the demand of some commodities, especially if the cost of serving a commodity is higher than the revenue associated with servicing its demand. In such a setting, the right objective is to maximize profit rather than minimizing cost so that the decision on how much demand of each commodity to satisfy depends on the trade-off between revenue and cost. Profit maximization is more complex than cost minimization as it incurs additional decisions, nevertheless, this is the actual problem setting for many applications.

The goal of this thesis is to model and solve profit maximizing hub location problems. In these problems, a portion of the demand can remain unserved when it is not profitable to be served. We define new problems and develop mathematical models determining

the locations of hubs, designing the hub networks, and routing the demand in order to maximize profit. Potential applications of profit maximizing hub location problems arise in the design of airline passenger and freight transportation networks, express shipment and postal delivery, truckload and less-than-truckload transportation, and any other industry that benefits from a hub network structure. To provide the big picture, in 2017 alone, worldwide airline industry provided services to more than 4.081 billion passengers across the world (IATA 2018); the world's largest package delivery company served 5.1 billion parcels and documents in the global delivery volume (UPS 2018), both by employing hub networks. Our models are applicable to the design of new hub networks as well as for improving existing ones. The developed models can be used as decision support tools to evaluate prospective locations of hubs and decide on the optimal shipment strategies while determining the proportion of demand to be served.

In this thesis, we first develop mathematical formulations for profit maximizing hub location problems considering all possible allocation strategies. As an extension, for each allocation strategy, we also model the cases in which direct connections between non-hub nodes are allowed. We evaluate the performances of the proposed models using well-known data sets from the literature and analyze the resulting hub networks under different parameter settings.

We then model capacity allocation decisions within profit maximizing hub location problems to satisfy demand of commodities from different market segments. Two exact algorithms based on a Benders reformulation are proposed to solve large-size instances of the problem. We develop a new methodology in this thesis to strengthen the Benders optimality cuts by decomposing the subproblem in a two-phase fashion. We further enhance these algorithms by the integration of improved variable fixing techniques.

Lastly, we address demand uncertainty and develop a two-stage stochastic program for profit maximizing hub location problems with capacity allocation. We then extend the model by investigating robust-stochastic formulations in which two different types of uncertainty including stochastic demand and uncertain revenue are simultaneously incorporated

into the problem. To embed uncertain revenues into the problem, robust optimization techniques are used and two particular cases including interval uncertainty with a max-min criterion and discrete scenarios considering a min-max regret objective are investigated. Mixed integer programming formulations for each of theses cases are presented. Exact algorithms based on Benders decomposition coupled with sample average approximation scheme are developed and enhanced by novel acceleration techniques to solve large-scale instances of the stochastic and robust-stochastic versions of the problem.

The rest of the thesis is organized as follows. Chapter 2 presents a review of the relevant literature on hub location problems. In Chapter 3, we formulate and solve mathematical models for different versions of the profit maximizing hub location problems. We include revenue management decisions and study profit maximizing hub location problems with capacity allocation in Chapter 4. In Chapter 5, we introduce and solve stochastic and robust-stochastic models by addressing different sources and types of uncertainty. Chapter 6 provides conclusions and a brief discussion on future research avenues.

Chapter 2

Literature Review

In this chapter, we classify and review the literature on relevant hub location problems. In particular, in Section 2.1, we review HLPs with different allocation strategies and inter-hub network topologies. In Section 2.2, we present an overview of the hub location problems with maximization objectives. In Section 2.3, we consider HLPs that model any source of uncertainty. Finally, we include publications employing Benders decomposition for solving HLPs in Section 2.4.

2.1 Hub Location and Hub Network Design

The subnetwork that constitutes the allocation links between demand nodes and hubs is referred to as the "access network". As mentioned in Chapter 1, there are two basic allocation strategies in hub network design; i.e., multiple allocation and single allocation. Hub location formulations vary a lot with the selection of the allocation strategy. A number of works on the multiple allocation problems that appeared in the literature are by Campbell [28], Ernst and Krishnamoorthy [47], Boland et al. [19], and Contreras et al. [35]. The single allocation version is studied by Ernst and Krishnamoorthy [46], O'Kelly

[75], Pirkul and Schilling [81], and Yaman [100]. Some studies considered both situations such as Campbell [29], Skorin-Kapov et al. [92], and O'Kelly et al. [78].

Regarding the subnetwork that constitutes the connections in-between hubs, designing complete inter-hub networks turned out to be a common assumption present in many hub location studies (for example, the seminal papers O'Kelly [74, 75], Campbell [29], Ernst and Krishnamoorthy [46], and Skorin-Kapov et al. [92]). For many studies, this is a direct consequence of having triangle inequality for transportation costs and not having any fixed costs for inter-hub links in the models. Another variant of the problem is to design incomplete inter-hub networks. Examples of such studies are Nickel et al. [73], Campbell et al. [31], Alumur et al. [6], Contreras et al. [38], and Alumur et al. [7].

Designing distinct topologies for inter-hub networks are also considered in the literature. Contreras et al. [38], and Martins de Sá et al. [68] studied the problem in which hubs are connected by means of a tree network. Potential applications arise when the set-up costs for hub links are high. Yaman [100] designed a hierarchical three-level hub network, where the top level consists of a complete network and the second and third levels are unions of star networks. Alumur et al. [9] studied the design of a hierarchical star-mesh-star hub network with multiple transportation modes. Yaman and Elloumi [102] modeled the design of two-level star networks taking service quality considerations into account. Contreras et al. [39] analyzed the case where the hubs are connected by means of a cycle, and Martins de Sá et al. [69] by means of a line.

In most of the hub location studies, direct connections between non-hub nodes is not possible. Some authors included this possibility in their models such as Aykin [11], Aykin [12], Nickel et al. [73], Sung and Jin [93], Wagner [98], and Mahmutoğulları and Kara [62].

An important extension to hub location problems is to incorporate capacity for hubs while designing hub networks. Capacitated versions of hub location problems are first formulated by Campbell [29] using path-based mixed integer programs that impose capacity constraints on the total incoming flow at hubs (i.e., flow arriving from both hub and non-hub nodes). A variant of this problem arises when capacities are applied only to the traffic

arriving directly from non-hub nodes. This variant is motivated from the postal-delivery applications and has been studied by Ebery et al. [44], Boland et al. [19], Marín [66], and Contreras et al. [37]. In some postal-delivery and express shipment networks (e.g. Canada Post, UPS), however, total incoming flow (regardless that is from a hub or a non-hub node) is sorted at every hub-stop. Moreover, the limiting capacity of a hub may not necessarily be on sorting or material handling, but, for example, on the available number of docks or gates.

2.2 Hub Location Problems with Maximization Objectives

There are not many studies in the literature focusing on maximization objectives within hub location problems. Perhaps, one of the early works is Campbell [29] introducing the hub maximal covering location models. Given a number of hub facilities to locate, the problem aims to maximize the demand covered. Campbell [29] defined different notions for coverage. Hwang and Lee [55] studied uncapacitated single allocation p-hub maximal covering problem and proposed a heuristic algorithm for the problem. More recently, Peker and Kara [80] extended the definition of coverage and introduced the notion of partial coverage that changes with distance. They developed mixed-integer programming formulations with partial coverage for single and multiple allocation versions.

Similar to hub maximal covering problems, we do not force all demand nodes to be served in profit maximizing hub location problems. However, we do not have a given budget for locating hubs and we optimize profit instead of maximizing the covered demand. Moreover, we also consider total transportation cost which is not taken into account in covering type hub location studies.

There are studies determining the locations of hubs within a competitive environment. In these studies, instead of having a single firm, there are a number of firms competing

to serve the demand. Hence, competitors' decisions affect the profit of a firm. Different objective functions are considered in competitive hub location problems, such as maximizing the demand captured, and maximizing total revenue or profit. Examples of studies considering a competitive environment include Marianov et al. [65], Eiselt and Marianov [45], Gelareh et al. [51], and Lüer-Villagra and Marianov [60]. There are also some studies considering a game theoretic framework in addressing competitive hub location problems such as Sasaki and Fukushima [87] and Sasaki et al. [86].

Even though objective functions of some competitive hub location studies also aim at maximizing profit, we do not consider a competitive environment in this study. In our study, there is only a single firm that wants to design its hub network in the most profitable way. Moreover, we do not force all demand to be served.

Alibeyg et al. [3] introduced a hub network design problem with profits. The problem aims to determine the locations of hubs, decide which edges to activate, select pairs of nodes and a set of commodities to be served, and make routing decisions with the objective of maximizing total profits. They considered a multiple allocation setting and assumed that each origin and destination path consists of at least one and at most two hub nodes. The demand between two pairs of nodes is served through at most three edges. They model different variations of the problem and use CAB dataset to test the performance of their models using CPLEX. In a subsequent study, Alibeyg et al. [4] proposed an exact algorithm for the profit-oriented models introduced by Alibeyg et al. [3]. They embedded Lagrangean relaxation within a branch-and-bound algorithm. They also used reduction tests and partial enumeration to reduce the problem size as well as the computational effort. Lin and Lee [59] consider a hub network design problem for time definite LTL freight transportation in which the carrier aims to determine hub locations, under price elasticity of demand, that maximize total profit. They show that profit optimization builds a denser hub network than cost minimization.

Profit maximizing hub location problems are also related to service network design problems, which determine the selection and scheduling of the services to operate as well

as the routes of flow to be shipped. The interested reader may refer to reviews on this area by Crainic [41] and Wieberneit [99]. In this study, unlike the service network design problem, we incorporate decisions on the locations of hubs.

2.3 Hub Location Problems under Uncertainty

There are a few studies incorporating various uncertainty aspects into the hub location problems. Marianov and Serra [64] study a problem within the context of airline transportation. A formula for the probability of a number of customers in the system is developed which is later employed to propose a capacity constraint and restrict the number of airplanes in the system. Yang [103] studies hub location problem within airline transportation under seasonal demand variations. He develops a two-stage stochastic programming model with finite set of scenarios and uses data from the air freight market in Taiwan and China to test the proposed model. Sim et al. [91] consider a stochastic p-hub center problem with normally distributed travel time. They employ chance constraints to model service level considerations.

Contreras et al. [36] study the stochastic uncapacitated multiple allocation hub location problem with uncertain demands and transportation costs. They show that the stochastic problem with uncertain demand is equivalent to its associated deterministic expected value problem where random variables are replaced by their expected value. However, when uncertainty is associated with transportation costs, this equivalence does not hold and an SAA method is developed to solve the corresponding stochastic problems. Numerical results on a set of instances with up to 50 nodes are reported.

Alumur et al. [8] address single and multiple allocation hub location problems in which two sources of uncertainty, set-up costs for the location of hubs and the demands to be transported between the nodes, are incorporated. They assume that no probabilistic information can be associated with uncertain setup costs and propose a min-max regret formulation. For the problem with uncertain demand, they consider a stochastic program-

ming model. They then merge these two models and propose a min-max regret stochastic formulation to model both sources of uncertainty. They generate a finite set of scenarios for the uncertain parameters (i.e., five scenarios for each parameter) and use CPLEX to solve instances with up to 25 nodes.

Meraklı and Yaman [71] model the robust uncapacitated multiple allocation p-hub median problem under polyhedral demand uncertainty with two different uncertainty sets; hose and hybrid. The hose model assumes that the only available information is the upper limit on the total flow adjacent at each node, while the hybrid model imposes lower and upper bounds on each pairwise demand. They adopt a min-max robustness criterion for a cost-based objective function and develop two exact algorithms based on Benders decomposition. Meraklı and Yaman [72] extend this study by incorporating capacity constraints for hubs and devise two different Benders decomposition algorithms capable of solving instances with up to 50 nodes.

Zetina et al. [104] present robust counterparts for uncapacitated hub location problems considering uncertain demands and transportation costs. They employ a budget of uncertainty to control the level of conservatism in their mathematical models. They implement a branch-and-cut algorithm on CPLEX solver and are able to solve instances with up to 50 nodes. Martins de Sá et al. [70] focus on a robust multiple allocation incomplete hub location problem in which a hub network can be partially interconnected by hub arcs, and both demand and transportation costs are subject to uncertainty. They develop Benders decomposition algorithm to solve their problem. More recently, Ghaffarinasab [52] considers robust multiple allocation p-hub median problem under polyhedral demand uncertainty. Three variants of polyhedral uncertainty models are used in the problem and a tabu search based matheuristic algorithm is developed to solve the presented models.

2.4 Benders Decomposition for Hub Location Problems

Most of the hub location problems mentioned in the previous sections are NP-hard except for some special cases. Hence, finding the exact solution for such problems is challenging, particularly when realistic problems are in large scale. Benders decomposition (BD) has received increased attention for solving several classes of HLPs to optimality. It is a partitioning method for solving mixed-integer linear programming and nonlinear programming problems where the general problem is split into two simpler ones: an integer master problem and a linear subproblem.

There are several successful BD implementations in the literature. Camargo et al. [25] is the first work using a Benders reformulation to solve the uncapacitated multiple allocation hub location problem. They present three variants of the algorithm: the classical BD algorithm, where a single cut is generated at each iteration, a multicut version where Benders cuts are generated for each origin-destination pair, and a variant that terminates when an ϵ-optimal solution is obtained. The proposed algorithms were applied to solve instances with up to 200 nodes. Rodriguez-Martin and Salazar-Gonzalez [84] consider a capacitated multiple allocation hub location problem in which the arcs connecting the hubs are not assumed to create a complete graph. They provide a formulation and design two exact solution algorithms relying on BD. The first one employs the classical BD approach and the second is a branch-and-cut algorithm based on a two-level nested decomposition scheme. The second outperforms the first approach in terms of computational time.

Contreras et al. [35] employ a Benders reformulation for the uncapacitated multiple allocation hub location problem which is enhanced through the use of a multicut reformulation, the generation of Pareto-optimal cuts, the integration of reduction tests, and the execution of a heuristic procedure. Contreras et al. [37] provide an extension of the BD approach proposed by Contreras et al. [35] to solve capacitated multiple allocation hub location problems. They apply Pareto-optimal Benders cuts as well as reduction tests to

improve the convergence of the algorithm, and solve instances with up to 300 nodes.

BD is also used to solve other variants of hub location problems, including flow dependent discounts for inter-hub links using a non-linear cost function (Camargo et al. 26), hub location-routing problems which incorporate routing decisions between non-hub nodes (Camargo et al. 24), hub location problems with single allocation under congestion (Camargo et al. 23 and Camargo and de Miranda Jr 22), problems with incomplete inter-hub networks (Camargo et al. 27 and Martins de Sá et al. 70), problems with distinct topologies of inter-hub networks such as tree-star networks (Martins de Sá et al. 68) and hub-line networks (Martins de Sá et al. 69), and hub location problems in liner shipping applications (Gelareh and Nickel 50).

Chapter 3

Profit Maximizing Hub Location Problems

In this chapter, we introduce profit maximizing hub location problems. Taking profit into consideration, we allow for the possibility of serving a subset of the demand. In this regard, we assume that a portion of the demand can be unserved when it is not profitable. This assumption actually provides a more realistic framework for designing hub networks.

One of the most related study in the literature is Alibeyg et al. [3]. Similar to Alibeyg et al. [3], we study hub network design problems with profits and introduce profit maximizing objective functions. However, in this thesis, we provide a new modeling framework for the problem. Unlike Alibeyg et al. [3], we do not assume that the demand between a pair of nodes can be served through at most two hubs or three edges. In our problem, the demand of an origin-destination pair can be shipped through any number of hubs and network connections as necessary. We include additional design variables to account for the design of the inter-hub network. Incomplete hub networks are employed in many real-life applications including, but not limited, to freight transportation, rapid transit systems, express shipment and postal delivery networks. Therefore, relaxing a commonly used assumption on the structure of the origin-destination paths, which limits the number of hub nodes to

two, leads to a more realistic model where non-trivial routing decisions are explicitly taken into account. In our computational analysis, we present a direct comparison of our results with one of the models presented in Alibeyg et al. [3]. Furthermore, we study multiple, single, and r-allocation versions of the problem and also allow for the possibility of direct connections between non-hub nodes.

The outline of this chapter is as follows: In the next section, we define the problem and introduce the notation to be used in the following sections. We model the profit maximizing hub location problems in Section 3.2. In Section 3.3, comprehensive computational results are presented on instances derived from the well-known data sets to determine the performance of the proposed models. Finally, Section 3.4 provides concluding remarks for this chapter.

3.1 Problem Definition and Notation

The profit maximizing hub location problems determine the locations of hubs and design of the hub network in order to maximize profit. The location decision focuses on the selection of a set of nodes to establish hubs, whereas the network design decisions deal with the design of the links to connect nodes of the network. The optimal routes of flows through the network are also to be determined.

There is a given set of nodes as well as the demand that can be served between them. Demand is defined between pairs of nodes. The problem is to determine which set of origin-destination (O-D) pairs to serve and how to serve them to maximize profit. Taking profit into consideration, the problem measures the trade-off between the revenue and cost in determining which O-D pairs to serve. In this regard, it is assumed that some O-D pairs can remain unserved if it is not profitable to serve them.

A set of hub nodes is to be located to serve the demand. All nodes can be potential hub facilities. A set of hub links to operate between hub nodes is also to be determined. We do not impose a fully interconnected hub network. Demand of an O-D pair can be shipped

on any number of network connections as necessary. Moreover, no particular network structure (such as a star or a tree network) is assumed for the inter-hub network.

For the design of the access network, we model the multiple and single allocation versions as well as the r-allocation strategy. For each allocation strategy, we also model the versions in which direct connections between non-hub nodes are allowed. Considering all the possibilities for shipments, the problem is to design the hub network in the most profitable way.

The objective of our problem is the maximization of total profit. Total profit is calculated by subtracting total cost from the total revenue. Revenue is obtained from satisfying the demand of each O-D pair. We assume that price is exogenously determined by the market and that the revenue is independent of the route of flow of the demand.

Total cost includes the variable transportation cost, the fixed installation cost of hubs, and the fixed cost of activating links. The transportation cost on the hub network between each O-D pair is calculated by the cost of transportation from origin-to-hub (collection), between hubs (transfer), and from hub-to-destination (distribution). In case of direct connections, there are no collection, transfer, and distribution legs. In this case, transportation cost is calculated by the cost of shipping all demand between an O-D pair using the direct connection in-between. Unit transportation costs do not need to satisfy triangle inequality. In addition to transportation cost, there is a fixed cost involved for operating an inter-hub link as well as a direct link between non-hub nodes. No operational cost is considered for the allocation connections.

There are economies of scale between hubs, for example, due to bulk transportation or frequent service. It is assumed that economies of scale are reflected on the transportation cost by a constant discount factor. We provide extensive analysis with varying values of the economies of scale factor.

We introduce the following notation for the parameters required for modeling the problem:

N	Set of nodes.
w_{ij}	Amount of demand to be shipped from node $i \in N$ to node $j \in N$. ($O_i = \sum_{j \in N} w_{ij}$ denotes the flow originated at node $i \in N$.)
r_{ij}	Revenue from satisfying a unit demand from node $i \in N$ to node $j \in N$.
c_{ij}	Unit cost of transportation from node $i \in N$ to node $j \in N$.
f_k	Fixed installation cost of a hub at node $k \in N$.
g_{kl}	Fixed cost of activating a hub link from hub $k \in N$ to hub $l \in N$.
q_{ij}	Fixed cost of activating a direct link from node $i \in N$ to node $j \in N$.
α	Transportation cost discount factor ($0 \leq \alpha < 1$).

In the sequel, we introduce the mathematical formulations of the problem.

3.2 Mathematical Formulations

In this section, we present mixed-integer linear programming (MILP) models for different versions of the profit maximizing hub location problem. We first introduce our MILP model for the multiple allocation problem. In Section 3.2.2, we present MILP models for the single allocation and the r-allocation versions of the problem. In Section 3.2.3, we introduce models allowing for direct connections with all allocation rules.

3.2.1 Multiple allocation model

We now introduce a mathematical model for the multiple allocation version of the problem. In this problem, a non-hub node can be allocated to as many hubs as it is profitable. So,

there is no limit on the number of hubs that a non-hub node can be allocated to. The decision variables that need to be defined for the multiple allocation model are as follows:

$$h_k = \begin{cases} 1, & \text{if a hub is located at node } k \in N, \\ 0, & \text{otherwise.} \end{cases}$$

$$y_{ijkl} = \begin{cases} 1, & \text{if the demand between node } i \in N \text{ and } j \in N \text{ is satisfied through a path} \\ & \text{with the first hub } k \in N \text{ and the last hub } l \in N, \\ 0, & \text{otherwise.} \end{cases}$$

$$z_{kl} = \begin{cases} 1, & \text{if an inter-hub link is operating from hub } k \in N \text{ to hub } l \in N, \\ 0, & \text{otherwise.} \end{cases}$$

f_{ikl} = Amount of demand originated at node $i \in N$ and routed on the inter-hub link from hub $k \in N$ to hub $l \in N$.

The *profit maximizing multiple allocation hub location problem* is modeled as:

$$\text{Max} \quad \sum_{i\in N}\sum_{j\in N}\sum_{k\in N}\sum_{l\in N} r_{ij}w_{ij}y_{ijkl} - \Big[\sum_{i\in N}\sum_{j\in N}\sum_{k\in N}\sum_{l\in N}(c_{ik}+c_{lj})w_{ij}y_{ijkl} + \sum_{i\in N}\sum_{k\in N}\sum_{l\in N}\alpha c_{kl}f_{ikl} + \sum_{k\in N} f_k h_k + \sum_{k\in N}\sum_{l\in N} g_{kl}z_{kl}\Big] \tag{3.1}$$

$$\text{s.t.} \quad \sum_{k\in N}\sum_{l\in N} y_{ijkl} \le 1 \qquad i,j \in N \tag{3.2}$$

$$\sum_{l\in N} y_{ijkl} + \sum_{l\in N: l\neq k} y_{ijlk} \le h_k \qquad i,j,k \in N \tag{3.3}$$

$$\sum_{l\in N,\, l\neq k} f_{ikl} - \sum_{l\in N,\, l\neq k} f_{ilk} = \sum_{j\in N}\sum_{l\in N} w_{ij} y_{ijkl} - \sum_{j\in N}\sum_{l\in N} w_{ij} y_{ijlk} \quad i,k \in N \tag{3.4}$$

$$f_{ikl} \leq O_i z_{kl} \quad i,k,l \in N, k \neq l \tag{3.5}$$

$$z_{kl} \leq h_k \quad k,l \in N, k \neq l \tag{3.6}$$

$$z_{kl} \leq h_l \quad k,l \in N, k \neq l \tag{3.7}$$

$$f_{ikl} \geq 0 \quad i,k,l \in N \tag{3.8}$$

$$h_k \in \{0,1\} \quad k \in N \tag{3.9}$$

$$y_{ijkl} \in \{0,1\} \quad i,j,k,l \in N \tag{3.10}$$

$$z_{kl} \in \{0,1\} \quad k,l \in N, k \neq l \tag{3.11}$$

The objective function value (3.1) represents net profit. Total cost is subtracted from the total revenue to calculate the net profit. The first term of the objective function calculates the revenue obtained from satisfying the demand. The terms in parenthesis represent the transportation cost, the installation cost of hubs, and the cost of operating hub links, respectively. While calculating the total transportation cost, the hub-to-hub transportation is discounted by the economies of scale discount factor, α.

Constraints (3.2) state that there must be a unique path recognized by the first and the last hubs, if the demand between a given pair of nodes is to be satisfied. Constraints (3.3) ensure that the demand between origin and destination nodes can be satisfied only through located hubs. Constraints (3.4) are the flow balance equations. Constraints (3.5) enforce that the flow is routed only on the operated hub links. Constraints (3.6) and (3.7) indicate that an inter-hub link can only be operated if both of the end nodes of that link are hubs. Constraints (3.8)-(3.11) represent the non-negative and binary variables.

In an uncapacitated environment, there always exists an optimal solution of the problem where the demand of each O-D pair is either satisfied fully or not satisfied at all. Therefore, we defined y_{ijkl} variables as binary. However, integrality property holds for these variables. Hence, even though if we let $y_{ijkl} \geq 0$ for all $i,j,k,l \in N$, there exists an optimal solution of this model where $y_{ijkl} \in \{0,1\}\ \forall\ i,j,k,l \in N$. In our computational experiments, we

solved the model with y_{ijkl} variables being binary as we obtained better solution times compared with real variables.

As mentioned in the problem definition, we assume that hubs have enough capacity to handle all flow. If this is not the case, then one may add the following sets of constraints into the model:

$$\sum_{i \in N} \sum_{l \in N} f_{ikl} \leq \Gamma_k h_k \qquad k \in N \tag{3.12}$$

$$y_{ijkl} \geq 0 \qquad i, j, k, l \in N \tag{3.13}$$

where Γ_k is defined as the available capacity of a hub located at node $k \in N$. In the presence of capacity constraints (3.12), y_{ijkl} variables should be defined as continuous routing variables denoting the fraction of the demand from node $i \in N$ to $j \in N$ that is satisfied through a path with the first hub $k \in N$ and the last hub $l \in N$.

3.2.2 Single allocation and r-allocation models

In this section, we first introduce the mathematical model for the single allocation profit maximizing hub location problem. In the single allocation problem, each non-hub node can be allocated to at most one hub node. To model this problem, in addition to the decision variables introduced in the previous section, we define an additional binary variable as follows:

$$x_{ik} = \begin{cases} 1, & \text{if demand node } i \in N \text{ is allocated to hub node } k \in N, \\ 0, & \text{otherwise.} \end{cases}$$

($x_{kk} = 1$ indicates that a hub is located at node $k \in N$.)

The rest of the variables are the same as introduced in the multiple allocation model.

The *profit maximizing single allocation hub location problem* is modeled as:

$$\text{Max} \quad \sum_{i\in N}\sum_{j\in N}\sum_{k\in N}\sum_{l\in N} r_{ij}w_{ij}y_{ijkl} - \Big[\sum_{i\in N}\sum_{j\in N}\sum_{k\in N}\sum_{l\in N}(c_{ik}+c_{lj})w_{ij}y_{ijkl} + \sum_{i\in N}\sum_{k\in N}\sum_{l\in N}\alpha c_{kl}f_{ikl} + \sum_{k\in N} f_k x_{kk} + \sum_{k\in N}\sum_{l\in N} g_{kl}z_{kl}\Big] \tag{3.14}$$

s.t. (3.2), (3.4), (3.5), (3.8), (3.10), (3.11)

$$\sum_{k\in N} x_{ik} \leq 1 \qquad i \in N \tag{3.15}$$

$$x_{ik} \leq x_{kk} \qquad i,k \in N \tag{3.16}$$

$$y_{ijkl} \leq x_{ik} \qquad i,j,k,l \in N \tag{3.17}$$

$$y_{ijkl} \leq x_{jl} \qquad i,j,k,l \in N \tag{3.18}$$

$$z_{kl} \leq x_{kk} \qquad k,l \in N, k \neq l \tag{3.19}$$

$$z_{kl} \leq x_{ll} \qquad k,l \in N, k \neq l \tag{3.20}$$

$$x_{ik} \in \{0,1\} \qquad i,k \in N \tag{3.21}$$

The objective function value (3.14) accounts for the net profit obtained from summing the total revenue minus total cost as in the multiple allocation version. Constraints (3.15) ensure that every demand node can be allocated to at most one hub node. To guarantee that the demand nodes can be allocated to only installed hubs, constraints (3.16) are included in the model. Constraints (3.17) and (3.18) link path variables with allocation decisions. Constraints (3.19) and (3.20) ensure that an inter-hub link is operated only in-between hubs. Constraints (3.21) are the domain constraints. The rest of the constraints are the same as introduced in the multiple allocation model.

As mentioned in Marin et al. [67], constraints (3.17) and (3.18) can be strengthened by

replacing them with the following sets of constraints:

$$\sum_{l \in N} y_{ijkl} \leq x_{ik} \qquad i, j, k \in N \tag{3.22}$$

$$\sum_{k \in N} y_{ijkl} \leq x_{jl} \qquad i, j, l \in N \tag{3.23}$$

Even though using the above strengthened constraints will result in a better LP relaxation bound, in our preliminary experiments, we observed that the solution times of the model using a commercial solver gets worse. Thus, we employed constraints (3.17) and (3.18) in our computational experiments.

Yaman [101] introduced the r-allocation version of a hub location problem where each node can be allocated to at most r hubs. This version is actually a generalization of the single and multiple allocation versions. When $r = 1$, the problem reduces to single allocation, whereas, when $r = |N|$, it reduces to multiple allocation. In order to model the r-allocation version of the profit maximizing hub location problem, we introduce the following set of constraints to replace constraints (3.15) in the single allocation model:

$$\sum_{k \in N} x_{ik} \leq r \qquad i \in N \tag{3.24}$$

The MILP formulation of the *profit maximizing r-allocation hub location problem* consists of the objective function (3.14) and constraints (3.2), (3.4), (3.5), (3.8), (3.10), (3.11), (3.16)-(3.21), and (3.24).

3.2.3 Models allowing for direct connections

In the previous models, we assumed that direct transportation between demand nodes (without using any hubs) is not allowed. In this section, we model the variation in which direct connections between non-hub nodes are allowed. To allow for direct services, we need to define an additional binary variable s_{ij} as follows:

$$s_{ij} = \begin{cases} 1, & \text{if there is a direct connection from non-hub node } i \in N \text{ to non-hub} \\ & \text{node } j \in N, \\ 0, & \text{otherwise.} \end{cases}$$

We first introduce the *profit maximizing multiple allocation hub location problem with direct connections*:

$$\begin{aligned} \text{Max} \quad & \sum_{i\in N}\sum_{j\in N}\sum_{k\in N}\sum_{l\in N} r_{ij}w_{ij}y_{ijkl} + \sum_{i\in N}\sum_{j\in N} r_{ij}w_{ij}s_{ij} - \Big[\sum_{i\in N}\sum_{j\in N}\sum_{k\in N}\sum_{l\in N}(c_{ik}+c_{jl})w_{ij}y_{ijkl} \\ & + \sum_{i\in N}\sum_{k\in N}\sum_{l\in N}\alpha c_{kl}f_{ikl} + \sum_{i\in N}\sum_{j\in N} w_{ij}c_{ij}s_{ij} + \sum_{k\in N} f_k h_k + \sum_{k\in N}\sum_{l\in N} g_{kl}z_{kl} + \sum_{i\in N}\sum_{j\in N} q_{ij}s_{ij}\Big] \end{aligned} \tag{3.25}$$

$$\text{s.t.} \quad (3.3) - (3.11)$$

$$s_{ij} + h_j \leq 1 \qquad i,j \in N \tag{3.26}$$

$$s_{ij} + h_i \leq 1 \qquad i,j \in N \tag{3.27}$$

$$s_{ij} + \sum_{k\in N}\sum_{l\in N} y_{ijkl} \leq 1 \qquad i,j \in N \tag{3.28}$$

$$s_{ij} \in \{0,1\} \qquad i,j \in N \tag{3.29}$$

The objective function (3.25) sums the revenues obtained from satisfying the demand through the hub network and also through direct connections. In addition to the previously defined costs, the total cost includes the cost of operating direct links between non-hub nodes as well. To guarantee that the direct connections are operated only between non-hub nodes, constraints (3.26) and (3.27) are included in the model. Constraints (3.28) result from modifying constraints (3.2) to ensure that there is either a unique path through the hub network or a direct link to satisfy the demand between a given pair of nodes. Finally, constraints (3.29) provide the domain for the binary direct-connection variables.

We also model the *profit maximizing single allocation hub location problem with direct*

connections:

$$\text{Max} \quad \sum_{i\in N}\sum_{j\in N}\sum_{k\in N}\sum_{l\in N} r_{ij}w_{ij}y_{ijkl} + \sum_{i\in N}\sum_{j\in N} r_{ij}w_{ij}s_{ij} - \Big[\sum_{i\in N}\sum_{j\in N}\sum_{k\in N}\sum_{l\in N}(c_{ik}+c_{jl})w_{ij}y_{ijkl} + \sum_{i\in N}\sum_{k\in N}\sum_{l\in N}\alpha c_{kl}f_{ikl} + \sum_{i\in N}\sum_{j\in N} w_{ij}c_{ij}s_{ij} + \sum_{k\in N} f_k x_{kk} + \sum_{k\in N}\sum_{l\in N} g_{kl}z_{kl} + \sum_{i\in N}\sum_{j\in N} q_{ij}s_{ij}\Big] \tag{3.30}$$

$$\text{s.t.} \quad (3.4), (3.5), (3.8), (3.10), (3.11), (3.15) - (3.21), (3.28), (3.29)$$

$$s_{ij} + x_{jj} \leq 1 \qquad i,j \in N \tag{3.31}$$

$$s_{ij} + x_{ii} \leq 1 \qquad i,j \in N \tag{3.32}$$

The objective function (3.30) calculates net profit considering the revenue obtained through direct connections as well as the cost of operating those links. Constraints (3.31) and (3.32) are included in the model to assure that direct connections are allowed only between non-hub nodes. The rest of the constraints are the same as introduced in the previous models.

For the r-allocation model with direct connections, we simply need to replace constraint (3.15) with constraint (3.24) in the single allocation version of the formulation.

3.2.4 Variable fixing

To decrease the computational burden with all the proposed models, the values of some decision variables can be fixed with preprocessing. To this end, we exploit the following properties of our mathematical models:

$$y_{ijkl} = 0 \qquad i,j,k,l \in N : r_{ij} < (c_{ik} + c_{lj}) \tag{3.33}$$

As noted in the problem definition, only profitable demand will be served. Hence, when the revenue from satisfying a unit demand between O-D pair $i,j \in N$ is strictly smaller than the sum of unit transportation costs from origin i to hub k (collection) and from hub l to destination j (distribution), no profit can be obtained from satisfying the demand of the

O-D pair $i, j \in N$ through hubs $k, l \in N$. Accordingly, the optimal value for the variable y_{ijkl} can be set to zero when the above mentioned condition is met.

In the next section, we present computational analysis with all of the introduced mathematical formulations.

3.3 Computational Results

We performed extensive computational experiments to analyze the resulting hub networks and the performance of the proposed mathematical models. We used two well-known benchmark data sets from the literature for hub location: the U.S. Civil Aeronautics Board (CAB) and the Australia Post (AP) datasets. Both of these datasets are readily available in OR Library [15].

Computational experiments were carried out on a workstation that contains: Intel Core i7-3930K 2.61GHz CPU, and 39 GB of RAM. The mathematical models were solved using IBM ILOG CPLEX 12.7. Variable fixing was employed as detailed in Section 3.2.4. All the instances were solved to optimality (10^{-5} gap) using the default settings.

The organization of this section is as follows: In the next section, we present computational results with the CAB dataset. In this section, we also provide some managerial insights obtained from solving the models on this data set. Section 3.3.2, presents analysis on the economies of scale factor. In Section 3.3.3, we compare our results with results from the relevant literature. To better understand the performance of the mathematical models from a computational point of view, we present numerical results with larger-sized instances derived from the AP dataset in Section 3.3.4.

3.3.1 Results with the CAB dataset

CAB dataset is based on airline passenger interactions between 25 cities in United States in 1970 (O'Kelly 75). OR Library provides the transportation costs (c_{ij}) and the demand

between each pair of cities (w_{ij}) for this dataset (Beasley 15). As customarily done in the literature, we scaled the demand values so that the total demand adds up to one. Since CAB dataset does not provide any information regarding the revenues, we used average transportation costs to estimate values for the revenues. We test three different values such that $r_{ij} \in \{1000, 1500, 2000\}$ for each O-D pair $i, j \in N$, referred to as low, medium, and high revenue levels, respectively. We also test three different values for hub installation costs generated by O'Kelly [76] such that $f_k \in \{50, 100, 150\}$ for all $k \in N$. Similarly, we refer these values as low, medium, and high cost levels, respectively. Cost of operating an inter-hub link is set to be 10% of hub installation costs; i.e., $g_{kl} = 0.1 f_k$ for all $k, l \in N$. The cost of operating a direct link, on the other hand, is set to be the 20% of the operational cost of an inter-hub link; i.e., $q_{ij} = 0.2 g_{ij}$ for all $i, j \in N$. These values can be interpreted by assuming that the frequency of service on the inter-hub links is five times more than that of direct connections. Operational costs are dependent on the level of hub installations costs (low, medium, or high) and taken to be the same for all potential links. The discount factor α is taken as 0.2, 0.4, 0.6, and 0.8 as customarily done in the literature. Table 3.1 summarizes the parameter settings with the CAB dataset.

Table 3.1: Parameter settings with the CAB dataset.

Description	**Parameter**	**Value**
Set of nodes	$\|N\|$	25
Demands	w_{ij}	OR Library [15]
Revenue per unit demand	r_{ij}	Low: 1000, Medium: 1500, High: 2000
Transportation cost per unit of flow	c_{ij}	OR Library [15]
Installation cost of a hub	f_k	Low: 50, Medium: 100, High: 150
Operational cost of an inter-hub link	g_{kl}	Low: 5, Medium: 10, High: 15
Operational cost of a direct link	q_{ij}	Low: 1, Medium: 2, High: 3
Discount factor for inter-hub connections	α	0.2, 0.4, 0.6, 0.8

We initially took runs with the multiple and single allocation models (without any direct connections) under different parameter values. The results obtained from solving the models are summarized in Table 3.2. The first two columns report the values of the

cost parameters and the discount factor, respectively. For each allocation rule, the next three columns indicate the maximum net profit, total percentage of satisfied demand, and the locations of the hub nodes, respectively, in the optimal solutions of the corresponding instances. The "CPU time (s)" columns present the run time of instances (in seconds) obtained from solving the problems to optimality. To demonstrate the results with different revenue levels, Table 3.2 is split horizontally into three parts for high, medium, and low revenue levels.

Observe from Table 3.2 that when the costs increase, net profit values decrease along with the percentage of satisfied demand. Note that net profit is directly proportional to the percent of satisfied demand. With increased cost levels, the models tend to result in locating fewer hubs. As expected, when the number of opened hubs in the solutions increase, CPU time required for solving the instances to optimality also increase. Hence, low cost instances tend to require more CPU time compared with high cost instances.

We next observe the effect of the economies of scale factor on the solutions presented in Table 3.2. When the α value increases; that is, when the effect of economies of scale on transportation costs is lower, the net profit values and the percentage of satisfied demand decrease. The number of located hubs, on the other hand, either decreases or remains the same. Note that, in Table 3.2, there are some instances with high cost levels resulted in locating only one hub. Economies of scale factor has no effect in such instances. For a given revenue and cost level, the instances resulted in opening one hub yield the same net profit value and the same percentage of satisfied demand independent from the value of α.

We tested all instances with three different revenue levels. When the revenue level decreases from high to low, the net profit values as well as the percentages of satisfied demand decrease. For a given cost level and α value, an increase in the revenue level results in satisfying more demand and may require opening more hubs.

The multiple allocation problem provides an upper bound for the single allocation problem in terms of net profit and percentage of satisfied demand. From the computational point of view, the single allocation model is more time consuming than the multiple alloca-

Table 3.2: Multiple and single allocation solutions with the CAB dataset.

		Multiple Allocation				Single Allocation			
Costs	α	Net profit	Satisfied demand (%)	Hub locations	CPU time (s)	Net profit	Satisfied demand (%)	Hub locations	CPU time (s)
		High revenue							
Low	0.2	1,190	100.00	4,7,12,14,17	4,891	1,181	99.67	4,7,12,14,17	12,343
	0.4	1,033	97.33	4,7,12,14,17	4,130	1,013	96.33	4,7,12,14,17	9,384
	0.6	926	94.00	4,7,12,14,17	2,428	874	83.50	4,12,17	8,933
	0.8	850	86.83	1,4,12,17	754	774	70.67	4,12,18	9,048
Medium	0.2	913	99.00	4,12,17,24	802	895	96.33	4,12,17	8,280
	0.4	804	93.00	4,12,17	615	790	92.00	4,12,17	7,271
	0.6	735	89.33	4,12,17	520	690	82.33	4,12,18	8,138
	0.8	681	79.67	18,21	57	649	67.00	20	4,102
High	0.2	740	97.00	4,12,17	550	735	96.33	4,12,17	8,738
	0.4	634	93.00	4,12,17	362	620	92.00	4,12,17	6,490
	0.6	599	67.00	20	90	599	67.00	20	1,363
	0.8	599	67.00	20	28	599	67.00	20	1,324
		Medium revenue							
Low	0.2	690	94.00	4,7,12,14,17	1,756	685	93.33	4,7,12,14,17	9,116
	0.4	550	89.00	4,7,12,14,17	1,249	532	86.33	4,7,12,14,17	7,924
	0.6	456	68.00	4,12,17	504	423	55.67	4,18	7,180
	0.8	426	64.00	4,12,17	283	371	51.67	4,18	5,597
Medium	0.2	429	83.17	4,12,17	549	418	81.67	4,12,17	4,329
	0.4	349	62.67	4,17	142	331	58.67	4,17	2854
	0.6	328	61.00	4,17	33	310	52.67	20	1,546
	0.8	325	61.00	4,18	23	310	52.67	20	1,388
High	0.2	267	62.67	4,17	214	262	62.00	4,17	3,414
	0.4	260	52.67	20	64	260	52.67	20	1,100
	0.6	260	52.67	20	19	260	52.67	20	1,073
	0.8	260	52.67	20	17	260	52.67	20	1,060
		Low revenue							
Low	0.2	199	58.83	4,12,14,17	80	192	57.33	4,12,14,17	6,057
	0.4	157	35.33	4,17	39	146	33.67	4,17	1,152
	0.6	142	33.33	4,17	11	119	27.33	4,17	1,031
	0.8	132	31.33	4,17	9	115	16.00	17	1,121
Medium	0.2	69	36.00	4,17	21	67	36.00	4,17	939
	0.4	65	16.00	17	13	65	16.00	17	802
	0.6	65	16.00	17	10	65	16.00	17	789
	0.8	65	16.00	17	7	65	16.00	17	895
High	0.2	15	16.00	17	7	15	16.00	17	622
	0.4	15	16.00	17	6	15	16.00	17	584
	0.6	15	16.00	17	6	15	16.00	17	591
	0.8	15	16.00	17	5	15	16.00	17	421

tion counterpart. In addition to the variables introduced for the multiple allocation model, recall that an additional binary variable was defined to model the single allocation problem. Hence, single allocation model is expected to be more challenging than the multiple allocation version.

The most time-consuming instance with the single allocation problem lasted around 3.43 hours, whereas the longest instance took 1.36 hours with the multiple allocation model. High revenue instances required more CPU time than medium and low revenue ones. This is because more hubs were opened with higher revenue levels to satisfy more demand. In general, the average CPU time requirements of the instances listed in Table 3.2 were 9.23 minutes and 1.13 hours for multiple and single allocation problems, respectively.

We also calculated the linear programming (LP) relaxation gaps of the multiple and single allocation models with all the instances listed in Table 3.2. Most of the gaps are strictly positive where the average LP gaps for the multiple and single allocation models are 4.46% and 15.87%, respectively. The LP gaps strongly vary with different parameter values. The maximum LP gap that we observed among the instances in Table 3.2 was 16.45% with the multiple allocation and 28.02% with the single allocation models, whereas the minimum was 0.02% with the multiple allocation and 7.24% with the single allocation model.

With both models, the locations of hubs and also the corresponding network designs differ greatly depending on the revenue and cost levels, and the α value. However, there are some common nodes that are selected as hubs in most of the instances, such as Chicago (4), Los Angeles (12), and New York (17). This is because these nodes generate higher amount of demand compared with other nodes in the CAB dataset.

We depict the optimal networks of a few instances from the multiple and single allocation solutions in Figures 3.1 and 3.2. In both of these figures, squares represent the established hubs, bold lines the inter-hub links, and the thin lines the allocation connections. Since the CAB dataset is symmetric, hub arcs are activated for both directions. Hence, the depicted links are undirected. There are some demand nodes in these figures

without any connections at all (see for example Figures 3.1d and 3.2d). In such cases, no demand generated from those nodes is served in the optimal solution of the problem.

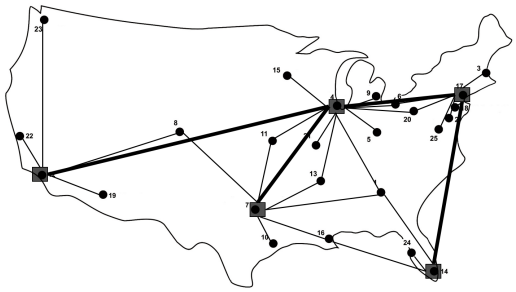

(a) High revenue, Low costs, $\alpha = 0.2$, Satisfied demand = 100%

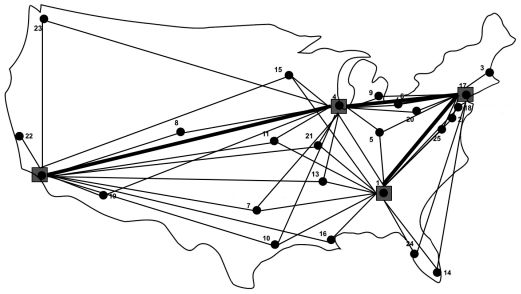

(b) High revenue, Low costs, $\alpha = 0.8$, Satisfied demand = 86.83%

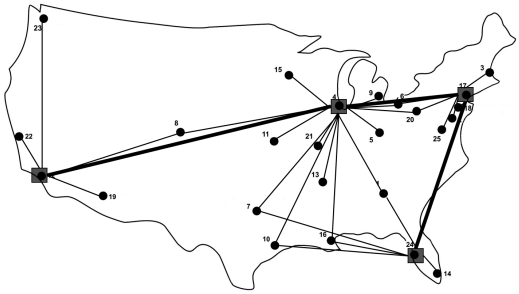

(c) High revenue, Medium costs, $\alpha = 0.2$, Satisfied demand = 99%

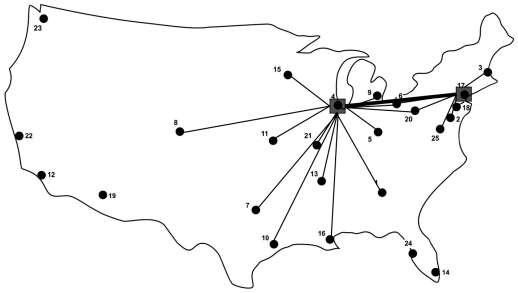

(d) Low revenue, Medium costs, $\alpha = 0.2$, Satisfied demand = 36%

Figure 3.1: Multiple allocation solutions.

Values of all the parameters except the α value are the same in Figures 3.1a and 3.1b. Observe that the number of allocation links used in Figure 3.1b is much higher than that of Figure 3.1a. This is because when $\alpha = 0.2$, most of the non-hub nodes are allocated to a single hub in order to take advantage from economies of scale, and, thus, decrease transportation cost of the flows via the inter-hub links. Whereas, when $\alpha = 0.8$, most of the non-hub nodes are allocated to at least two hubs. In this case, more flow is shipped using one hub on a route rather than using more hubs and inter-hub links. Moreover, when the discount due to economies of scale is high ($\alpha = 0.2$), the percentage of satisfied demand

goes up to 100%.

Figure 3.1a corresponds to an instance with low cost level, whereas Figure 3.1c corresponds to medium costs. All the parameter values except the cost levels are the same in these two figures. When the cost level is increased from low to medium, note that one less hub is opened and the percentage of satisfied demand drops from 100% to 99%. The 1% of unsatisfied demand in Figure 3.1c refers to the demand between O-D pairs Dallas (7)–Seattle (23), Houston (10)–Seattle (23), and New Orleans (16)–Seattle (23). The demand between those city pairs are not served as it is not profitable.

The only difference between the instances depicted in Figures 3.1c and 3.1d is the revenue level. When the revenue level is high (Figure 3.1c), four hubs are opened with 99% of total satisfied demand. On the other hand, when the revenue level is low (Figure 3.1d) the number of opened hubs reduces to two, and only 36% of the total demand is served. Note that some demand nodes in Figure 3.1d are not served at all. The demand generated from the cities on the East Coast and South–West (Los Angeles (12), Miami (14), Phoenix (19), San Francisco (22), Seattle (23), and Tampa (24)) remain entirely unserved in the optimal solution.

Figure 3.2 depicts instances from the single allocation solutions. In Figure 3.2a, when the revenue level is high, five hubs are located and 99.68% of the demand is satisfied. The only unserved O-D pair is Denver(8)–Seattle (23) in this instance. On the other hand, in Figure 3.2b, when the revenue level is low, one less hub is opened and the percentage of satisfied demand drops down to 56.33%. Similarly, when Figures 3.2c and 3.2d are compared, one less hub is opened and the percentage of satisfied demand decreases from 92.00% to 58.67% when the revenue level is reduced from high to medium.

All the parameters in Figures 3.1a and 3.2a are the same; the only difference is the allocation strategies. Note that both of the models resulted in exactly the same hub locations and inter-hub networks. The differences between the resulting networks of these two instances are the consequence of the allocation strategies. In particular, Denver (8) is allocated to hubs located in Dallas (7) and Los Angeles (12) with the multiple allocation

model (Figure 3.1a), whereas it is allocated to a single hub located in Dallas (7) with the single allocation model (Figure 3.2a). All demand is satisfied in the multiple allocation solution, whereas the percentage of satisfied demand is 99.68% with single allocation. Allocating Denver (8) to Los Angeles (12) in addition to Dallas (7), makes it possible to serve the demand between the O-D pair Denver(8)–Seattle (23) in the optimal solution.

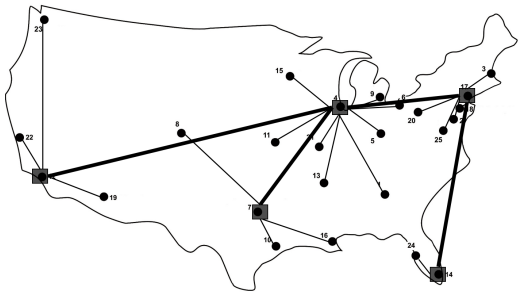

(a) High revenue, Low costs, $\alpha = 0.2$, Satisfied demand = 99.67%

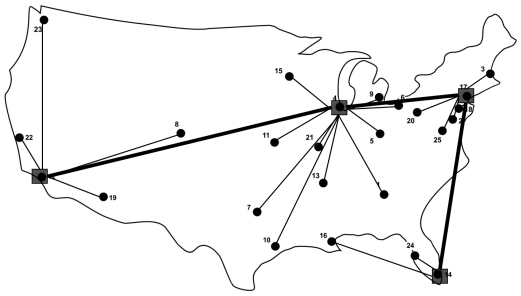

(b) Low revenue, Low costs, $\alpha = 0.2$, Satisfied demand = 57.33%

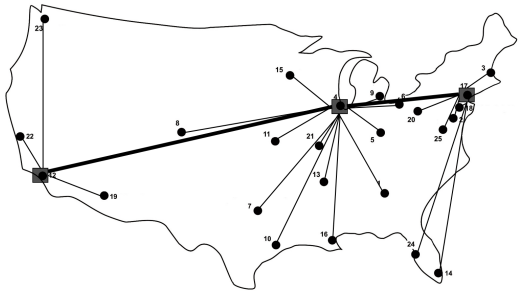

(c) High revenue, Medium costs, $\alpha = 0.4$, Satisfied demand = 92.00%

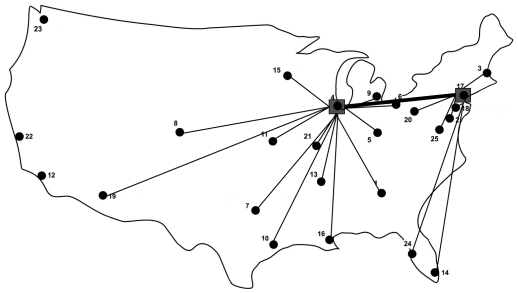

(d) Medium revenue, Medium costs, $\alpha = 0.4$, Satisfied demand = 58.67%

Figure 3.2: Single allocation solutions.

Observe from Figures 3.1 and 3.2 that Chicago (4), Los Angeles (12), and New York (17) are commonly preferred cities for locating hub nodes. Moreover, except for the 2-hub networks, note that the most profitable inter-hub networks are not fully interconnected, they are incomplete.

Next, we solve our models with direct connections under the same parameter values.

The results for the multiple and single allocation models with direct connections are reported in Table 3.3. In addition to the columns in Table 3.2, columns labeled 'Satisfied demand–direct (%)" are included in Table 3.3 to highlight the percentage of the demand satisfied only through direct connections.

Similar conclusions can be drawn from Table 3.3 as from Table 3.2. An increase in the cost level results in a decrease in the percentage of satisfied demand and net profit. Besides, an increase in the α value may also yield to a decrease in net profit. As expected, a decrease in the revenue level results in a decrease in net profit as well.

Multiple allocation with direct connections problem provides again an upper bound for the single allocation with direct connections problem. Thus, multiple allocation results in better net profits. Observe from Table 3.3 that in the instances with the same set of parameter values, percentage of satisfied demand with direct connections obtained with the single allocation model is higher than that of the multiple allocation model. That is, more demand is shipped through direct connections with the single allocation model compared with multiple allocation.

There are some instances with a hyphen sign (-) written under the hub locations columns in Table 3.3. No hubs are established in such instances, and, hence, the demand is satisfied only through direct connections. In this case, both allocation strategies yield the same net profit for the same set of parameter values.

Observe from Table 3.3 that percentage of satisfied demand through direct connections increases when fewer hubs are opened in the solutions. Moreover, when Tables 3.2 and 3.3 are compared, the models with direct connections result in opening fewer hubs. Fewer hubs are required with direct connections because a certain portion of the demand is served through direct service. Also note that the models with direct connections result in higher net profit values compared with the models not allowing for direct connections. If it was not profitable to serve the demand through direct connections, then no direct links would be established in the resulting networks. Hence, allowing for direct connections provide an upper bound for no-direct-connection problems.

Table 3.3: Solutions allowing for direct connections with the CAB dataset.

		Multiple Allocation with Direct Connections					Single Allocation with Direct Connections				
Costs	α	Net profit	Satisfied demand–total (%)	Satisfied demand–direct (%)	Hub locations	CPU time (s)	Net profit	Satisfied demand–total (%)	Satisfied demand–direct (%)	Hub locations	CPU time (s)
		High revenue									
Low	0.2	1,192	100.00	0.33	4,7,12,14,17	6,537	1,190	99.67	1.00	4,7,12,14,17	11,628
	0.4	1,042	97.83	0.67	4,7,12,14,17	6,171	1,027	95.33	3.00	4,12,14,17	9,143
	0.6	945	94.50	2.33	4,7,12,25	2,948	909	79.00	9.67	4,20	8,457
	0.8	904	82.83	8.33	20,21	619	889	77.67	16.00	5	2,018
Medium	0.2	925	99.00	1.33	4,12,18,24	3,331	917	96.00	1.67	4,12,17	8,675
	0.4	826	93.33	2.00	4,12,18	2,666	814	91.67	2.33	4,12,18	7,299
	0.6	779	76.00	7.00	5	264	779	76.00	7.00	5	1,856
	0.8	779	76.00	7.00	5	27	779	76.00	7.00	5	1,325
High	0.2	750	97.33	1.33	4,12,17	2,461	738	96.67	1.33	4,12	5,448
	0.4	696	69.33	4.33	20	88	696	69.33	4.33	20	1,933
	0.6	696	69.33	4.33	20	35	696	69.33	4.33	20	1,332
	0.8	696	69.33	4.33	20	41	696	69.33	4.33	20	1,379
		Medium revenue									
Low	0.2	694	94.67	0.67	4,7,12,14,17	4,322	689	93.67	1.00	4,7,12,14,17	10,296
	0.4	558	83.17	1.67	4,12,14,17	2,868	547	81.33	3.33	4,12,14,17	8,612
	0.6	505	67.00	5.33	4,18	536	497	59.00	11.33	20	1,923
	0.8	497	59.00	11.33	20	159	497	59.00	11.33	20	1,118
Medium	0.2	451	84.33	1.67	4,12,17	2,491	431	83.00	1.67	4,12,17	4,404
	0.4	401	55.67	6.00	20	223	401	55.67	6.00	20	1,421
	0.6	401	55.67	6.00	20	44	401	55.67	6.00	20	1,077
	0.8	401	55.67	6.00	20	36	401	55.67	6.00	20	957
High	0.2	325	54.33	3.33	20	34	325	54.33	3.33	20	1,123
	0.4	325	54.33	3.33	20	31	325	54.33	3.33	20	891
	0.6	325	54.33	3.33	20	32	325	54.33	3.33	20	948
	0.8	325	54.33	3.33	20	31	325	54.33	3.33	20	919
		Low revenue									
Low	0.2	213	49.33	2.00	4,14,17	2,101	210	48.00	1.67	4,14,17	2,527
	0.4	181	31.67	5.67	20	56	181	31.67	5.67	20	890
	0.6	181	31.67	5.67	20	42	181	31.67	5.67	20	783
	0.8	181	31.67	5.67	20	39	181	31.67	5.67	20	795
Medium	0.2	119	5.67	5.67	-	32	119	5.67	5.67	-	665
	0.4	119	5.67	5.67	-	29	119	5.67	5.67	-	618
	0.6	119	5.67	5.67	-	35	119	5.67	5.67	-	664
	0.8	119	5.67	5.67	-	36	119	5.67	5.67	-	635
High	0.2	89	4.33	4.33	-	32	89	4.33	4.33	-	699
	0.4	89	4.33	4.33	-	29	89	4.33	4.33	-	651
	0.6	89	4.33	4.33	-	31	89	4.33	4.33	-	654
	0.8	89	4.33	4.33	-	30	89	4.33	4.33	-	637

The single allocation with direct connections model is computationally more difficult than the multiple allocation version. The increase in run times is a consequence of the additional binary variable defined for the single allocation version of the problem. The average CPU time requirements for the instances listed in Table 3.3 is 17.81 minutes for the multiple allocation, and 48.33 minutes for the single allocation model.

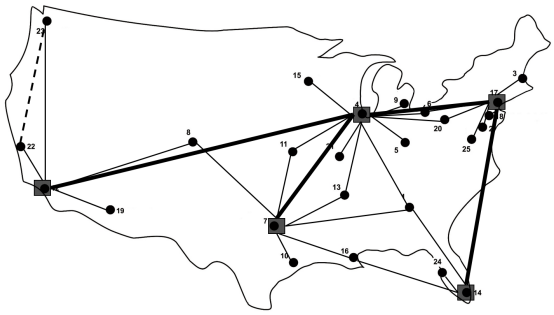

(a) Multiple allocation: High revenue, Low costs, Satisfied demand = 100% (0.33% with direct connections)

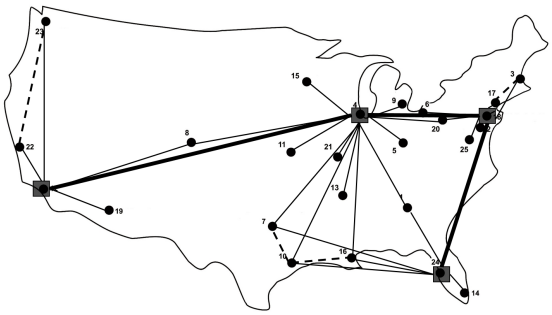

(b) Multiple allocation: High revenue, Medium costs, Satisfied demand = 99.00% (1.33% with direct connections)

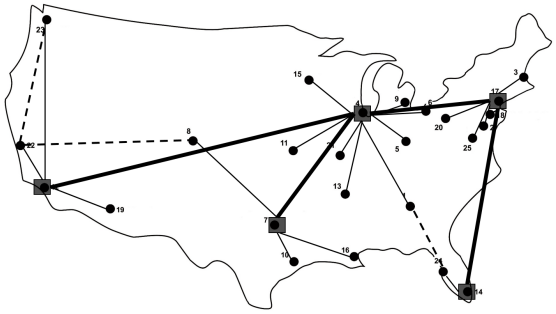

(c) Single allocation: High revenue, Low costs, Satisfied demand = 99.67% (1.00% with direct connections)

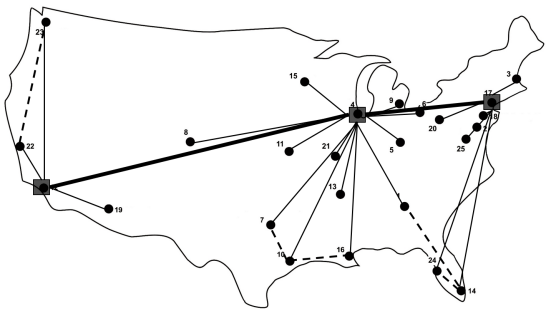

(d) Single allocation: High revenue, Medium costs, Satisfied demand = 96.00% (1.67% with direct connections)

Figure 3.3: Multiple and single allocation solutions with direct connections when $\alpha = 0.2$.

Figure 3.3 provides optimal networks of some instances with direct connections when $\alpha = 0.2$. Figures 3.3a and 3.3b depict multiple allocation instances, while Figures 3.3c and

3.3d depict their single allocation counterparts. The dash-lines in these figures indicate the direct connections between non-hub nodes. Note that resulting optimal inter-hub networks are all incomplete.

When the cost level is increased from low (Figures 3.3a and 3.3c) to medium (Figures 3.3b and 3.3d), fewer hubs are opened, and more demand is satisfied through direct connections. Figures 3.3a and 3.3c that correspond to multiple and single allocation problems, respectively, resulted in locating exactly the same hubs and the same inter-hub network design. However, the allocation links and the direct connections are different. In Figures 3.3b and 3.3d, when the allocation strategy is changed from multiple to single, one less hub is opened and the percentage of satisfied demand through direct connections increased from 1.33% to 1.67%.

Next, we compare instances presented in Figures 3.1, 3.2, and 3.3. Note that the values of all the parameters are the same in Figures 3.1a, 3.2a, 3.3a, and 3.3c. Each of these figures corresponds to an optimal solution obtained under a different model. However, all optimal solutions resulted in opening the same set of hubs and inter-hub links. The only differences are the allocation links and direct connection decisions. Shipping the demand between San Francisco (22) and Seattle (23) directly as seen in Figure 3.3a resulted in an increase in the net profit value from 1190 to 1192 compared with Figure 3.1a. Total percentage of satisfied demand in the instances depicted in Figures 3.2a and 3.3c are exactly the same (99.67%). However, 1% of the demand is satisfied through direct connections in Figure 3.3c, and this resulted in an increase in the net profit from 1181 to 1190.

We also want to analyze the performance of the r-allocation models. Looking at the optimal multiple allocation solutions, we observed that a non-hub node is allocated to at most three hubs with the CAB dataset. Therefore, when $r = 3$, r-allocation problems reduce to multiple allocation on this dataset. We thus set r to 2 and 3 to take runs with the two r-allocation models under different parameter values. Table 3.4 presents the results obtained with the r-allocation models.

Note that, when $r = 3$, r-allocation models result in exactly the same optimal solutions

Table 3.4: r-allocation solutions with the CAB dataset.

		r-Allocation without Direct Connections				r-Allocation with Direct Connections			
		r=2		r=3		r=2		r=3	
Cost	α	Net profit	CPU time (s)	Net profit	CPU time (s)	Net profit	CPU time (s)	Net profit	CPU time (s)
		High revenue							
Low	0.2	1,187	20,788	1,190	21,895	1,191	20,001	1,192	21,174
	0.4	1,021	20,700	1,033	2,1134	1,034	19,108	1,042	20,602
	0.6	897	18,534	926	20,409	921	16,800	945	17,418
	0.8	835	15,671	850	17,381	904	4,149	904	4,287
Medium	0.2	905	18,890	913	19,924	925	18,144	925	19,147
	0.4	804	16,423	804	16,562	826	16,722	826	17,015
	0.6	735	14,544	735	15,276	779	1,312	779	1,245
	0.8	681	10,500	681	10,662	779	1,216	779	1,422
High	0.2	740	14,719	740	15,283	750	14,603	750	15,067
	0.4	634	11,466	634	12,084	696	1,301	696	1,385
	0.6	599	2,140	599	2,266	696	1,434	696	1,283
	0.8	599	2,130	599	2,160	696	1,430	696	1,323
		Medium revenue							
Low	0.2	687	17,332	690	18,037	692	19,527	694	21,001
	0.4	542	16,749	550	17,712	552	16,899	558	19,084
	0.6	456	14,959	456	15,134	505	4,897	505	5,242
	0.8	426	14,279	426	14,623	497	1,295	497	1,448
Medium	0.2	429	7,578	429	7,982	451	13,212	451	14,154
	0.4	349	7,053	349	7,379	401	1,898	401	2,138
	0.6	328	4,741	328	5,044	401	2,012	401	1,980
	0.8	325	3,191	325	3,335	401	1,827	401	2,001
High	0.2	267	5,763	267	6,182	325	1,416	325	1,461
	0.4	260	1,786	260	1,644	325	1,323	325	1,526
	0.6	260	1,500	260	1,587	325	1,284	325	1,315
	0.8	260	1,401	260	1,509	325	1,217	325	1,542
		Low revenue							
Low	0.2	195	12,633	199	14,689	213	4,010	213	4,142
	0.4	157	1,913	157	2,133	181	779	181	785
	0.6	142	1,332	142	1,428	181	764	181	791
	0.8	132	804	132	1,044	181	873	181	803
Medium	0.2	69	825	69	998	119	623	119	675
	0.4	65	205	65	225	119	651	119	602
	0.6	65	187	65	243	119	604	119	634
	0.8	65	186	65	214	119	652	119	704
High	0.2	15	45	15	49	89	623	89	637
	0.4	15	43	15	46	89	640	89	662
	0.6	15	43	15	44	89	638	89	651
	0.8	15	42	15	46	89	681	89	676

obtained with the multiple allocation models. Moreover, when $r = 2$, most of the instances again resulted in the same optimal solutions with $r = 3$. Hence, we only report net profit values and CPU times in Table 3.4. Note that instances with $r = 3$ provides an upper bound for $r = 2$. Thus, for the same set of parameters, when r value is increased from 2 to 3, the net profit value either increases or remains the same.

Regarding the CPU time requirements, r-allocation models turned out to be the most challenging set of models compared with single and multiple allocation. They are computationally more difficult than multiple allocation models because an additional set of binary variables needs to be defined. Compared with single allocation, allowing the models search for r allocations instead of just one seems to increase the CPU times considerably as well. The most time-consuming instance with the r-allocation models took a little less than 6 hours to solve to optimality. The averages of the CPU times listed in Table 3.4 is 1.89 hours.

Net profits change significantly with the cost levels and the economies of scale factor under different allocation strategies. Figure 3.4 provides an insight for the change in net profits under different parameter values.

Each graph presented in Figure 3.4 corresponds to a different level of revenue: high, medium, and low. For each revenue level, we depict optimal net profit values obtained with four different models under different cost levels and discount factor α.

Observe from Figure 3.4 that multiple allocation model with direct connections results in the best net profit values. As already discussed, this model actually provides an upper bound for all the remaining models. The lowest profits are obtained with the single allocation model when direct connections are not allowed.

Figure 3.4 also illustrates the impact of α on net profit. It is clear that profits decrease with increasing α, for a given cost level. The effect of α on profits is higher with lower cost levels. Note that there are some instances in which the profits are insensitive to α. In such instances, either no hub or one hub is opened in the optimal solutions. In other words, no economies of scale are achieved as there is no inter-hub transportation. In such

cases, multiple and single allocation strategies result in exactly the same net profits.

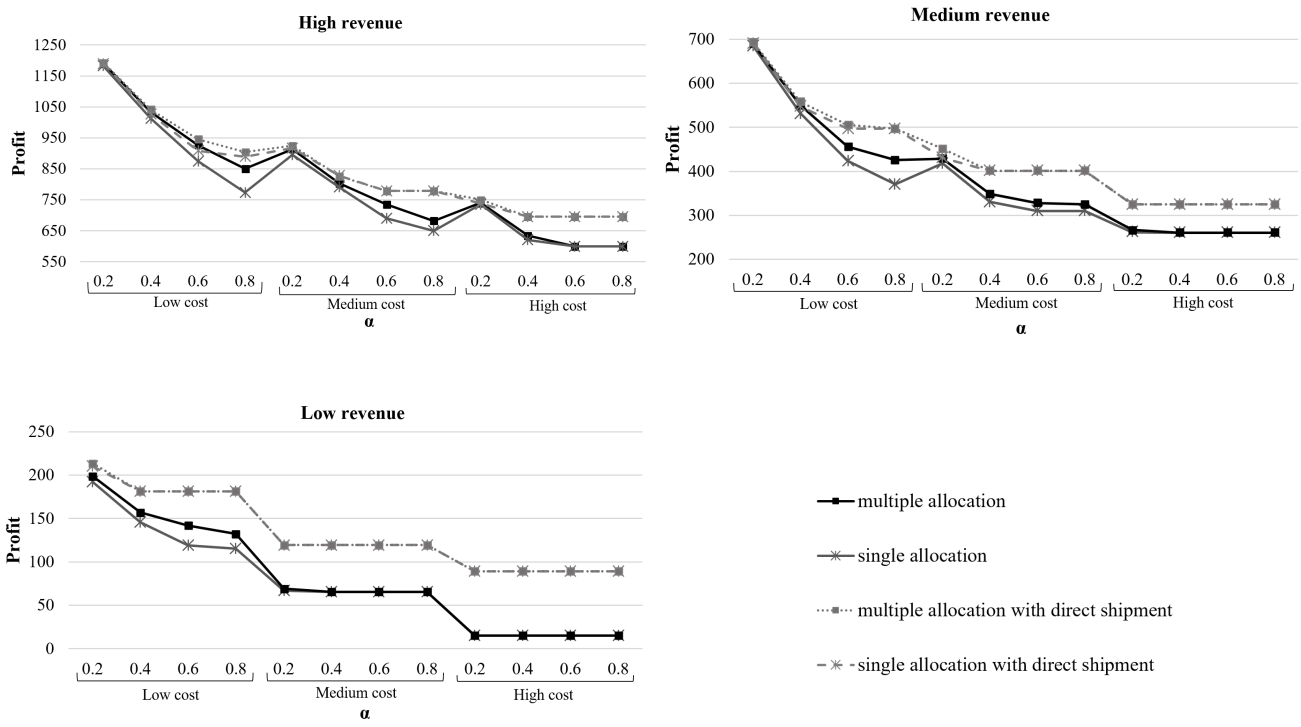

Figure 3.4: Profit comparison under different parameter values with four different models.

In general, we can conclude from Figure 3.4 that when the effect of economies of scale on transportation costs is higher (when α value is lower), the decision maker can obtain significantly more profit. Hence, economies of scale are an important factor in designing and operating hub networks. As noted in the problem definition, we assume that economies of scale are exploited only on the inter-hub links and that it is independent from the amount of flow. This is a simplification of real-life for the sake of modeling the problem efficiently. We next want to analyze the consequences of this simplification.

3.3.2 Economies of scale analysis

We analyzed optimal flows on all network connections in the resulting solutions. The amount of flow routed on the inter-hub links and allocation connections are obviously less when direct connections between non-hub nodes are allowed. Hence, we concentrated on the optimal flows with the models allowing for direct connections to observe if the amount of flow routed on the inter-hub links justify economies of scale. For this analysis, we sorted flows on all links of the network to see if there are any allocation links or direct links carrying larger flows than inter-hub links. We could identify only a few such instances where the flow on one allocation link exceeded the flow on an inter-hub link. For example, in the instance from Table 3.3 with high revenue and medium cost levels with $\alpha = 0.4$, the allocation link New York (17)–Philadelphia (18) carries more flow than the inter-hub link Chicago (4)–Los Angeles (12). This is because all demand originating at New York and destined to all other cities has to use the allocation link from New York to Philadelphia. However, as mentioned above, only a few instances do not justify economies of scale in our experimentation. This is because our models do not enforce the establishment of fully interconnected inter-hub networks. Note that in all of our solutions with more than two hubs, the resulting inter-hub networks are incomplete. By the inclusion of inter-hub network design decisions in hub location models, more flow is consolidated on hub-to-hub links.

We also wanted to analyze the impact of using a flow-independent economies of scale factor on the inter-hub links. Incorporating a flow-dependent economies of scale factor in our models would computationally be impractical due to its non-linear nature. Instead, we decided to recalculate the transportation costs of our optimal solutions by using flow-dependent discounts. For this analysis, we adopted the non-linear concave function introduced in O'Kelly and Bryan [77]. While recalculating the transportation costs, we replaced α and for each inter-hub link $k, l \in N$, we calculated the discount through the

function:

$$1 - \theta(\sum_{i \in N} f_{ikl})^{\beta} \qquad k, l \in N \tag{3.34}$$

where $0 < \theta \leq 1$, $\beta > 0$, and $\sum_{i \in N} f_{ikl}$ is the amount of flow routed on the inter-hub link from hub k to hub l. Note that since total demand is scaled and it adds up to one, we do not need to scale the flows in this calculation.

For each instance with the given revenue and cost levels, we compared net profits obtained from using different combinations of constant and flow-dependent discount factors, α, θ, and β. We observed through this analysis that for any given value of α, there is a valid combination of θ and β values which results in comparable transportation costs. For example, in the instances with high revenue and low cost levels, total transportation cost recalculated by using $\theta = 0.9$ and $\beta = 0.1$ in the above function results in a 2% decrease in the net profit on average when compared with using $\alpha = 0.2$, which is the highest economies of scale discount that we used in our experimentation. Similarly, with high revenue and medium cost levels, using the combination of $\theta = 0.75$ and $\beta = 0.2$ results in only a 0.23% decrease in the net profit on average compared with using $\alpha = 0.4$. This analysis shows that the α values used in our computational experiments actually provide good estimates for flow-dependent discounts.

We would like to note that the analysis that we performed with this flow-dependent discount function is post-processing. As noted by O'Kelly and Bryan [77], modeling the problem assuming a fixed discount factor not only miscalculate the total network cost but may also wrongly select optimal hub locations and allocations. Incorporating a more realistic calculation of economies of scale within the proposed models is definitely an important avenue for future research.

3.3.3 Comparison with the literature

As discussed in our introduction, hub location problems with profits considering the multiple allocation strategy were already introduced in Alibeyg et al. [3]. In this chapter, in

addition to studying all allocation possibilities, we included additional design variables to account for the design of the inter-hub network which in turn makes the problem more complicated. To justify the increased complexity of the proposed models, we present a computational comparison of our multiple allocation model and the PO_1 model presented in Alibeyg et al. [3, 4]. For this comparison, we concentrated on the instances resulted in opening more than two hubs in the optimal solutions obtained from our multiple allocation model. Table 3.5 presents the results.

Table 3.5: Comparison of our multiple allocation model with PO_1 from Alibeyg et al. [3, 4].

		PO_1				Multiple Allocation Model				
Cost	alpha	Net profit	Satisfied demand (%)	LP gap (%)	CPU time (s)	Net profit	Satisfied demand (%)	LP gap (%)	CPU time (s)	Profit gap (%)
		High revenue								
Low	0.2	1,146	100.00	3.49	1,851	1,190	100.00	2.73	4,891	3.86
	0.4	991	95.67	3.61	1,611	1,033	97.33	4.31	4,130	4.23
	0.6	889	91.67	5.28	1,084	926	94.00	2.77	2,428	4.19
	0.8	832	85.33	7.95	449	850	86.83	2.27	754	2.21
Medium	0.2	887	97.05	6.05	764	913	99.00	7.31	801	2.96
	0.4	791	88.33	4.91	416	804	93.00	5.84	615	1.62
	0.6	723	85.67	9.09	287	735	89.33	3.70	521	1.63
High	0.2	723	93.33	6.22	325	740	97.00	8.04	550	2.27
	0.4	619	88.33	13.52	144	634	93.00	9.45	362	2.31
		Medium revenue								
Low	0.2	656	88.00	3.35	1,081	690	94.00	4.91	1,756	5.16
	0.4	517	83.00	6.95	605	550	89.00	6.43	1,249	6.36
	0.6	440	64.00	4.24	427	456	68.00	3.49	504	3.65
	0.8	411	61.00	6.61	212	426	64.00	2.85	283	3.56
Medium	0.2	401	82.00	17.73	324	429	83.17	12.63	549	6.98
		Low revenue								
Low	0.2	183	55.33	8.99	111	199	58.83	4.79	80	8.74

For each instance, Table 3.5 provides the net profit, percentage of satisfied demand, LP relaxation gap, and the run time of the instances obtained by solving the PO_1 model from Alibeyg et al. [3, 4] and our multiple allocation model introduced in Section 3.2.1.

The last column of Table 3.5 presents the percentage of the gap between the net profits obtained from these two models.

Firstly, a comparison of the CPU times and LP relaxation gaps reported in Alibeyg et al. [3] with Table 3.5 reveals that our test instances are computationally more challenging than the ones reported in Alibeyg et al. [3]. We would like to note that we used variable fixing while solving both of the models under the default settings of CPLEX.

Our multiple allocation model provides an upper bound in terms of the net profit value and the percentage of satisfied demand. Observe from Table 3.5 that all the profit gaps are strictly positive. This is because in all of our solutions with more than two hubs, there exist paths in which more than two hubs are used to satisfy the demand between O-D pairs. PO_1 model needs to activate additional hub links to satisfy the same or even less amount of demand that is satisfied with our multiple allocation model. For example, with high revenue and low cost levels when $\alpha = 0.2$, 100% of the demand is satisfied under both of the models. In this instance, our multiple allocation solution resulted in operating an incomplete inter-hub network (Figure 3.1a) and 14% of the total flow is routed using more than two hubs on a route. While, the PO_1 solution, which restricts the number of hubs on a route to at most two and activates hub arcs of a fully inter-connected hub network, resulted in a 3.83% decrease in the net profit. The percent gap in profits goes up to 8.74% in the instances listed in Table 3.5. Moreover, since the demand is scaled in our data, the magnitude of the objective function value is relatively low in our experiments, otherwise the difference in the net profits would have been higher. We believe these results provide a clear indication of the added benefit of incorporating more complex paths into the models.

3.3.4 Results with the AP dataset

In this section, we test the performance of our models on a 40-node subset of the Australia Post (AP) dataset (Ernst and Krishnamoorthy 46). The distances and the demand between each pair of cities are provided in OR Library (Beasley 15). Collection and distributions costs per unit are taken equal to one. For the revenue of each O-D pair, we again test three

different values such that $r_{ij} \in \{20, 30, 50\}$ for all $i, j \in N$. We refer to these values as low, medium, and high revenues, respectively. There are two different sets for hub installation costs available on the AP dataset referred to as loose and tight. Cost of operating an inter-hub link is assumed to be 10% of the average installation costs from the AP data. Similar to the CAB dataset, the cost of operating a direct link is taken to be the 20% of the operational cost of an inter-hub link. Operational costs are assumed to be the same for all potential links. For all instances, the discount factor α is taken as 0.75, as defined in the AP dataset (Beasley 15).

The results obtained from solving the multiple and single allocation models without and with direct connections are summarized in Tables 3.6 and 3.7, respectively. As noted in the first two columns, we tested three different revenue and two different cost levels.

Table 3.6: Multiple and single allocation solutions with the AP dataset.

		Multiple Allocation				Single Allocation			
Revenue	Costs	Net profit	Satisfied demand (%)	Hub locations	CPU time (h)	Net profit	Satisfied demand (%)	Hub locations	CPU time (h)
High	Loose	118,303	98.13	12,22,26,28	3.82	73,384	91.25	11,12,22,28	6.87
	Tight	105,850	97.75	11,14,29	3.07	46,736	90.38	11,14,29	6.12
Medium	Loose	42,868	77.69	12,22,26,28	2.91	36,904	64.06	11,22,28	5.04
	Tight	32,716	69.13	14,29	0.09	29,569	51.56	29	1.20
Low	Loose	14,099	22.63	28	0.03	14,099	22.63	28	0.53
	Tight	6,404	23.50	29	0.05	6,404	23.50	29	0.48

Similar conclusions can be drawn with the AP dataset as with the CAB dataset. Net profits and the percentage of satisfied demand decrease with decreasing revenue levels. Tight (high) fixed cost instances result in lower net profits. In the models with direct connections (Table 3.7), a decrease in the revenue level results in an increase in the percentage of satisfied demand through direct connections.

Table 3.7: Solutions allowing for direct connections with the AP dataset.

		Multiple Allocation with Direct Connections					Single Allocation with Direct Connections				
Revenue	Costs	Net profit	Satisfied demand-total (%)	Satisfied demand-direct (%)	Hub locations	CPU time (h)	Net profit	Satisfied demand-total (%)	Satisfied demand-direct (%)	Hub locations	CPU time (h)
High	Loose	119,998	98.50	1.00	12,18,22,28	4.61	76,026	87.00	4.75	11,12,22,28	7.01
	Tight	106,614	95.25	1.13	14,29	3.66	48,101	86.13	5.38	11,14,29	6.59
Medium	Loose	44,222	76.06	1.19	11,22,28	3.05	38,694	63.19	5.56	11,22,28	5.82
	Tight	36,252	71.00	5.25	19,22	0.57	34,179	54.75	12.31	29	2.15
Low	Loose	15,077	23.44	1.31	28	0.04	15,077	23.44	1.31	28	0.39
	Tight	6,677	23.63	0.25	29	0.09	6,677	23.63	0.25	29	0.34

The CPU times obtained from solving the models with the AP dataset indicate that larger-sized instances are more challenging, and, consequently, more time consuming than small-sized instances, as expected. Because of the higher run times, CPU times in Tables 3.6 and 3.7 are reported in hours. Note that, in addition to the size of the instances, computation times also vary a lot with different parameter values as well as allocation strategies. In particular, when the revenue level decreases from high to low, the CPU times in Table 3.6 drops from about 7 hours to less than 1 hour. The most difficult instances were with the single allocation model allowing for direct connections. Average CPU time requirement of the instances presented in Tables 3.6 and 3.7 with the 40-node AP dataset is 2.66 hours.

3.4 Conclusions

In this chapter, we studied hub location problems with the aim of maximizing profit. We defined new problems and developed efficient mathematical models addressing the questions of where to locate hubs and how to design hub networks in order to maximize profit. We determined optimal routes of flow to transport the demand between origin-

destination pairs while allowing a portion of the demand to be unserved. We introduced mixed-integer linear programming models for multiple, single, and r-allocation versions of the problem. We also modeled the possibility of direct connections for each allocation strategy. The proposed models design hub networks in the most profitable way considering all possibilities for shipments.

We performed computational experiments on the well-known CAB and AP datasets to analyze the resulting hub networks and performance of the proposed mathematical models. We tested all models under various different parameter settings. We varied revenues, costs, and the economies of scale discount factor, and analyzed the optimal locations of hubs, design of the hub network, and percentage of satisfied demand.

The results provided insights on where to locate hubs, how to design hub networks, what portion of the demand to serve, and how to route flows. The most profitable inter-hub network designs with more than two hubs turned out to be incomplete. Trade-off between different allocation strategies as well as the impact of allowing for direct connections is explored. The best net profit values were obtained with the multiple allocation model allowing for direct connections, whereas, the lowest profits were obtained with the single allocation model when direct connections are not allowed. The choice of the allocation strategy did not result in a significant difference on the locations of hubs in the optimal solutions. The effect of the economies of scale discount on total profit is also analyzed. The results showed that the decision maker can obtain significantly more profit when the discount on transportation costs due to economies of scale is higher.

Chapter 4

Profit Maximizing Hub Location Problems with Capacity Allocation

In many real-life hub networks, the demand of commodities usually consists of different classes (e.g., for regular and priority service). The decision maker thus needs to consider how to allocate the available capacity to these different demand segments, while determining the proportion of the demand to serve for each class. In airline passenger networks, different classes of demand may include the demand for, for example, the first, business, and economy class service. In express shipment delivery networks, on the other hand, there is a demand for services such as priority, express, and standard mail. Incurring these revenue management decisions surely bring on extra challenges yet this is a much more realistic problem setting.

In this chapter, we incorporate revenue management decisions within hub location problems and determine how to allocate available capacities of hubs to demand of commodities from different market segments. *The profit maximizing hub location problems with capacity allocation* introduced in this chapter seek to find an optimal hub network structure, maximizing total profit to provide services to a set of commodities while considering the design cost of the network. The decisions to be made are the optimal number and loca-

tions of hubs, allocation of demand nodes to these hubs, and the optimal routes of flow of different classes of commodities that are selected to be served. We consider a hub location problem with multiple assignments, and allow a path of an origin-destination pair to pass through at most two hubs. Direct connections between non-hub nodes are not allowed; all commodities must be routed via a set of hubs. Demand is segmented into different classes and revenue is obtained from satisfying demands for the commodities of each class. The model is to decide how much demand to serve from each class considering the available capacity. Each demand class from each commodity can be partially satisfied.

We first present a strong mixed-integer programming formulation of the profit maximizing hub location problem with capacity allocation and then present two exact algorithms based on a Benders decomposition of the formulation. Since the subproblem is inseparable, solving it can be as challenging as solving the original problem. Moreover, due to degeneracy in the subproblem, straightforward implementation of Benders decomposition suffers from low convergence. Alleviating these deficiencies, we propose a general methodology for decomposing inseparable subproblems into smaller problems in a two-phase fashion, where optimality and strength of the cuts are guaranteed in phase I and phase II, respectively. More specifically, for the profit maximizing hub location problem with capacity allocation, we prove that the second phase can be solved as a set of LP-relaxations of maximum weighted matching problems, or as a series of LP-relaxations of knapsack problems. We enhance these algorithms by incorporating improved variable fixing techniques. Moreover, we perform extensive computational experiments to evaluate the efficiency and robustness of the proposed algorithms and solve large-scale instances of the problem.

The outline of this chapter is organized as follows. We introduce the notation and formulate the mixed-integer linear programming model in Section 4.1. Section 4.2 contains the basic Benders decomposition algorithm and our introduction of several features that improve the convergence and efficiency of the problem. We perform extensive computational experiments in Section 4.3 to test our mathematical model and evaluate our algorithms. Section 4.4 provides some concluding remarks for this chapter.

4.1 Mathematical Formulations

This section first introduces the notation and then presents mathematical formulation of the problem.

4.1.1 Notation

Let $G = (N, A)$ be a complete digraph, where N is the set of nodes and A is the set of arcs. Adapting the notation used by Contreras et al. [37], we define a hub arc as an ordered set $a \in A$ and a loop a as $\{a_1, a_2\}$ if $|a| = 2$, and as $\{a_1\}$ if $|a| = 1$. Let $H \subseteq N$ be the set of potential hub locations, and K represent the set of commodities whose origin and destination points belong to N. Demand of commodities are segmented into M classes. For each commodity $k \in K$ of class $m \in M$, w_k^m is defined as the amount of commodity k of class m to be routed from the origin $o(k) \in N$ to the destination $d(k) \in N$. Satisfying a unit commodity $k \in K$ of class $m \in M$ produces a per unit revenue of r_k^m. Let f_i and Γ_i denote the installation cost and the available capacity of a hub located at node $i \in H$, respectively. The transportation cost from node $i \in N$ to node $j \in N$ is defined as $c_{ij} = \gamma d_{ij}$, where d_{ij} denotes the distance from node i to node j, and γ is the resource cost per unit distance. Distances are assumed to satisfy the triangle inequality,

Each path of an origin-destination pair contains at least one and at most two hubs. Thus, paths are of the form $(o(k), i, j, d(k))$, where $(i, j) \in H \times H$ represents the ordered pair of hubs to which $o(k)$ and $d(k)$ are allocated, respectively. The transportation cost of routing one unit of commodity k along path $(o(k), i, j, d(k))$ can be calculated by $C_{ijk} = \chi c_{o(k)i} + \alpha c_{ij} + \delta c_{jd(k)}$, where χ, α, δ represent the collection, transfer, and distribution costs, respectively. The economies of scale between hubs are reflected by assuming $\alpha < \chi$ and $\alpha < \delta$.

A few characteristics of the multiple allocation hub location problem can be employed in modeling profit maximizing hub location problems with capacity allocation as detailed below:

Property 1. *In any optimal solution, a commodity can be routed via a path containing two distinct hubs only if it is not cheaper to do so using one of the hubs (Boland et al. [19]).*

Property 2. *In any optimal solution, every commodity $k \in K$ uses at most one of the paths $o(k), i, j, d(k)$ and $o(k), j, i, d(k)$; the one with the lower transportation cost (Contreras et al. [35]).*

Consequently, each commodity defines its own set of potential hub arcs. Henceforth, we replace C_{ijk} with $\hat{C}_{ijk} = \min\{C_{ijk}, C_{jik}\}$, and reduce the set of candidate hub arcs for commodity $k \in K$ to A_k as defined in (4.1), which can be used to reduce the size of the mathematical formulations.

$$A_k = \{(i,j) \in A : i \leq j, \hat{C}_{ijk} \leq \min\{C_{iik}, C_{jjk}\}\} \tag{4.1}$$

4.1.2 Model

Let y_i equal to 1 if a hub is established at node $i \in H$, and 0 otherwise. Moreover, let x_{ak}^m determine the fraction of commodity $k \in K$ of class $m \in M$ that is satisfied through a path with hub arc $a \in A_k$. The *The profit maximizing hub location problems with capacity allocation* is then modeled as:

$$\text{Maximize} \quad \sum_{m \in M} \sum_{k \in K} \sum_{a \in A_k} (r_k^m - \hat{C}_{ak}) w_k^m x_{ak}^m - \sum_{i \in H} f_i y_i \tag{4.2}$$

$$\text{s.t.} \quad \sum_{a \in A_k} x_{ak}^m \leq 1 \qquad k \in K, m \in M \tag{4.3}$$

$$\sum_{a \in A_k : i \in a} x_{ak}^m \leq y_i \qquad i \in H, k \in K, m \in M \tag{4.4}$$

$$\sum_{m \in M} \sum_{k \in K} \sum_{a \in A_k : i \in a} w_k^m x_{ak}^m \leq \Gamma_i y_i \qquad i \in H \tag{4.5}$$

$$x_{ak}^m \geq 0 \qquad k \in K, m \in M, a \in A_k \tag{4.6}$$

$$y_i \in \{0,1\} \qquad i \in H. \tag{4.7}$$

The objective function (4.2) represents net profit, which is calculated by subtracting total cost from total revenue. If demand of a commodity from a given class is to be satisfied, then by constraints (4.3) flow must be routed via hubs. Each demand class from each commodity can be partially satisfied through different paths. Constraints (4.4) ensure that demand of commodities can be satisfied only through open hubs. Constraints (4.5) restrict capacity on the total incoming flow at a hub via both hub and non-hub nodes. Finally, constraints (4.6) and (4.7) define the non-negative and binary variables.

Remark 1. *For integer values of y, constraints (4.3) and (4.5) imply constraints (4.4). Hence, constraints (4.4) act as valid inequalities for the mathematical model (4.2)-(4.7).*

Since our solution method is based on Benders decomposition, and it is known that Benders decomposition performs better with stronger formulations (Magnanti and Wong [61]), we choose to keep these constraints in our mathematical model.

Note that when revenue from satisfying the commodity $k \in K$ of class $m \in M$ is strictly smaller than the unit transportation cost of routing commodity k along a path containing a hub arc $a \in A_k$, no profit can be obtained from satisfying the demand for commodity $k \in K$ of class $m \in M$ through that path. Accordingly, the optimal value for the corresponding variable x_{ak}^m can then be set to zero as noted in Property 3 below:

Property 3. *For every $k \in K$, $m \in M$ and $a \in A_k$, if $r_k^m < \hat{C}_{ak}$, then $x_{ak}^m = 0$ in any optimal solution to (4.2)-(4.7).*

4.2 Benders Decomposition

We introduce a Benders decomposition methodology for the solution of our models. Benders decomposition is well suited for hub location problems especially with multiple allocation structure as the problem can be decomposed into linear subproblems by fixing the integer variables for the location of hubs. In this section, we first present the Benders

reformulation of the model and the Benders decomposition algorithm; we then detail our solution strategies for the subproblems.

4.2.1 Benders reformulation and algorithm

Given the mixed integer formulation (4.2)-(4.7), in the Benders reformulation of the problem, the hub location decisions are handled in the master problem and the rest is left to the subproblem. By fixing the values of the integer variables $y_i = y_i^e$, we obtain the following linear *primal subproblem* (PS):

$$\text{(PS)} \quad \text{Maximize} \quad \sum_{m\in M}\sum_{k\in K}\sum_{a\in A_k}(r_k^m - \hat{C}_{ak})w_k^m x_{ak}^m \tag{4.8}$$

$$\text{s.t.} \quad \sum_{a\in A_k} x_{ak}^m \leq 1 \qquad k\in K, m\in M \tag{4.9}$$

$$\sum_{a\in A_k: i\in a} x_{ak}^m \leq y_i^e \qquad i\in H, k\in K, m\in M \tag{4.10}$$

$$\sum_{m\in M}\sum_{k\in K}\sum_{a\in A_k: i\in a} w_k^m x_{ak}^m \leq \Gamma_i y_i^e \qquad i\in H \tag{4.11}$$

$$x_{ak}^m \geq 0 \qquad k\in K, m\in M, a\in A_k. \tag{4.12}$$

We derive the dual of PS by associating the dual variables α_k^m, u_{ik}^m, and b_i to the constraints (4.9), (4.10), and (4.11), respectively. We then have the following *dual subproblem* (DS):

$$\text{(DS)} \quad \text{Minimize} \quad \sum_{k\in K}\sum_{m\in M}\alpha_k^m + \sum_{i\in H} y_i^e(\Gamma_i b_i + \sum_{k\in K}\sum_{m\in M} u_{ik}^m) \tag{4.13}$$

$$\text{s.t.} \quad \alpha_k^m + u_{ik}^m + u_{jk}^m + w_k^m(b_i+b_j) \geq (r_k^m - \hat{C}_{ijk})w_k^m \qquad k\in K, m\in M, (i,j)\in A_k : i\neq j \tag{4.14}$$

$$\alpha_k^m + u_{ik}^m + w_k^m b_i \geq (r_k^m - \hat{C}_{iik})w_k^m \qquad k\in K, m\in M, i\in H \tag{4.15}$$

$$\alpha_k^m, u_{ik}^m, b_i \geq 0 \qquad k\in K, m\in M, i\in H \tag{4.16}$$

Let P denote the polyhedron defined by (4.14)-(4.16), and let $\hat{P}$ be the set of extreme points of P. The primal and dual subproblems are always feasible and bounded, hence an optimal solution of DS is one of the extreme points of P. Note that $\hat{P}$ does not depend on y_i^e; hence, for any arbitrary y, DS can be restated as

$$\min_{(\alpha,u,b)\in\hat{P}} \quad \sum_{k\in K}\sum_{m\in M}\alpha_k^m + \sum_{i\in H} y_i(\Gamma_i b_i + \sum_{k\in K}\sum_{m\in M} u_{ik}^m). \tag{4.17}$$

Let η denote the overall revenue obtained by satisfying the demand; the Benders *master problem* (MP) can then be formulated as:

$$\text{(MP)} \quad \text{Maximize} \quad \eta - \sum_{i\in H} f_i y_i \tag{4.18}$$

$$\text{s.t.} \quad \eta \le \sum_{k\in K}\sum_{m\in M}\alpha_k^m + \sum_{i\in H} y_i(\Gamma_i b_i + \sum_{k\in K}\sum_{m\in M} u_{ik}^m) \quad (\alpha,u,b)\in\hat{P} \tag{4.19}$$

$$y_i \in \{0,1\} \qquad i \in H. \tag{4.20}$$

Note that MP contains an exponential number of constraints. We can work around this difficulty by employing a cutting-plane method. Starting with an empty set $\hat{P}$, we iteratively solve a relaxed master problem with a small subset of $\hat{P}$ and keep adding new extreme points to $\hat{P}$ by solving dual subproblems, until the optimal solution to MP is found.

An overview of the basic BD algorithm is given in Algorithm 1. In this algorithm, UB, LB, e, z_{MP}^e, and z_{DS}^e stand for the current upper and lower bounds, the iteration counter, and the optimal solutions obtained from the master problem and dual subproblem at iteration e, respectively.

The computational efficiency of the Benders decomposition algorithm generally depends on the number of iterations required to obtain an optimal solution and the computational effort needed to solve MP as well as DS at each iteration. In the following sections, we first describe how the size of the problem can be reduced via variable fixing and then explain how the subproblem can be solved efficiently.

Algorithm 1 Benders decomposition

1: $UB \leftarrow +\infty, LB \leftarrow -\infty, e \leftarrow 0, \hat{P} \leftarrow \emptyset$
2: **while** $(LB < UB)$ **do**
3: **SOLVE** MP and obtain y^e and z^e_{MP}
4: $UB \leftarrow z^e_{MP}$
5: **SOLVE** DS and obtain $(\alpha, u, b)^e$ and z^e_{DS}
6: $LB \leftarrow \max\{LB, z^e_{DS} - \sum_{i \in H} f_i y^e_i\}$
7: **ADD** $(\alpha, u, b)^e$ to $\hat{P}$
8: $e \leftarrow e + 1$
9: **end while**

4.2.2 Variable fixing

Variable fixing can improve the efficiency of the Benders decomposition algorithm by reducing the computational time of solving the master problems and subproblems due to solution space reduction. The dominance properties presented in Section 4.1 reduce the size of the model significantly via preprocessing. We can further reduce the size by eliminating hubs that cannot be open in an optimal solution. Contreras et al. [35] propose two reduction tests that eliminate such hubs by using the information obtained during the inner iterations of the Benders algorithm. In this thesis, we adapt and improve on these tests for eliminating hubs from H and the associated variables from the model.

The first reduction test is based on the primal information obtained by solving the LP-relaxation of MP. Let MP^e_{LP} denote the LP-relaxation of MP at iteration e, z^e_{LP} its optimal value, and rc_i the reduced cost associated with variable y_i for $i \in H$. Let LB be a known lower bound on the optimal value of MP. Since $z^e_{LP} + rc_i$ provides a lower bound on the optimal value of MP, any hub $i \in H$ for which $z^e_{LP} + rc_i < LB$ cannot be open in any optimal solution. Hence, such hubs and their associated variables in the master and subproblem can be discarded in subsequent iterations.

The second reduction test relies on eliminating a set of hubs $Q \subset H$ that are proved

to be closed in an optimal solution. Let $\text{MP}^e(Q)$ denote the MP at iteration e with the additional constraint $\sum_{i \in Q} y_i \geq 1$, and $z^e_{MP}(Q)$ its optimal value. Let LB be a lower bound on the optimal value of MP. Note that $\text{MP}^e(Q)$ provides a lower bound on the optimal value of MP^e. Hence, if $z^e_{MP}(Q) < LB$, then none of these hubs can be open in any optimal solution. Therefore, the hubs contained in Q and their associated variables can be discarded in subsequent iterations.

The performance of this reduction test highly depends on the choice of Q. The hubs contained in Q should ideally have the least chance of being open in an optimal solution. Note that it is vital to eliminate potentially non-optimal hubs in the earlier iterations of the Benders algorithm. To increase the chance of a successful test, we make the following two modifications on the settings of the second reduction test of Contreras et al. [35].

The first modification addresses the choice of Q. Rather than setting $Q = H$ at the beginning of the Benders algorithm, we set Q to a certain proportion p_Q (e.g., 75%) of the hubs that are less likely to be open in an optimal solution. A simple greedy way of identifying such hubs is to sort the hubs in a nondecreasing order of their ratio of fixed cost (f) to capacity (Γ). At iteration e, we discard from Q the set of hubs opened in the optimal solution of MP as well as the nodes that satisfy the first reduction test. We then perform the second reduction test and if it fails, we further remove from Q the open hubs in the optimal solution of $\text{MP}^e(Q)$. As the Benders algorithm proceeds, Q may become empty (either because of successful tests or discarding open hubs), and we must thus reset Q. This time, rather than greedily sorting the hubs in nondecreasing order of $f/_\Gamma$, we sort them in nonincreasing order of the number of times the hubs have been opened in previous iterations of the Benders algorithm, and select the first p_Q of the sorted hubs.

The second modification addresses the weakness of the bound obtained by $z^e_{MP}(Q)$. Rather than running a single test at each iteration, we split Q into a certain number n_Q of (not necessarily mutually exclusive) smaller subsets. We then run a reduction test for each subset and remove all the nodes in the subset that results in a successful reduction test. Although this modification requires solving multiple integer programs at each iteration

of the Benders algorithm, the time required for solving these programs is negligible and compensated by the improved effectiveness of the resulting tests when proper values of p_Q and n_Q are selected. Our computational experiments show that both of these modifications considerably increase the performance of the second reduction test.

4.2.3 A two-phase method for solving the subproblem

Solving the dual subproblem is the most challenging part of the BD algorithm. Due to different definition of capacity usage of hubs in our problems, unlike Contreras et al. [37], we can no longer cast the subproblem (4.13)-(4.16) as a transportation problem. Moreover, the algorithm may suffer from slow convergence due to weakness of the generated cuts.

Pareto-optimal (PO) cuts (Magnanti and Wong [61]) have been extensively used in the literature for generating strong optimality cuts. This method relies on solving two subproblems. In the first problem, the optimal value of the subproblem is calculated. In the second problem (known as the PO subproblem), using a *core point*, a PO cut is generated. By fixing b at specific values, Contreras et al. [37] generate good cuts by approximating the PO subproblem (Contreras et al. [35]). Because of the structural differences of our problem, as we will demonstrate via computational experiments, the method proposed by Contreras et al. [37] does not generate good enough cuts for our problem, or it comes with a high computational burden. Hence, we seek a method for generating good optimality cuts with less computational effort.

In this thesis, we propose a method for solving the subproblem in two sequential phases based on the set of values of the binary variables at which the subproblem is evaluated, and reduce each phase into simpler problems. Our approach for breaking the subproblem into two phases is analogous to the idea of approximating the PO cuts. In Phase I, we obtain the optimal value of the subproblem, whereas in Phase II, we strengthen the cut while preserving the optimality and feasibility of the solution.

At iteration e of the BD algorithm, we obtain an optimal solution y^e from MP. Let

$H_1^e = \{i : y_i^e = 1\}$ be the set of open hubs and $H_0^e = \{i : y_i^e = 0\}$ be the set of closed hubs. Moreover, let A_{ke}^1 denote the set of distinct potential open hubs of commodity k at iteration e (i.e., $A_{ke}^1 = \{(i,j) \in A_k \cap H_1^e \times H_1^e : i \neq j\}$.) Note that any feasible value of b_i and u_{ik}^m would be optimal when $i \in H_0^e$. Hence, we can solve the subproblem in two phases. In *Phase I*, we remove the variables b_i and u_{ik}^m and their corresponding constraints from DS associated with $i \in H_0^e$, and compute the values of the remaining variables by solving the following *Phase I* subproblem.

$$\text{(DS-I)} \quad \text{Minimize} \quad \sum_{k\in K}\sum_{m\in M} \alpha_k^m + \sum_{i\in H_1^e}(\Gamma_i b_i + \sum_{k\in K}\sum_{m\in M} u_{ik}^m) \tag{4.21}$$

$$\text{s.t.} \quad \alpha_k^m + u_{ik}^m + u_{jk}^m + w_k^m(b_i + b_j) \geq (r_k^m - \hat{C}_{ijk})w_k^m \quad k \in K, m \in M, (i,j) \in A_{ke}^1 \tag{4.22}$$

$$\alpha_k^m + u_{ik}^m + w_k^m b_i \geq (r_k^m - \hat{C}_{iik})w_k^m \quad k \in K, m \in M, i \in H_1^e \tag{4.23}$$

$$\alpha_k^m, u_{ik}^m, b_i \geq 0 \quad k \in K, m \in M, i \in H_1^e \tag{4.24}$$

Note that α_k^m variables are independent from i, accordingly, solving DS-I results in obtaining the optimal values of all α_k^m variables. Hence, in *Phase II*, we find feasible values of b_i and u_{ik}^m for $i \in H_0^e, k \in K, m \in M$ with respect to constraints (4.14)-(4.16), aiming to generate optimality cuts as strong as possible.

Let $A_{ke}^0 = \{(i,j) \in A_k \cap H_0^e \times H_0^e : i \neq j\}$ denote the set of distinct potential closed hub arcs of commodity $k \in K$ at iteration e, and let $H_1^{ei} = \{j \in H_1^e : (i,j) \in A_k \text{ or } (j,i) \in A_k\}$ be the set of open hubs that together with the closed hub $i \in H_0^e$ form a potential hub arc for commodity $k \in K$. Updating DS by fixing the value of the computed variables and

removing the already satisfied constraints, we get the following *Phase II* subproblem:

$$\text{(DS-II)} \quad \text{Minimize} \quad \sum_{i \in H_0^e} (\Gamma_i b_i + \sum_{k \in K} \sum_{m \in M} u_{ik}^m) \tag{4.25}$$

$$\text{s.t.} \quad u_{ik}^m + u_{jk}^m + w_k^m (b_i + b_j) \geq \rho_{ij}^{km} \quad k \in K, m \in M, (i,j) \in A_{ke}^0 \tag{4.26}$$

$$u_{ik}^m + w_k^m b_i \geq \rho_{ii}^{km} \quad k \in K, m \in M, i \in H_0^e \tag{4.27}$$

$$u_{ik}^m, b_i \geq 0 \quad k \in K, m \in M, i \in H_0^e \tag{4.28}$$

where $\rho_{ij}^{km} = (r_k^m - \hat{C}_{ijk}) w_k^m - \alpha_k^m$ and

$$\rho_{ii}^{km} = \max\{\max_{j \in H_1^{ei}} \{(r_k^m - \hat{C}_{ijk}) w_k^m - u_{jk}^m - w_k^m b_j\}, (r_k^m - \hat{C}_{iik}) w_k^m\} - \alpha_k^m. \tag{4.29}$$

We propose two algorithms tailored to the special structure of the Phase II subproblem. First, we show that DS-II can be viewed as a set of LP-relaxations of maximum weighted matching problems for a given value of b_i for $i \in H_0^e$. In the second approach, we show that Phase II can be solved as a sequence of LP-relaxations of knapsack problems. In the following sections, we present some theoretical insights and discuss how to solve the two phases efficiently.

4.2.3.1 Solving the Phase I subproblem

We simplify DS-I (4.21)-(4.24) by showing that $u_{ik}^m = 0$, for $k \in K$, $m \in M$ and $i \in H_1^e$, in an optimal solution of DS-I.

Proposition 1. *There exists an optimal solution to DS-I, in which* $u_{ik}^m = 0$ *for* $k \in K$, $m \in M$ *and* $i \in H_1^e$.

Proof. For any arbitrary value of b (including the optimal solution) and for each $k \in K$ and $m \in M$, DS-I (4.21)-(4.24) can be decomposed into smaller problems of the following form:

$$\text{(DS-I}(km)\text{)} \quad \text{Minimize} \quad \alpha_k^m + \sum_{i \in H_1^e} u_{ik}^m \tag{4.30}$$

$$\text{s.t.} \quad \alpha_k^m + u_{ik}^m + u_{jk}^m \geq (r_k^m - \hat{C}_{ijk} - b_i - b_j) w_k^m \quad (i,j) \in A_{ke}^1 \tag{4.31}$$

$$\alpha_k^m + u_{ik}^m \geq (r_k^m - \hat{C}_{iik} - b_i) w_k^m \quad i \in H_1^e \tag{4.32}$$

$$\alpha_k^m, u_{ik}^m \geq 0 \quad i \in H_1^e. \tag{4.33}$$

Define $\beta_{ij} = (r_k^m - \hat{C}_{ijk} - b_i - b_j) w_k^m$ for $(i,j) \in A_{ke}^1$, and $\beta_{ii} = (r_k^m - \hat{C}_{iik} - b_i) w_k^m$ for $i \in H_1^e$. Let μ_{ij} and μ_{ii} be the dual variables associated with (4.31) and (4.32), respectively, for $(i,j) \in A_{ke}^1$ and $i \in H_1^e$. Dual of DS-I(km) can be formulated as:

$$\text{(Dual DS-I}(km)\text{)} \quad \text{Maximize} \quad \sum_{a \in \hat{A}_{ke}^1} \mu_a \beta_a \tag{4.34}$$

$$\text{s.t.} \quad \sum_{a \in \hat{A}_{ke}^1} \mu_a \leq 1 \tag{4.35}$$

$$\sum_{a \in \hat{A}_{ke}^1 : i \in a} \mu_a \leq 1 \quad i \in H_1^e \tag{4.36}$$

$$\mu_a \geq 0 \quad a \in \hat{A}_{ke}^1 \tag{4.37}$$

where $\hat{A}_{ke}^1 = A_{ke}^1 \cup \{(i,i) : i \in H_1^e\}$. Constraints (4.36) are clearly dominated by (4.35) for every $i \in H_1^e$, thus can be removed entirely from the dual problem. Accordingly, it is optimal to set the dual variables associated with (4.36) to zero, i.e. $u_{ik}^m = 0$ for $i \in H_1^e$. □

The outcome of Proposition 1 is that we can compute the optimal solution of DS-I(km) and its dual, by using the corollaries stated below:

Corollary 1. *In the optimal solution of DS-I(km),* $\alpha_k^m = \max_{a \in \hat{A}_{ke}^1} \{\beta_a, 0\}$.

Corollary 2. *Let* $a^* = \arg\max_{a \in \hat{A}_{ke}^1} \{\beta_a\}$, *where ties are broken arbitrarily. In the optimal solution of Dual DS-I(km),* $\mu_a = 0$ *for* $a \in \hat{A}_{ke}^1 \setminus \{a^*\}$. *If* $\beta_{a^*} > 0$, *then* $\mu_{a^*} = 1$, *otherwise* $\mu_{a^*} = 0$.

Consequently, DS-I can be solved using a nested cutting-plane algorithm, where b is the master problem variable and α is the subproblem variable, and the dual subproblems are solved using Corollary 2.

4.2.3.2 Solving the Phase II subproblem as maximum weighted matching problems

For a given vector $(b_i)_{i\in H_0^e}$, DS-II can be restated for each $k \in K$ and $m \in M$ as:

$$\text{(DS-II)}(km) \quad \text{Minimize} \quad \sum_{i\in H_0^e} u_{ik}^m \tag{4.38}$$

$$\text{s.t.} \quad u_{ik}^m + u_{jk}^m \geq \rho_{ij}^{km} - w_k^m(b_i + b_j) \quad (i,j) \in A_{ke}^0 \tag{4.39}$$

$$u_{ik}^m \geq \rho_{ii}^{km} - w_k^m b_i \quad i \in H_0^e \tag{4.40}$$

$$u_{ik}^m \geq 0 \quad i \in H_0^e. \tag{4.41}$$

Observe that (4.40) together with (4.41) serve as lower bounds on u_{ik}^m. Define $t_{ik}^m = u_{ik}^m - lb_{ik}^m$, where $lb_{ik}^m = \max\{\rho_{ii}^{km} - w_k^m b_i, 0\}$. DS-II($km$) can be restated as:

$$\text{(MWC)}(km) \quad \text{Minimize} \quad \sum_{i\in H_0^e} t_{ik}^m \tag{4.42}$$

$$\text{s.t.} \quad t_{ik}^m + t_{jk}^m \geq \beta_{ij}^{km} \quad (i,j) \in A_{ke}^0 \tag{4.43}$$

$$t_{ik}^m \geq 0 \quad i \in H_0^e, \tag{4.44}$$

where $\beta_{ij}^{km} = \rho_{ij}^{km} - w_k^m(b_i + b_j) - lb_{ik}^m - lb_{jk}^m$ for $(i,j) \in A_{ke}^0$. Assume without loss of generality that β_{ij}^{km} values are nonnegative, otherwise their corresponding constraints can be dropped. Problem (4.42)-(4.44) is commonly known as the *Minimum Weight Cover (MWC)* problem (see e.g. Galil 49), which is the dual of the LP-relaxation of the *Maximum Weighted Matching (MWM)* problem in the edge-weighted graph $G_{km} = (H_0^e, A_{ke}^0)$, where edges are weighted according to β_{ij}^{km}.

LP-relaxation of MWM can be formulated as

$$\text{(LP-MWM}(km)\text{)} \quad \text{Maximize} \quad \sum_{a\in A^0_{ke}} \mu^{km}_a \beta^{km}_a \tag{4.45}$$

$$\text{s.t.} \quad \sum_{a\in A^0_{ke}: i\in a} \mu^{km}_a \leq 1 \quad i \in H^e_0 \tag{4.46}$$

$$\mu^{km}_a \geq 0 \qquad a \in A^0_{ke}, \tag{4.47}$$

where μ^{km}_a is the dual variable associated with (4.43) and represents the extent to which edge $a \in A^0_{ke}$ is picked in the MWM. Unlike the LP-relaxation of the MWM problem in general graphs, LP-relaxation of the MWM problem in bipartite graphs (MWMB) guarantees integrality of the solutions. Hence, methods proposed for solving the MWMB can also be used for solving its LP-relaxation. Below, we show that the MWM problem (4.45)-(4.47) can be transformed into the MWMB problem in an equivalent sparse bipartite graph.

Define bipartite graph $G^B_{km} = (V_1, V_2, B)$, where $V_1 = \{v^1_i\}_{i\in H^e_0}$, $V_2 = \{v^2_i\}_{i\in H^e_0}$, and $B = \{(v^1_i, v^2_j) \in V_1 \times V_2 : (i,j) \in A^0_{ke}\}$. Let μ^B be a maximum weighted matching in G^B_{km}, and let

$$\mu^{km}_{ij} = \frac{1}{2}(\mu^B_{(v^1_i, v^2_j)} + \mu^B_{(v^1_j, v^2_i)}) \quad \forall (i,j) \in A^0_{ke}. \tag{4.48}$$

Proposition 2. *$\mu^{km} = (\mu^{km}_{ij})_{(i,j)\in A^0_{ke}}$ defined in (4.48) is optimal to LP-MWM(km) (4.45)-(4.47).*

Proof. μ^B being a matching in G^B_{km} requires

$$\sum_{j\in H^e_0:(i,j)\in A^0_{ke}} \mu^B_{(v^1_i, v^2_j)} \leq 1 \quad \forall v^1_i \in V_1 \text{ (or equivalently } i \in H^e_0) \tag{4.49}$$

$$\sum_{j\in H^e_0:(i,j)\in A^0_{ke}} \mu^B_{(v^1_j, v^2_i)} \leq 1 \quad \forall v^2_i \in V_2 \text{ (or equivalently } i \in H^e_0). \tag{4.50}$$

Summing (4.49) and (4.50) and dividing the resulting inequality by 2 yields

$$\sum_{j\in H^e_0:(i,j)\in A^0_{ke}} \frac{1}{2}(\mu^B_{(v^1_i, v^2_j)} + \mu^B_{(v^1_j, v^2_i)}) = \sum_{j\in H^e_0:(i,j)\in A^0_{ke}} \mu^{km}_{ij} \leq 1 \quad \forall i \in H^e_0, \tag{4.51}$$

which implies (4.46), hence μ^{km} defined in (4.48) is feasible for LP-MWM(km). Now we show that μ^{km} is also optimal for LP-MWM(km). By contradiction assume that μ^{km} is not optimal for LP-MWM(km), hence there exists a solution $\hat{\mu}^{km}$ with a strictly higher total weight. We show that this contradicts with optimality of μ^B. Define $\hat{\mu}^B$ as

$$\hat{\mu}^B_{(v_i^1,v_j^2)} = \hat{\mu}^B_{(v_j^1,v_i^2)} = \hat{\mu}^{km}_{ij} \quad \forall (i,j) \in A^0_{ke}. \tag{4.52}$$

$\hat{\mu}^B$ clearly satisfies (4.49) and (4.50), hence is a feasible matching for the bipartite graph G^B_{km}. Moreover, note that

$$\sum_{(i,j)\in A^0_{ke}} (\hat{\mu}^B_{(v_i^1,v_j^2)} + \hat{\mu}^B_{(v_j^1,v_i^2)}) = 2 \sum_{(i,j)\in A^0_{ke}} \hat{\mu}^{km}_{ij} > 2 \sum_{(i,j)\in A^0_{ke}} \mu^{km}_{ij} = \sum_{(i,j)\in A^0_{ke}} (\mu^B_{(v_i^1,v_j^2)} + \mu^B_{(v_j^1,v_i^2)}), \tag{4.53}$$

which implies that $\hat{\mu}^B$ is a better matching than μ^B, contradicting the optimality of μ^B. □

The optimal solution to MWC(km) (4.42)-(4.44) can be obtained in a similar manner. Let t^B be a minimum weight cover in G^B_{km}, and let

$$t^m_{ik} = \frac{1}{2}(t^B_{v_i^1} + t^B_{v_i^2}) \quad \forall i \in H^e_0. \tag{4.54}$$

Proposition 3. *$t^m_k = (t^m_{ik})_{i\in H^e_0}$ defined in (4.54) is optimal to MWC(km) (4.42)-(4.44).*

Proof. t^B being a cover in G^B_{km} implies that

$$t^B_{v_i^1} + t^B_{v_j^2} \geq \beta^{km}_{ij} \quad \forall (i,j) \in A^0_{ke} \tag{4.55}$$

$$t^B_{v_j^1} + t^B_{v_i^2} \geq \beta^{km}_{ji} \quad \forall (j,i) \in A^0_{ke}. \tag{4.56}$$

Since β^{km} is symmetric, summing (4.55) and (4.56) and dividing the resulting inequality by 2 implies (4.43); hence, t^m_k defined in (4.54) is feasible for MWC(km). Now, by contradiction assume that t^m_k is not optimal, hence there exists a solution $\hat{t}^m_k$ with a strictly lower cover weight. Define $\hat{t}^B$ as

$$\hat{t}^B_{v_i^1} = \hat{t}^B_{v_i^2} = \hat{t}^m_{ik} \quad \forall i \in H^e_0. \tag{4.57}$$

$\hat{t}^B$ clearly satisfies (4.55) and (4.56), and has a lower cover weight than t^B, contradicting the optimality of t^B. □

Propositions 2 and 3 indicate that it is enough to find a MWM in bipartite graph G^B_{km} to solve MWC(km) and LP-MWM(km).

Several algorithms have been proposed for solving the MWMB. (For a review on recent methods, see, e.g., Burkard et al. 21.) As a byproduct of solving the MWM problem (4.45)-(4.47), we eventually need to find the optimal value of (4.38)-(4.41). Hence, we adapt a primal-dual algorithm due to Galil [49], which can be solved in $O(an \log_{\lceil a/n+1 \rceil} n)$, where $n = |H^e_0|$ and $a = |A^0_{km}|$ are the number of nodes and edges, respectively.

The strength of the cut generated using this method depends highly on the value at which vector $(b_i)_{i \in H^e_0}$ is fixed. One could simply set b_i to zero for $i \in H^e_0$, or to the average of b_i in previous iterations of the BD algorithm; however, this will likely result in weak cuts. Moreover, note that larger values of b result in fewer positive β^{km}_a values, thus reducing the number of edges (i.e. $|A^0_{km}|$), and consequently the computational time for solving the MWM problems. In A.1, we explain how proper values of $(b_i)_{i \in H^e_0}$ can be calculated efficiently using a relaxation of DS-II.

4.2.3.3 Solving the Phase II subproblem as knapsack problems

At each iteration of the BD algorithm, we obtain a solution y with a set of open/closed hubs. The open hubs are potentially the ones with desirable properties; e.g., with high capacity, low installation cost, and/or profitable flows through these hubs. Hence, the most frequently opened hubs in the preceding iterations of BD are more likely to be opened again in the subsequent iterations. To strengthen the cut, we must prioritize minimizing the coefficients of these hubs over the hubs that are less likely to be open. In light of this observation, solving DS-II at iteration e, we sequentially minimize the coefficient of y_i for one closed hub $i \in H^e_0$ at a time, in a particular order of H^e_0, rather than minimizing the summation of coefficients of all closed hubs simultaneously.

Let $O_i^e = \sum_{h:h\leq e} y_i^h$ denote the number of times that hub i has been opened prior to or at iteration e of BD. A higher value of O_i^e implies a higher chance for hub i to be open at iteration $e+1$. We first solve DS-II (4.25)-(4.28) as if $i = \arg\max_{j\in H_0^e}\{O_j^e\}$ is the only hub in H_0^e:

$$\text{(DS-II}(i)\text{)} \quad \text{Minimize} \quad \Gamma_i b_i + \sum_{k\in K}\sum_{m\in M} u_{ik}^m \tag{4.58}$$

$$\text{s.t.} \quad u_{ik}^m + w_k^m b_i \geq \rho_{ii}^{km} \quad k\in K, m\in M \tag{4.59}$$

$$u_{ik}^m, b_i \geq 0 \quad k\in K, m\in M. \tag{4.60}$$

Note that since i is assumed to be the only hub in H_0^e, constraints (4.26) do not appear in this model, but will be satisfied by the next closed hubs in the sequence by means of updating the respective ρ_{ii}^{km} values using (4.29).

Upon solving DS-II(i), we obtain the values of all dual variables associated with hub i (i.e., u_{ik}^m and b_i). Consequently, we fix these values, add i to H_1^e and remove i from H_0^e. We continue this procedure with the next closed hub $i = \arg\max_{j\in H_0^e}\{O_j^e\}$ with ρ_{ii}^{km} values updated according to the new sets H_1^e and H_1^{ei}. We replicate this procedure until values of all dual variables are computed; i.e., until H_0^e becomes empty. An overview of this procedure is presented in Algorithm 2.

Algorithm 2 Solving DS-II via sequential knapsack problems

1: **while** $(H_0^e \neq \emptyset)$ **do**
2: $\quad i \leftarrow \arg\max_{j\in H_0^e}\{O_j^e\}$
3: $\quad$ Compute ρ_{ii}^{km} values using (4.29) for the selected i and each $k\in K$ and $m\in M$ with respect to the updated H_1^e and H_1^{ei}.
4: $\quad$ **SOLVE** DS-II(i) and obtain b_i and u_{ik}^m for $k\in K$ and $m\in M$.
5: $\quad H_0^e \leftarrow H_0^e \setminus \{i\}$
6: $\quad H_1^e \leftarrow H_1^e \cup \{i\}$
7: **end while**

Observe that DS-II(i) is the dual of the LP-relaxation of a knapsack problem (KP) with knapsack capacity Γ_i, and items $(k,m) \in K \times M$ with weight w_k^m and profit ρ_{ii}^{km}, as formulated in (4.61)-(4.63):

$$\text{(LP-KP}(i)) \quad \text{Maximize} \quad \sum_{(k,m)\in K\times M} \rho_{ii}^{km}\mu_k^m \tag{4.61}$$

$$\text{s.t.} \quad \sum_{(k,m)\in K\times M} w_k^m \mu_k^m \leq \Gamma_i \tag{4.62}$$

$$0 \leq \mu_k^m \leq 1 \qquad (k,m) \in K \times M, \tag{4.63}$$

where μ_k^m is the dual variable associated with (4.59), and represents the extent to which item $(k,m) \in K \times M$ is picked. Note that the items with a non-positive profit (i.e., $\rho_{ii}^{km} \leq 0$) can be discarded from the problem. Dantzig [42] showed that the optimal solution to this problem can be found by filling the knapsack in a non-increasing order of profit-to-weight ratio ρ_{ii}^{km}/w_k^m of the items, until we reach the first item that does not fit into the knapsack. This item is called the break item $(\bar{k},\bar{m})$, which is partially picked according to the residual capacity. Using the complementary-slackness conditions, it can be verified that the optimal value of b_i is the profit-to-weight ratio of the break item; i.e.,

$$b_i = \rho_{ii}^{\bar{k}\bar{m}}/w_{\bar{k}}^{\bar{m}}. \tag{4.64}$$

Moreover, using (4.59) and (4.60), the optimal value of u_{ik}^m can be calculated by setting $u_{ik}^m = \max\{\rho_{ii}^{km} - w_k^m b_i, 0\}$. Balas and Zemel [14] showed that the LP-relaxation of knapsack problem can be solved in $O(n)$, where $n = |K||M|$, by finding the break item as a weighted median, rather than by explicitly sorting the items. This implies that the optimal values of b and u can be found in the same time bound.

4.3 Computational Experiments

We use the well-known Australia Post (AP) dataset to test our models and algorithms. AP dataset contains postal service data of 200 nodes in Australia and it is the most

commonly used dataset in hub location literature (Ernst and Krishnamoorthy 46). The distances (d_{ij}) and the postal flow between pairs of nodes (w_k) are provided in OR Library, and a computer code is presented to generate smaller subsets of the data by grouping cities (Beasley 15). We assume that the demand of commodities are segmented into 3 classes; i.e., $|M| = 3$, where $w_k^1 = 0.2w_k$, $w_k^2 = 0.3w_k$, and $w_k^3 = 0.5w_k$. Motivated from the postal delivery applications, where the price of sending a parcel depends on its size and the distance between the origin-destination, and also considering revenue elasticity of demand, the revenue per unit demand is taken to be dependent on the distance, class, and the amount of commodity to be shipped. Hence, for the revenue from commodity $k \in K$ of class $m \in M$, we generate random values as $r_k^m = \gamma^m \frac{c_k}{w_k^m}$, where $\gamma^1 \sim U[50, 60]$, $\gamma^2 \sim U[40, 50]$, and $\gamma^3 \sim U[30, 40]$. Collection, transfer, and distribution costs per unit are taken as $\chi = 2$, $\alpha = 0.75$, and $\delta = 3$ as defined in the AP dataset (Beasley 15). We test instances with $|N| \in \{10, 20, 25, 40, 50, 75, 100, 200\}$.

There are two different sets for installation costs and capacities of hubs available on the AP dataset referred to as loose and tight. The opening cost of hubs in the instances with tight (T) installation costs is larger than those with loose (L) installation costs. In contrast, instances with tight (T) capacities have smaller available capacities compared to the instances with loose (L) capacities. Hence, there are four instances for a given node size corresponding to different combinations of installation costs and capacities. We denote each instance as $nf\Gamma$ where n is the instance size, f is the installation costs, and Γ is the capacity.

Computational experiments were carried out on a workstation that contains: Intel Core i7-3930K 2.61GHz CPU, and 39 GB of RAM. The algorithms were coded in $C\#$ and the time limit was set to 15 hours. The master problems of all versions of the Benders decomposition algorithms as well as the Phase I subproblems were solved using the callable library of CPLEX 12.7. We used $p_Q = 75\%$ and $n_Q = 6$ in all our tests, which are the best values for the corresponding parameters based on the results provided in Appendix A.2.

We first evaluate the performance and effectiveness of the algorithms proposed in Sec-

tion 4.2 for the MILP model. We implemented two different versions of Algorithm 1 referred to as BD1 and BD2, corresponding to different solution strategies of Phase II. In BD1, Phase II is solved as LP-relaxations of maximum weighted matching problem, whereas in BD2, Phase II is solved as LP-relaxations of knapsack problem. For comparison, we also implemented Pareto-optimal cuts (PO), the best known cuts from the literature, to solve our subproblems. We use the two reduction tests as described in Section 4.2.2 to eliminate candidate hubs within all of the three algorithms: PO, BD1, and BD2.

The detailed results of the comparison between these Benders algorithms using the AP instances are provided in Table 4.1. The first column represents the name and size of the instance. The next four columns labeled "Total time (sec)" present the computational time of instances (in seconds) obtained from solving the problems to optimality by using CPLEX, PO, BD1, and BD2, respectively. The next three columns labeled "Iterations" provide the required number of iterations for the convergence of the algorithms PO, BD1, and BD2, respectively. The columns labeled "% hubs elim." present the percentage of the total candidate hubs eliminated by algorithms PO, BD1, and BD2, respectively. The last two columns labeled "Optimal solution" indicate the maximum net profit and the locations of hub nodes, respectively, for the optimal solution found for each of the considered instances. Whenever an algorithm is not able to solve an instance within the time limit (15 hours of CPU time) to optimality, we write "Time" in the corresponding entry of the table. If an algorithm runs out of memory, we write "Mem".

Our goal of presenting the results of PO in Table 4.1 is to compare the strength of the cuts generated by BD1 and BD2 with this method. We use the decomposition scheme proposed by Contreras et al. [37] for solving the Pareto-optimal subproblem. In this method, at iteration e of Algorithm 1, by fixing the value of $(b_i)_{i\in H_1^e}$ at the optimal values obtained from the original subproblem, and by setting $(b_i)_{i\in H_0^e}$ to zero, they decompose the PO subproblem into $|K|$ (here $|K||M|$) independent problems. These problems can be solved using an LP solver, however, as Contreras et al. [35] argue, for computational tractability, they sacrifice the strength of the cuts by solving the resulting problems via an approximation technique. Since our goal of implementing PO method is to compare the strength

Table 4.1: Comparison of Benders reformulations and CPLEX with the AP dataset.

	Total time (sec)				Iterations			% hubs elim.			Optimal solution	
$\|N\|$	CPLEX	PO	BD1	BD2	PO	BD1	BD2	PO	BD1	BD2	Profit	Open hubs
10LL	1.02	1.37	0.13	0.01	7	4	4	50.0	60.0	60.0	20,417	5,6,9,10
10LT	0.89	0.94	0.03	0.01	5	4	4	60.0	80.0	80.0	3,336	5
10TL	1.00	0.81	0.03	0.07	9	6	6	50.0	60.0	60.0	13,488	5,9
10TT	1.16	0.26	0.03	0.03	4	3	3	80.0	90.0	90.0	2,682	5
20LL	9.64	35.64	1.70	2.11	51	11	11	70.0	65.0	80.0	100,443	7,9,10,19
20LT	11.38	45.26	0.97	1.34	60	7	7	65.0	65.0	65.0	57,139	5,10,12,14,19
20TL	10.34	21.52	0.84	0.99	37	9	9	75.0	80.0	85.0	49,559	5,7,10
20TT	6.17	4.51	0.22	0.29	11	3	3	70.0	95.0	95.0	10,135	10
25LL	15.42	68.03	7.91	6.31	48	18	18	76.0	72.0	72.0	125,390	7,14,17,23
25LT	12.82	157.51	3.27	2.35	93	7	7	68.0	72.0	72.0	88,022	6,9,10,12,14,25
25TL	14.21	53.80	2.12	2.09	40	9	9	76.0	72.0	72.0	76,933	6,9,14,23
25TT	12.30	100.76	2.02	1.92	71	10	10	80.0	76.0	76.0	35,121	6,10,14,25
40LL	79.23	261.31	52.57	42.47	48	64	58	70.0	82.5	85.0	76,995	12,22,26,29
40LT	83.18	623.02	39.58	28.93	66	42	38	82.5	82.5	82.5	66,860	12,14,26,29,30,38
40TL	41.25	71.96	9.53	5.26	13	14	11	85.0	82.5	82.5	62,960	14,19,29
40TT	39.21	209.68	6.80	5.49	24	11	11	87.5	82.5	90.0	49,938	14,19,25,38
50LL	142.18	466.78	64.34	39.92	49	42	38	76.0	88.0	86.0	73,054	15,28,33,35
50LT	138.98	666.23	33.69	26.67	24	19	17	76.0	86.0	82.0	68,904	6,26,32,46
50TL	115.73	188.11	11.01	8.06	14	11	13	88.0	88.0	88.0	54,009	3,26,45
50TT	105.01	303.43	7.42	5.23	20	7	7	88.0	88.0	92.0	45,506	17,26,48
75LL	Mem	8,979.00	525.81	387.66	111	105	88	85.3	89.3	86.7	142,551	14,23,35,37,56
75LT	Mem	8,327.27	137.00	87.58	73	23	15	90.7	92.0	90.7	110,194	14,25,32,35,38,59
75TL	Mem	3,918.76	69.85	71.12	26	13	13	92.0	92.0	96.0	89,562	14,35,37
75TT	Mem	4,986.99	42.92	33.84	36	12	11	93.3	90.7	90.7	81,697	25,32,38,59
100LL	Mem	32,872.67	904.00	665.94	58	53	54	94.0	94.0	94.0	1,777,224	29,55,64,73
100LT	Mem	Time	1,078.75	684.20	-	63	56	-	92.0	92.0	1,775,001	29,44,54,68,96
100TL	Mem	4,236.89	87.64	76.50	13	12	13	94.0	93.0	95.0	1,724,826	5,52,95
100TT	Mem	6,743.21	156.57	159.85	13	13	13	95.0	93.0	93.0	1,712,163	5,34,44,52,95
200LL	Mem	Time	11,435.00	6,430.31	-	40	39	-	96.0	96.0	1,102,073	43,95,159
200LT	Mem	Time	12,404.83	7,120.03	-	53	46	-	95.0	95.5	1,087,014	41,96,168,171
200TL	Mem	Time	953.94	879.52	-	12	12	-	97.5	97.5	1,068,431	54,95,186
200TT	Mem	Time	783.13	673.33	-	6	6	-	97.5	97.5	1,055,760	52,54,115,168,186

of the resulting cuts with our proposed methods, after decomposing the PO subproblem into $|K||M|$ independent problems, rather than employing the approximation technique, we solve the dual of the resulting problems using the CPLEX LP solver. Note that the number of iterations cannot be reduced by the approximation algorithm, hence the number of iterations of PO as presented in Table 4.1 provides a lower bound on the number of iterations that we would obtain using the approximation technique proposed by Contreras et al. [35].

Table 4.1 shows that both algorithms BD1 and BD2 outperform CPLEX in terms of computational time and the number of instances solved to optimality. Additionally, the results of Table 1 clearly indicate that our algorithms (BD1 and BD2) outperform PO, with the only exception of instance 40LL.

Each of the Benders algorithms proposed in this thesis is able to solve all considered instances to optimality within an hour of CPU time, with the exception of instances 200LL and 200LT, which take approximately 3.3 hours for BD1 and 1.9 hours for BD2, respectively. The columns % hubs elim. show that a large percentage of candidate hubs can be eliminated by variable fixing. The columns Total time (sec) and Iterations indicate that the convergence of the Benders algorithm is improved by solving Phase II as LP-relaxations of knapsack problem, especially for the larger size instances. This implies that BD2 outperforms BD1; hence, we use BD2 for the rest of the computational experiments.

Table 4.1 also shows the locations of installed hubs in optimal solutions, where the optimal number of hubs to locate varies between one and six. It seems that, in these particular instances, the number of installed hubs does not depend on the size of the instance; it is rather more dependent on hub installation costs and capacities. For example, in the instances with tight installation costs and loose capacities, the problem tends to result in locating fewer hubs.

In Table 4.2, we observe the percentages of satisfied demand from different market segments. The averages for each demand class are calculated over instances from Table 4.1 with the same type of installation costs and capacities. The last column provides the aver-

Table 4.2: Percentage of total demand satisfied for each demand class.

Instance type	Demand class			Average
	1	2	3	
LL	98.32%	94.58%	71.74%	88.21%
LT	98.32%	87.95%	55.83%	80.70%
TL	98.32%	93.45%	59.99%	83.92%
TT	93.00%	75.45%	39.64%	69.37%

age percentages of total satisfied demand. Among the three demand classes, the first class is the one with the highest percentages of satisfied demand, as serving this class of demand yields the highest revenue. On the other hand, for the instances with the same configuration of hub installation costs and capacities, the third demand class, having the least revenues, has the least percentages of satisfied demand as expected. Moreover, instances with loose capacities (LL and TL) result in higher percentages on average compared to the instances with tight capacities (LT and TT).

To better understand the performance of the proposed algorithms from a computational point of view, we also present computational results with larger-size instances introduced by Contreras et al. [35], and later extended by Contreras et al. [37]. There are three different sets of instances, referred as Set I, Set II, and Set III, which are constructed by considering three different levels of magnitude for the amount of flow originating at a given node: low-level (LL) nodes, medium-level (ML) nodes, and high-level (HL) nodes. The total outgoing flow of LL, ML and HL nodes are obtained from the interval [1,10], [10,100], and [100,1000], respectively. Capacities of hubs are generated by using the formula provided in Ebery et al. [44] in which parameter ρ is taken to be 0.5 and 1.5 for the loose (L) and tight (T) types of capacities, respectively. The other sets of parameters are as described in the beginning of Section 4.3. For Sets I, II, and III, we test instances with $|N| \in \{50, 100, 150, 200, 250, 300\}$. The detailed results are provided in Table 4.3 where the column titles have the same meanings as in the previous table.

Table 4.3: Computational results using BD2 with Sets I, II, and III instances.

Instance	Total time (sec)	Iterations	% hubs elim.	Profit	#open hubs
Set I					
50L	22.30	31	88.0	21,765	6
50T	15.49	19	90.0	16,943	4
100L	45.43	36	94.0	30,273	4
100T	50.18	23	95.0	30,215	4
150L	648.31	65	93.3	77,667	7
150T	523.05	25	94.7	74,952	6
200L	1,734.22	30	96.0	155,097	8
200T	3,160.84	33	95.5	144,874	7
250L	19,441.16	69	96.0	325,657	9
250T	4,861.76	37	97.2	181,027	5
300L	20,132.06	75	96.0	388,322	11
300T	14,885.61	52	97.7	188,944	6
Set II					
50L	64.29	35	88.0	85,327	6
50T	50.78	27	86.0	60,174	5
100L	224.41	48	92.0	201,451	7
100T	448.40	58	90.0	199,819	8
150L	3,785.39	121	91.3	458,915	12
150T	2,904.36	38	92.7	438,771	9
200L	1,442.94	25	95.0	236,247	8
200T	3,556.37	21	94.5	216,241	9
250L	10,414.33	62	95.2	437,819	11
250T	5,589.51	47	96.0	354,688	10
300L	17,367.18	68	96.0	1,532,224	10
300T	16,399.61	49	97.0	986,373	7
Set III					
50L	32.50	37	88.0	19,037	5
50T	19.93	32	90.0	16,353	5
100L	736.18	21	88.0	511,879	9
100T	530.51	16	91.0	39,672	7
150L	5,945.02	28	91.3	129,155	12
150T	5,327.03	27	92.7	964,137	9
200L	7,920.45	49	90.0	144,503	15
200T	6,738.52	45	93.5	103,987	11
250L	12,166.41	41	92.8	992,585	16
250T	11,057.31	32	95.2	710,562	11
300L	22,565.61	39	93.3	1,004,591	17
300T	18,349.47	34	95.0	903,773	14

All of the instances presented in Table 4.3 from Sets I, II, and III are solved to optimality. The most time-consuming instance in Sets I, II, and III took around 6, 5, and 6 hours, respectively, to solve to optimality. The averages of the computational times reported in Table 4.3 for the Sets I, II, and III are 1.5, 1.4, and 2.1 hours, respectively.

Table 4.4: Computational results of Sets I and II instances with $|N| \in \{350, 400, 500\}$.

Instance	Total time (sec)	Iterations	% hubs elim.	Profit	#open hubs
Set I					
350L	28,118.49	19	96.9	188,759	11
350T	21,881.74	15	97.7	147,501	7
400L	43,942.63	16	97.0	248,458	12
400T	35,763.21	14	97.5	186,239	9
500L	83,149.54	15	95.4	1,137,769	23
500T	54,731.43	11	97.0	821,439	14
Set II					
350L	31,025.56	31	95.7	682,514	15
350T	23,149.81	26	96.6	530,697	11
400L	40,209.23	29	95.3	852,627	19
400T	33,195.23	22	95.3	671,734	13
500L	Time	17	71.8	965,113	25
500T	82,296.42	14	96.6	583,129	17

Lastly, we present additional runs from Sets I and II with $|N| \in \{350, 400, 500\}$ to analyze the limit of our algorithm. We have extended the CPU time limit to 24 hours for these instances. The results are presented in Table 4.4. Our algorithm is able to solve all of the instances to optimality within the time limit, except for the instance 500L in Set II. That particular instance resulted in an optimality gap of 2.52%. These results further confirm the efficiency and robustness of the BD2 algorithm when considering more challenging and larger-size instances.

4.4 Conclusion

In this chapter, we defined the profit maximizing hub location problem with capacity allocation by incorporating revenue management decisions, and embedding more realistic and challenging capacity constraints for hubs. We presented a strong path-based mixed integer programming formulation of the problem. We described two Benders-based algorithms to solve large-scale instances of the problem by developing a new decomposition methodology for solving the Benders subproblems. We proved that the subproblems can be viewed as a set of LP-relaxations of maximum weighted matching problems (BD1), or as a series of LP-relaxations of knapsack problems (BD2). We further enhanced the algorithms by incorporating improved variable fixing techniques.

We performed extensive computational experiments on the well-known AP dataset, and also on larger-size instances from the literature, to analyze the performance of the proposed algorithms. In view of our computational results, both algorithms outperform the best known cuts (Pareto-optimal cuts), in terms of computational efficiency and also quality. The results further show that BD2 outperforms BD1 particularly on larger instances. BD2 succeeded to optimally solve instances with up to 500 nodes and 750,000 commodities of different demand classes. These results clearly confirm the efficiency and robustness of our algorithms.

Chapter 5

Profit Maximizing Hub Location Problems Under Uncertainty

Profit maximizing hub location problems are network design problems involving strategic decisions. In strategic planning, decisions need to be held for a considerable time frame. During this time, in real world, many unpredictable causes may lead to changes in operating conditions. For example, the amount of demand may be greater or smaller than its expected value. Changes may also occur in the amount of revenue obtained from the satisfied demand due to some unpredictable variations in a competitive environment. In these conditions, solving a deterministic model may result in wrong and costly decisions. Hence, taking uncertainty into account in the decision process is a necessity. To provide more reliable models, we consider two typical sources of uncertainty in profit maximizing HLPs with capacity allocation. We assume that demand of commodities and revenues are not precisely known and the optimal decisions have to be anticipated under uncertainty.

Optimization under uncertainty generally consists of two streams of research: stochastic and robust optimization. In stochastic optimization, there are some known probability distributions describing the behavior of uncertain parameters and these distributions can be used to optimize the expected value of the objective function. In robust optimization, on

the other hand, no probabilistic information is available for the uncertain parameters. In this case, uncertainty can be described by using a finite set of scenarios or can be modeled assuming that the values of the uncertain parameters can change within predefined intervals (for more information on robust optimization see, e.g., Bertsimas and Sim [18], Ben-Tal et al. [16], Bertsimas et al. [17], Gabrel et al. [48], and Correia and Saldanha-da Gama [40]).

In this chapter, we consider two sources of uncertainty: demand and revenue. Because of the availability of historical data, we assume that demand is described by a known probability distribution. On the other hand, since revenue might be affected by unpredictable external sources (e.g., economical conditions or competition) and historical data cannot effectively describe such variations, it may not make sense to assume a probability distribution for the revenue describing its behavior. Hence, we use robust optimization techniques to incorporate uncertain revenues into the problem by considering both interval representation and discrete scenarios. Modeling profit maximizing hub location problems using both robust and stochastic optimization techniques surely brings on extra computational challenges, yet we believe this is a much more realistic problem setting with respect to information availability.

We first incorporate demand uncertainty into the problem and develop a two-stage stochastic program considering stochastic demand. The first stage decision is the location of hubs, while the assignment of demand nodes to hubs, optimal routes of flows, and capacity allocation decisions are made in the second stage. We then model the robust-stochastic problem when there is uncertainty associated with revenues under stochastic demand.

To incorporate uncertain revenues into the problem, we first propose a robust-stochastic model by taking interval uncertainty into account for revenues using the max-min criterion with a budget of uncertainty. The max-min criterion maximizes profit under the worst case scenario. Then, we propose a min-max regret stochastic model by considering a finite set of scenarios that describe uncertainty associated with the revenues. With the

min-max regret criterion, the decision maker decides based on the regret (or opportunity loss) from not selecting the best strategy. Both max-min and min-max regret criteria fit a conservative decision maker approach (Aissi et al. [2]). We model both approaches to empirically show the level of robustness and conservatism of each metric in addressing the uncertainty associated with revenues.

We develop exact algorithms based on Benders decomposition coupled with a sample average approximation (SAA) scheme to solve the problems with a continuous demand distribution and an infinite number of scenarios. Inspired by the repetitive nature of SAA, we additionally propose novel acceleration techniques to enhance the convergence of the algorithms. We assess the efficiency of the proposed algorithms through extensive computational experiments. Furthermore, we investigate the effects of uncertainty under different settings on optimal hub networks and empirically evaluate the quality of the solutions obtained from different modeling approaches under various parameter settings.

The outline of this chapter is organized as follows. In Section 5.1, we define the problem and introduce the notation. In Section 5.2, we present a two-stage stochastic program of the problem, propose an SAA algorithm coupled with Benders decomposition, and provide computational experiments. Section 5.3 presents mathematical formulations for the robust-stochastic versions of the problem, solution schemes for these models, and computational experiments to evaluate the quality of the solutions obtained from different modeling approaches. Finally, Section 5.4 provides concluding remarks.

5.1 Problem Definition

We consider a directed complete graph $G = (N, A)$, where N is the set of nodes and A is the set of arcs representing possible direct links between the nodes. We allow the arc set A to have both an ordered set and a self-loop by defining $\{a_1, a_2\}$ if $|a| = 2$, and $\{a_1\}$ if $|a| = 1$, respectively. We denote the set of potential hub locations by $H \subseteq N$ and assume that there is an installation cost as well as an available capacity for a hub located at node

$i \in H$ denoted by f_i and Γ_i, respectively.

There is demand for a set of commodities denoted by $K \subseteq N \times N$. Each $k \in K$ indicates an O-D pair whose origin and destination points belong to N. The demand for commodities are stochastic and segmented into M classes. Let $w_k^m(\xi)$ be the random variables representing the future demand for commodity $k \in K$ of class $m \in M$ to be routed from origin $o(k) \in N$ to destination $d(k) \in N$. We assume that demands of different commodities are independent random variables associated with a known probability distribution, while different demand classes of each commodity are dependent and correlated. A per unit revenue, denoted by r_k^m, is obtained from satisfying a unit commodity $k \in K$ of class $m \in M$.

Each arc has a transportation cost defined as $c_{ij} = \gamma d_{ij}$, where d_{ij} represents the distance between nodes $i \in N$ and $j \in N$ and γ is the resource cost per unit distance. We assume that distances satisfy the triangle inequality, and thus every path between an origin $o(k)$ and a destination $d(k)$ will contain at least one and at most two hubs represented by $(o(k), i, j, d(k))$, where $(i, j) \in H \times H$ is the ordered pair of hubs. Accordingly, the unit transportation cost of routing commodity k along path $(o(k), i, j, d(k))$ is expressed as $C_{ijk} = \chi c_{o(k)i} + \alpha c_{ij} + \delta c_{jd(k)}$, where χ, α, δ are the collection, transfer, and distribution costs along the path. To reflect economies of scale between hubs, we assume that $\alpha < \chi$ and $\alpha < \delta$.

Note that in any optimal solution, every commodity $k \in K$ uses at most one of the paths $o(k), i, j, d(k)$ and $o(k), j, i, d(k)$; the one with the lower transportation cost. This property can be used to reduce the size of the mathematical formulations. Accordingly, we replace C_{ijk} with $\hat{C}_{ijk} = \min\{C_{ijk}, C_{jik}\}$, and reduce the set of candidate hub arcs for commodity $k \in K$ to A_k by defining $A_k = \{(i, j) \in A : i \leq j, \hat{C}_{ijk} \leq \min\{C_{iik}, C_{jjk}\}\}$.

5.2 Stochastic Model

We now model the problem with uncertain demand assuming that the uncertainty associated with demands is described by a known probability distribution. If E_ξ denotes the expectation with respect to ξ, and Ξ the support of ξ, then the *profit maximizing hub location problem with capacity allocation and stochastic demand* can be modeled as:

$$\text{Maximize} \quad E_\xi\Big[\sum_{m\in M}\sum_{k\in K}\sum_{a\in A_k}(r_k^m-\hat{C}_{ak})w_k^m(\xi)x_{ak}^m(\xi)\Big]-\sum_{i\in H}f_iy_i \tag{5.1}$$

$$\text{s.t.} \quad \sum_{a\in A_k}x_{ak}^m(\xi)\le 1 \qquad k\in K, m\in M, \xi\in\Xi \tag{5.2}$$

$$\sum_{a\in A_k:i\in a}x_{ak}^m(\xi)\le y_i \qquad i\in H, k\in K, m\in M, \xi\in\Xi \tag{5.3}$$

$$\sum_{m\in M}\sum_{k\in K}\sum_{a\in A_k:i\in a}w_k^m(\xi)x_{ak}^m(\xi)\le \Gamma_i y_i \qquad i\in H, \xi\in\Xi \tag{5.4}$$

$$x_{ak}^m(\xi)\ge 0 \qquad k\in K, m\in M, a\in A_k, \xi\in\Xi \tag{5.5}$$

$$y_i\in\{0,1\} \qquad i\in H. \tag{5.6}$$

The above model forms a two-stage stochastic program. The first stage problem corresponds to strategic hub location decisions. These long-term decisions will not be influenced by demand variations, accordingly, the variables y_i become known in this stage. However, the allocation decisions and the optimal routes of flows through the network, as well as the decision on how much of total capacity should be allocated to demand from different classes, do vary in response to the change of demand and, thus, are influenced by the stochastic demand. These tactical decisions are determined in the second stage depending on the particular realization of the random vector $\xi\in\Xi$. Accordingly, the variables x_{ak}^m become known in the second stage.

The objective function (5.1) contains a deterministic term which calculates the installation cost of the hubs, and the expectation of the second stage objective which calculates the expected value of revenue and transportation cost. Constraints (5.2) ensure that if the demand of commodity is to be satisfied, the flow should be routed via hubs. Constraints (5.3) prevent the demand of commodities to be satisfied through non-hubs nodes. Constraints (5.4) model capacity restriction on the total incoming flow at a hub. Note that constraints (5.2) and (5.4) imply constraints (5.3); however, we keep these in the model to have a stronger formulation. Finally, constraints (5.5)-(5.6) represent the non-negative and binary variables.

5.2.1 Solution scheme for the stochastic model

In this section, we present an algorithm to solve the profit maximizing hub location problem with capacity allocation and stochastic demand. The methodology integrates a sampling technique, named as *sample average approximation* (SAA) algorithm (the reader may refer to Shapiro and Homem-de Mello [90], Mak et al. [63], Kleywegt et al. [57]) with the Benders decomposition algorithm detailed in Sections 5.2.1.1 and 5.2.1.2.

5.2.1.1 Sample Average Approximation

SAA is a Monte Carlo simulation based approach to stochastic discrete optimization problems. The main idea of this method is to reduce the size of the problem by generating a random sample and approximating the expected value of the corresponding sample average function. The sample average optimization problem is then solved (using the BD algorithm in our case), and the procedure is repeated. The SAA scheme has previously been applied to stochastic supply chain design as well as hub location problems with a large number of scenarios (see, e.g., Santoso et al. [85], Schütz et al. [88], Contreras et al. [36], and Adulyasak et al. [1]).

The main challenge in solving the stochastic problem (5.1)-(5.6) is the evaluation of the

expected value of the objective function (Kleywegt et al. [57]). To deal with this problem, we use a SAA scheme in which a random sample of realizations of the random vector $n \in \mathcal{N}$ is generated, and the second-stage expectation

$$E_{\xi}\Big[\sum_{m\in M}\sum_{k\in K}\sum_{a\in A_k}(r_k^m - \hat{C}_{ak})w_k^m(\xi)x_{ak}^m(\xi)\Big]$$

is approximated by the sample average function

$$\tfrac{1}{|\mathcal{N}|}\sum_{n\in\mathcal{N}}\sum_{m\in M}\sum_{k\in K}\sum_{a\in A_k}(r_k^m - \hat{C}_{ak})w_k^{mn}x_{ak}^{mn},$$

where w_k^{mn} and x_{ak}^{mn} denote the amount of commodity $k \in K$ of class $m \in M$ to be shipped from origin $o(k) \in N$ to destination $d(k) \in N$ under sample $n \in \mathcal{N}$, and the fraction of commodity $k \in K$ of class $m \in M$ that is satisfied through a hub link $a \in A_k$ under scenario $n \in \mathcal{N}$, respectively. Accordingly, the approximated form of the stochastic problem by the SAA algorithm is modeled as:

$$\text{Maximize} \quad \frac{1}{|\mathcal{N}|}\sum_{n\in\mathcal{N}}\sum_{m\in M}\sum_{k\in K}\sum_{a\in A_k}(r_k^m - \hat{C}_{ak})w_k^{mn}x_{ak}^{mn} - \sum_{i\in H} f_i y_i \tag{5.7}$$

$$\text{s.t.} \quad \sum_{a\in A_k} x_{ak}^{mn} \le 1 \qquad k \in K, m \in M, n \in \mathcal{N} \tag{5.8}$$

$$\sum_{a\in A_k: i\in a} x_{ak}^{mn} \le y_i \qquad i \in H, k \in K, m \in M, n \in \mathcal{N} \tag{5.9}$$

$$\sum_{m\in M}\sum_{k\in K}\sum_{a\in A_k: i\in a} w_k^m x_{ak}^{mn} \le \Gamma_i y_i \qquad i \in H, n \in \mathcal{N} \tag{5.10}$$

$$x_{ak}^{mn} \ge 0 \qquad k \in K, m \in M, a \in A_k, n \in \mathcal{N} \tag{5.11}$$

$$y_i \in \{0,1\} \qquad i \in H. \tag{5.12}$$

Hereafter, we use the above approximated model (5.7)-(5.12) as the mathematical model for the profit maximizing hub location problem with capacity allocation and stochastic demand.

The optimal solution and the optimal value of the SAA problem (5.7)-(5.12) converge with probability one to their true counterpart (5.1)-(5.6) as the sample size increases (Kleywegt et al. [57]). Assuming that the SAA problem is solved within an optimality gap of $\delta > 0$, and by letting $\varepsilon > \delta$ and $\alpha \in (0, 1)$, then a sample size of

$$|\mathcal{N}| \geq \frac{3\sigma_{max}^2}{(\varepsilon - \delta)^2} \log(\frac{|Y|}{\alpha}) \tag{5.13}$$

guarantees that the SAA solution is an ε-optimal solution to the true problem with a probability of at least $1 - \alpha$, where σ_{max}^2 is the maximal variance of certain function differences (the readers may refer to Kleywegt et al. [57] for details).

To choose $\mathcal{N}$ in practice, one should take into account the trade-off between the quality of the solution obtained from the SAA problem and the computational time required to solve it. Hence, it can be more efficient to solve the SAA problem (5.7)-(5.12) with independent samples repeatedly rather than increasing the sample size $\mathcal{N}$. We now describe our procedure:

1. Generate $\mathcal{M}$ independent samples each of size $\mathcal{N}$; i.e., $\xi_j^1, \ldots, \xi_j^{|\mathcal{N}|}$, for $j \in \mathcal{M}$ and solve the corresponding SAA problem (5.7)-(5.12) for each sample $\mathcal{N}_j$ to optimality employing the BD algorithm detailed in Section 5.2.1.2. Let $\mathcal{V}^{\mathcal{N}_j}$ and $\hat{y}^{\mathcal{N}_j}$, $j \in \mathcal{M}$, be the corresponding optimal objective value and an optimal solution, respectively.

2. Calculate the average of all optimal solution values from the SAA problems and their variance:

$$\bar{\mathcal{V}}_{\mathcal{M}}^{\mathcal{N}} = \tfrac{1}{|\mathcal{M}|} \sum_{j \in \mathcal{M}} \mathcal{V}^{\mathcal{N}_j}$$

$$\sigma^2_{\bar{\mathcal{V}}_{\mathcal{M}}^{\mathcal{N}}} = \tfrac{1}{(|\mathcal{M}|-1)|\mathcal{M}|} \sum_{j \in \mathcal{M}} (\mathcal{V}^{\mathcal{N}_j} - \bar{\mathcal{V}}_{\mathcal{M}}^{\mathcal{N}})^2$$

   The expected value of $\bar{\mathcal{V}}_{\mathcal{M}}^{\mathcal{N}}$ provides an upper statistical bound for the optimal value of the original problem, and $\sigma^2_{\bar{\mathcal{V}}_{\mathcal{M}}^{\mathcal{N}}}$ is an estimate of the variance of this estimator.

3. Pick a feasible solution $\hat{y} \in Y$ for problem (5.1)-(5.6), for example, use one of the previously computed solutions $\hat{y}^{\mathcal{N}_j}$. Estimate the objective function value of the original problem by using this solution as follows:

$$\mathcal{V}_{\mathcal{N}'}(\hat{y}) = \frac{1}{|\mathcal{N}'|}\Big[\sum_{k\in K}\sum_{a\in A_k}\sum_{m\in M}(r_k^m - \hat{C}_{ak})w_k^{mn}x_{ak}^{mn}\Big] - \sum_{i\in H} f_i\hat{y}_i$$

where $\xi_j^1, \ldots, \xi^{|\mathcal{N}'|}$ is a sample of size $\mathcal{N}'$ generated independently of the samples used in the SAA problems. Note that since the first-stage variables are fixed, one can take much larger number of scenarios for $|\mathcal{N}'|$ than the sample size $|\mathcal{N}|$ used to solve the SAA problems. The estimator $\mathcal{V}_{\mathcal{N}'}(\hat{y})$ serves as a lower bound on the optimal objective function value. We can estimate the variance of $\mathcal{V}_{\mathcal{N}'}(\hat{y})$ as follows:

$$\sigma^2_{\mathcal{N}'}(\hat{y}) = \frac{1}{(|\mathcal{N}'|-1)|\mathcal{N}'|}\sum_{n\in\mathcal{N}'}\Big([\sum_{k\in K}\sum_{a\in A_k}\sum_{m\in M}(r_k^m - \hat{C}_{ak})w_k^{mn}x_{ak}^{mn}] - \sum_{i\in H} f_i\hat{y}_i - \mathcal{V}_{\mathcal{N}'}(\hat{y})\Big)^2$$

4. Calculate the estimators for the optimality gap and its variance. Employing the estimators computed in steps 2 and 3, we get:

$$gap_{\mathcal{N},\mathcal{M},\mathcal{N}'}(\hat{y}) = \bar{\mathcal{V}}^{\mathcal{N}}_{\mathcal{M}} - \mathcal{V}_{\mathcal{N}'}(\hat{y})$$

$$\sigma^2_{gap} = \sigma^2_{\bar{\mathcal{V}}^{\mathcal{N}}_{\mathcal{M}}} + \sigma^2_{\mathcal{N}'}(\hat{y})$$

We can then use these estimators to construct a confidence interval for the optimality gap.

5.2.1.2 Benders Decomposition for the SAA Problem

In this section, we present a Benders decomposition algorithm coupled with SAA to solve the profit maximizing hub location problem with capacity allocation and stochastic demand. By approximating the second-stage expectation via the sample average function as described in the previous section, the stochastic problem can be formulated as (5.7)-(5.12).

At each replication of the sample average optimization problem, we solve the SAA counterpart of the problem (5.1)-(5.6) using a Benders decomposition algorithm. As explained in previous chapters, BD is based on the premise that for fixed values of integer variables, the resulting problem, known as the primal subproblem, is relatively easier to solve compared to the original problem. In BD, the problem is reformulated based on the information inferred from the dual space of the continuous variables. The equivalent reformulation, known as the master problem, contains the integer variables and exponentially many constraints corresponding to the dual variables. Therefore, MP is usually solved using a cutting-plane method, where relaxations of MP are iteratively solved until the optimal solution is obtained.

We assume that the hub location decisions are handled in the master problem, while the rest is left to the subproblem. For a given sample $\mathcal{N}$ and fixed value of the integer variables $y_i = y_i^e$, the *primal subproblem* PS($\mathcal{N}$) reads as

$$\text{PS}(\mathcal{N}) \quad \text{Maximize} \quad \frac{1}{|\mathcal{N}|} \sum_{n\in\mathcal{N}} \sum_{m\in M} \sum_{k\in K} \sum_{a\in A_k} (r_k^m - \hat{C}_{ak}) w_k^{mn} x_{ak}^{mn} \tag{5.14}$$

$$\text{s.t.} \quad \sum_{a\in A_k} x_{ak}^{mn} \leq 1 \qquad k\in K, m\in M, n\in\mathcal{N} \tag{5.15}$$

$$\sum_{a\in A_k: i\in a} x_{ak}^{mn} \leq y_i^e \qquad i\in H, k\in K, m\in M, n\in\mathcal{N} \tag{5.16}$$

$$\sum_{m\in M} \sum_{k\in K} \sum_{a\in A_k: i\in a} w_k^{mn} x_{ak}^{mn} \leq \Gamma_i y_i^e \qquad i\in H, n\in\mathcal{N} \tag{5.17}$$

$$x_{ak}^{mn} \geq 0 \qquad k\in K, m\in M, a\in A_k, n\in\mathcal{N}. \tag{5.18}$$

Observe that PS($\mathcal{N}$) can be decomposed into $|\mathcal{N}|$ independent subproblems of the form PS (4.8)-(4.12) for each $n \in \mathcal{N}$. Consequently, the dual subproblem associated with each n can be formulated as DS (4.13)-(4.16) and solved using the techniques proposed in Section 4.2.3. In the following, we denote the DS under scenario $n \in \mathcal{N}$ by DS($\mathcal{N}, n$), in which w_k^m is replaced with w_k^{mn}, for each $k \in K$ and $m \in M$.

Let $\hat{P}_{\mathcal{N}}^n$ for $n \in \mathcal{N}$ denote the set of extreme points of the polyhedron defined by feasible

region of DS($\mathcal{N}, n$). The master problem can then be stated as

$$\text{MP}(\mathcal{N}) \quad \text{Maximize} \quad \frac{1}{|\mathcal{N}|}\sum_{n\in\mathcal{N}}\eta^n - \sum_{i\in H} f_i y_i \tag{5.19}$$

$$\text{s.t.} \quad \eta^n \leq \sum_{k\in K}\sum_{m\in M}\alpha_k^{mn} + \sum_{i\in H} y_i(\Gamma_i b_i^n + \sum_{k\in K}\sum_{m\in M} u_{ik}^{mn}) \quad n \in \mathcal{N}, (\alpha^n, u^n, b^n) \in \hat{P}_{\mathcal{N}}^n \tag{5.20}$$

$$y_i \in \{0,1\} \qquad i \in H \tag{5.21}$$

This problem contains an exponential number of constraints, which can be tackled by employing a cutting plane method, where a sequence of relaxed master problems and dual subproblems are solved, until the optimal solution is found.

5.2.1.3 Acceleration Techniques for the SAA Problem

The variable fixing techniques presented in Section 4.2.2 can be applied to each sample of the stochastic model. We further enhance the convergence of our SAA algorithm as detailed below.

Because of the repetitive structure of the SAA algorithm, we must solve $|\mathcal{M}|$ replications of problem (5.7)-(5.12). Consequently, upon solving MP($\hat{\mathcal{N}}$) for a specific sample $\hat{\mathcal{N}}$, we obtain dual solutions $(\hat{\alpha}^{\hat{n}}, \hat{u}^{\hat{n}}, \hat{b}^{\hat{n}}) \in \hat{P}_{\hat{\mathcal{N}}}^{\hat{n}}$ for each $\hat{n} \in \hat{\mathcal{N}}$. Now, assume that we want to solve MP($\mathcal{N}$) for a different sample $\mathcal{N}$. Solving MP($\mathcal{N}$) with initially empty $\hat{P}_{\mathcal{N}}^n$ sets would disregard the fact that the optimal solution of MP($\hat{\mathcal{N}}$) is potentially a near-optimal solution to MP($\mathcal{N}$). We can exploit this property and retrieve feasible solutions $(\alpha^n, u^n, b^n) \in \hat{P}_{\mathcal{N}}^n$ for scenario n of sample $\mathcal{N}$ from the solutions contained in $\hat{P}_{\hat{\mathcal{N}}}^{\hat{n}}$ for $\hat{n} \in \hat{\mathcal{N}}$.

Given a feasible solution for DS($\hat{\mathcal{N}}, \hat{n}$), the following proposition provides a feasible solution for DS($\mathcal{N}, n$).

Proposition 4. *Let $(\hat{\alpha}^{\hat{n}}, \hat{u}^{\hat{n}}, \hat{b}^{\hat{n}}) \in \hat{P}_{\hat{\mathcal{N}}}^{\hat{n}}$ be a feasible solution for DS($\hat{\mathcal{N}}, \hat{n}$), and $\hat{w}_k^{m\hat{n}}$ be the demand for commodity $k \in K$ of class $m \in M$ under scenario $\hat{n} \in \hat{\mathcal{N}}$. (α^n, u^n, b^n) defined*

by (5.22)-(5.24) *is feasible for* $DS(\mathcal{N}, n)$*:*

$$b_i^n = \hat{b}_i^{\hat{n}} \qquad i \in H \tag{5.22}$$

$$\alpha_k^{mn} = \frac{w_k^{mn}}{\hat{w}_k^{m\hat{n}}} \hat{\alpha}_k^{m\hat{n}} \qquad k \in K, m \in M \tag{5.23}$$

$$u_{ik}^{mn} = \frac{w_k^{mn}}{\hat{w}_k^{m\hat{n}}} \hat{u}_{ik}^{m\hat{n}} \qquad k \in K, m \in M, i \in H \tag{5.24}$$

Corollary 3. *The solution obtained by* (5.22)-(5.24) *provides a valid cut for* $MP(\mathcal{N})$*.*

Note that for a given scenario $n \in \mathcal{N}$, each scenario $\hat{n} \in \hat{\mathcal{N}}$ can provide a valid cut for MP($\mathcal{N}$). To avoid adding too many cuts, we select and add the best potential cut, which belongs to scenario $\hat{n}^* \in \hat{\mathcal{N}}$ with the least demand deviation from the demand under scenario $n \in \mathcal{N}$, i.e.

$$\hat{n}^* = \arg\min_{\hat{n} \in \hat{\mathcal{N}}} \left\{ \sum_{(k,m) \in K \times M} |w_k^{m\hat{n}} - w_k^{mn}| \right\}. \tag{5.25}$$

It should, however, be noted that when generating valid cuts from sample $\hat{\mathcal{N}}$ for sample $\mathcal{N}$, both instances should have the same set of hubs. In other words, if in the process of solving MP($\hat{\mathcal{N}}$), we eliminate a number of hubs via variable fixing, we will not calculate the dual variables associated with the eliminated hubs, hence the incomplete solution obtained by (5.22)-(5.24) may not provide a valid cut for MP($\mathcal{N}$). To tackle this problem, we solve the first sample of the SAA algorithm without using any variable fixing to ensure that the resulting cuts can be used for the subsequent samples of SAA. Once these solutions are obtained, we add the respective cuts obtained from the first sample to the master problem of the subsequent samples and continue with performing variable fixing as introduced in Section 4.2.2.

5.2.2 Computational results for the stochastic model

To perform computational experiments with the stochastic model, we use the same parameter setting and the same workstation as detailed in Section 4.3. We use instances

with $|N| \in \{10, 20, 25, 40, 50, 75\}$ and set the time limit to 24 hours. We first focus on the practical convergence of the SAA scheme using the stochastic model, we then test the performance of our methods on the instances involving up to 75 nodes.

5.2.2.1 Sample generation

We generate independent samples for demands of commodities using a normal distribution parameterized as follows: Let $\bar{w}_k^m$ be the demand of commodity k of class m in the deterministic case. Moreover, let $\bar{w}_k = \sum_{m \in M} \bar{w}_k^m$ be the total demand of commodity k, and $\rho_m^k = \frac{\bar{w}_k^m}{\bar{w}_k}$ be the proportion of demand of segment m of commodity k. We assume that the total demand of k (i.e. w_k) is drawn from a normal distribution in which the mean demand is set to $\bar{w}_k$ and the standard deviation is equal to $\sigma_k = \nu \bar{w}_k$, where ν is the coefficient of variation. Consequently, once the total demand of commodity k is realized, the correlated demand of class m is computed as $w_k^m = \rho_m^k w_k$.

5.2.2.2 Practical convergence of the SAA algorithm

The aim of this section is to analyze the practical convergence of the SAA scheme in order to choose a sample size $|\mathcal{N}|$ and the number of replications $|\mathcal{M}|$ that provide the best trade-off between solution quality and computational time. To this end, we perform computational tests with sample sizes $|\mathcal{N}| \in \{50, 100, 500, 1000\}$ and a number of replications $|\mathcal{M}| \in \{10, 20, 40, 60, 80\}$. We select two 10-node instances of the AP dataset and generate independent samples as explained above, with ν set to 0.5. The sample size of $|\mathcal{N}'| = 10,000$ is used to evaluate the SAA gap.

Figures 5.1 and 5.2 plot the optimality gap, standard deviation for the optimality gap, and the computational time required for the SAA algorithm for different sample sizes $|\mathcal{N}|$ and $|\mathcal{M}|$, with AP10LL and AP10TL, respectively. Figures 1(a) and 2(a) clearly indicate that larger sample size result in smaller optimality gap on average. It is also observed that as the sample sizes $|\mathcal{N}|$ and $|\mathcal{M}|$ increase, the corresponding standard deviation for

the optimality gap decreases (Figures 1b and 2b), whereas the corresponding computation time increases significantly (Figures 1c and 2c), for both AP10LL and AP10TL instances. In general, the largest sample size $|\mathcal{N}| = 1000$ provides the best average SAA gap with the least variation, and the sample size $|\mathcal{N}| = 50$ is the best in terms of the trade-off between solution quality and computational time. For this reason, we use sample sizes $|\mathcal{N}| = 50$ and $|\mathcal{M}| = 60$ during the rest of our computational experiments.

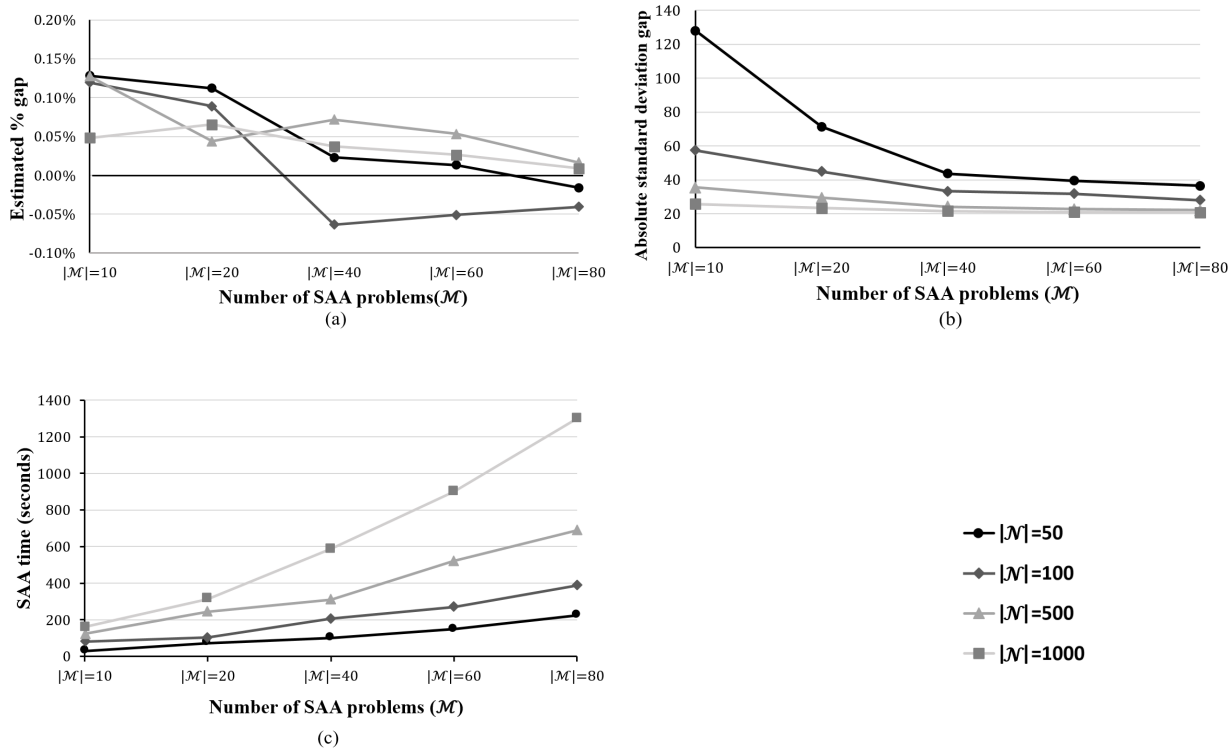

Figure 5.1: Optimality gap, standard deviation for the optimality gap, and the total CPU time required for the SAA algorithm for different sample sizes $|\mathcal{N}|$ and $|\mathcal{M}|$ with AP10LL.

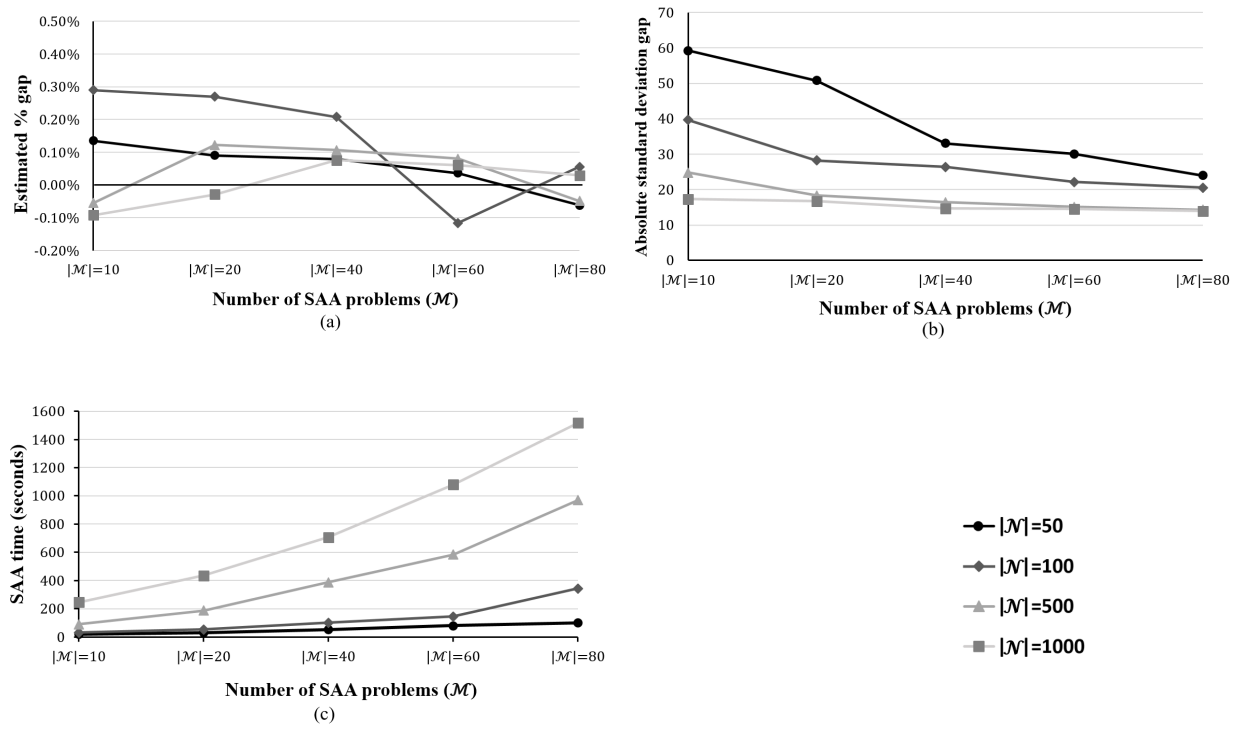

Figure 5.2: Optimality gap, standard deviation for the optimality gap, and the total CPU time required for the SAA algorithm for different sample sizes $|\mathcal{N}|$ and $|\mathcal{M}|$ with AP10TL.

5.2.2.3 Solving larger-size instances

We first evaluate the performance of the acceleration techniques proposed for SAA. To this end, we took runs with and without the implementation of the acceleration techniques on the 10-25 node instances from the AP dataset. For each instance, we consider two values 0.5 and 1 as the coefficient of variation to represent the amount of uncertainty in the stochastic demand. We compare the computational times in Table 5.1. The first two columns report the instance size and the coefficient of variation. The third and fourth columns labeled "Time (sec)" report the computation times in seconds without and with the implementation of the acceleration techniques, respectively. The last two rows report the averages.

The results provided in Table 5.1 indicate that the algorithm performs more than two times faster on average with the implementation of the proposed acceleration techniques. In particular, for the larger-size instances, the algorithm runs up to five times faster with the implementation of the acceleration techniques. Hence, all computational experiments with the stochastic model are carried out using the acceleration techniques.

We now analyze and evaluate the performance of the SAA algorithm on larger-size instances with up to 75 nodes from the AP dataset. The computational results are summarized in Table 5.2. The first two columns provide the number of nodes and the coefficient of variation. The next three columns labeled "Optimal solution" present the net profit ($\bar{\mathcal{V}}^{\mathcal{N}}_{\mathcal{M}}$), the best hub locations, and the run time of instances (in seconds) obtained from solving the SAA algorithm, respectively. The next column labeled "% Gap" provides the percent optimality gap relative to the best solution obtained by the SAA algorithm. The last two columns labeled "CI for SAA % gap at" give the 95% and 99% confidence interval for the optimality gap of the best solution obtained by the SAA algorithm, respectively.

The results provided in Table 5.2 indicate that the estimated optimality gaps obtained by the SAA algorithm are always below 0.2%, and that the corresponding confidence intervals for the optimality gaps are quite narrow for both 95% and 99%. These confirm the efficiency of the SAA algorithm proposed for the problem with stochastic demand, and

Table 5.1: Computational times for the stochastic model with and without the implementation of the acceleration techniques for SAA.

$\|H\|$	ν	Time (sec)	
		Without acceleration	With acceleration
10LL	0.5	55.29	50.82
	1	47.38	41.76
10LT	0.5	18.42	15.39
	1	21.80	18.33
10TL	0.5	38.63	33.89
	1	53.46	53.48
10TT	0.5	17.34	14.97
	1	15.10	13.11
20LL	0.5	8,723.45	1,553.42
	1	6,601.72	2,713.17
20LT	0.5	2,892.03	1,442.36
	1	3,303.61	1,907.56
20TL	0.5	3,528.43	1,089.42
	1	4,202.39	1,173.79
20TT	0.5	249.41	101.11
	1	197.85	76.78
25LL	0.5	5,494.94	1,418.24
	1	6,653.34	2,014.32
25LT	0.5	15,617.96	3,218.51
	1	8,327.14	3,832.22
25TL	0.5	3,577.96	1,127.83
	1	4,382.44	1,613.32
25TT	0.5	5,053.09	1,420.91
	1	3,152.68	1,711.33
Average	0.5	3,772.25	957.24
	1	3,079.91	1,264.10

Table 5.2: Computational results for the stochastic model with 48 instances of the AP dataset.

Instance		Optimal solution			% Gap	CI for SAA % gap at	
$\|H\|$	ν	Profit	Open hubs	Time (sec)	SAA	95%	99%
10LL	0.5	21,380	5,6,9,10	50.82	0.08	(-6.16, 11.73)	(-8.74, 14.31)
	1	22,529	5,6,9,10	41.76	-0.04	(-4.91, 13.47)	(-7.47, 16.03)
10LT	0.5	3,344	5	15.39	0.06	(-9.96, 13.67)	(-13.45, 17.16)
	1	3,358	5,6	18.33	0.18	(-7.24, 15.50)	(-9.29, 17.55)
10TL	0.5	13,890	4,5,9	33.89	0.14	(-14.02, 7.87)	(-18.39, 12.24)
	1	14,586	4,5,9	53.48	-0.04	(-11.05, 8.37)	(-12.19, 9.51)
10TT	0.5	2,690	5	14.97	0.03	(-9.96, 13.67)	(-13.56, 17.27)
	1	2,683	5	13.11	0.14	(-6.42, 16.57)	(-10.60, 20.75)
20LL	0.5	105,282	7,9,10,19	1,553.42	0.04	(-15.15, 14.31)	(-16.73, 15.89)
	1	113,599	7,9,10,14,19	2,713.17	0.03	(-9.92, 15.72)	(-14.67, 20.47)
20LT	0.5	59,727	5,9,10,12,14,19	1,442.36	0.05	(-4.45, 8.72)	(-9.21, 13.48)
	1	63,731	5,9,10,12,14,19	1,907.56	0.04	(-3.72, 10.74)	(-7.05, 14.07)
20TL	0.5	53,035	5,7,10	1,089.42	0.08	(-11.67, 10.97)	(-16.07, 15.37)
	1	57,511	5,7,10	1,173.79	0.06	(-8.60, 15.09)	(-11.86, 18.35)
20TT	0.5	13,672	10	101.11	0.02	(-10.62, 10.07)	(-11.90, 11.35)
	1	13,984	10	76.78	-0.03	(-8.08, 12.76)	(-10.94, 15.62)
25LL	0.5	133,240	7,14,17,23	1,418.24	-0.03	(-10.32, 13.46)	(-13.03, 16.17)
	1	140,164	7,14,17,23	2,014.32	-0.02	(-6.47, 14.83)	(-11.33, 19.69)
25LT	0.5	92,042	6,10,12,14,25	3,218.51	-0.01	(-6.23, 10.47)	(-11.13, 15.37)
	1	98,570	9,10,12,14,19,25	3,832.22	0.01	(-9.87, 11.51)	(-14.58, 16.22)
25TL	0.5	81,755	6,9,14,23	1,127.83	-0.02	(-8.48, 10.26)	(-9.95, 11.73)
	1	87,625	6,9,14,23	1,613.32	-0.02	(-5.98, 12.38)	(-10.64, 17.04)
25TT	0.5	36,956	6,10,14,25	1,420.91	0.00	(-9.16, 8.70)	(-11.60, 11.14)
	1	39,992	6,9,10,14,25	1,711.33	-0.01	(-7.18, 10.91)	(-8.92, 12.65)
40LL	0.5	80,696	12,22,26,29	15,219.35	-0.03	(-18.92, 17.71)	(-22.80, 21.59)
	1	86,456	9,22,26,29,38	17,612.49	0.02	(-15.39, 19.48)	(-16.88, 20.97)
40LT	0.5	71,192	12,14,26,29,30,38	20,369.86	-0.04	(-19.32, 22.57)	(-21.37, 24.62)
	1	76,989	5,14,19,26,29,30,38	22,928.64	0.04	(-16.86, 23.36)	(-18.55, 25.05)
40TL	0.5	65,621	14,19,29	7,549.28	-0.03	(-14.74, 19.37)	(-18.99, 23.62)
	1	71,406	14,19,29	8,084.24	0.05	(-12.37, 21.22)	(-14.30, 23.15)
40TT	0.5	52,843	14,19,25,38	9,672.36	-0.04	(-17.53, 19.75)	(-19.06, 21.28)
	1	57,349	5,19,25,30	10,836.71	0.05	(-15.95, 23.42)	(-20.59, 28.06)
50LL	0.5	77,216	15,28,33,35	13,565.38	0.03	(-19.46, 25.37)	(-27.00, 32.91)
	1	83,180	5,15,28,33,35	15,738.46	-0.03	(-17.11, 26.23)	(-25.07, 34.19)
50LT	0.5	73,467	6,26,32,46	11,874.35	0.05	(-15.83, 21.64)	(-22.38, 28.19)
	1	79,923	6,19,26,30,46	14,969.23	-0.06	(-13.26, 23.83)	(-16.90, 27.47)
50TL	0.5	58,384	3,26,45	5,595.46	0.05	(-16.30, 16.99)	(-20.26, 20.95)
	1	60,756	3,14,29,45	7,304.05	-0.09	(-12.61, 18.28)	(-17.92, 23.59)
50TT	0.5	48,376	6,26,48	6,393.29	0.12	(-14.67, 16.36)	(-20.39, 22.08)
	1	53,261	6,26,48	7,141.92	-0.07	(-12.71, 18.49)	(-17.16, 22.94)
75LL	0.5	145,792	14,23,35,37,56	43,955.24	0.10	(-17.54, 12.63)	(-23.37, 18.46)
	1	198,962	5,14,19,26,29,30,38	46,085.51	0.04	(-12.46, 18.49)	(-16.55, 22.58)
75LT	0.5	113,510	14,25,32,35,38,59	36,666.45	-0.08	(-14.29, 18.81)	(-18.50, 23.02)
	1	122,007	14,26,32,35,46,59	39,157.63	0.04	(-11.39, 19.41)	(-16.60, 24.62)
75TL	0.5	92,609	14,35,37	24,531.79	0.16	(-21.74, 19.83)	(-29.04, 27.13)
	1	96,829	14,35,37	25,742.90	0.07	(-18.25, 22.49)	(-24.14, 28.38)
75TT	0.5	81,697	25,32,38,59	32,559.79	0.14	(-23.67, 16.74)	(-31.43, 24.50)
	1	84,157	25,26,32,38,59	34,637.15	-0.10	(-17.34, 18.51)	(-22.33, 23.50)

also imply that the solutions produced by our algorithm are good enough to be used in practical applications.

We next observe the effects of variability in uncertain demands on the solutions reported in Table 5.2. When the ν value increases, that is, when the variability in the uncertain demand increases, the net profit values and the computation time required for the SAA algorithm also increase. Note that the best found hub locations do not change significantly under these variations. We can identify a few instances in which hub locations change by demand variation, and in most of the instances, the locations of the hubs obtained with the deterministic and stochastic models are identical (Tables 4.1 and 5.2). It seems that, in these particular instances, the long-term location decisions are dependent more on the configuration of hub installation costs and capacities than the demand.

5.3 Robust-Stochastic Models

We now model the robust-stochastic problem when there is uncertainty associated with revenues under stochastic demand. We present two mathematical formulations for the robust-stochastic version of the problem. We first model a max-min criterion and then a min-max regret.

5.3.1 Case I: max-min criterion

We use interval uncertainty for revenues in which each parameter r_k^m for $k \in K, m \in M$ takes values in $[\bar{r}_k^m - \hat{r}_k^m, \bar{r}_k^m]$, where $\bar{r}_k^m$ is the nominal value of revenue and $\hat{r}_k^m \geq 0$ represents the deviation from the nominal value. Let $\gamma_r \in [0, |K| \times |M|]$ be an integer value controlling the level of conservatism in the objective and denote the uncertainty budget on the maximum number of revenue parameters r_k^m whose value is allowed to differ from its nominal value. We are interested in finding an optimal solution that optimizes against all realizations under which a number γ_r of the revenue coefficients can vary in

such a way as to maximally influence the objective (Bertsimas and Sim [18]). The *robust-stochastic model with max-min criterion* for the profit maximizing hub location problem with capacity allocation is then modeled as:

$$\text{RS-I} \qquad \max_{(x,y)\in\mho} \; E_\xi\Big[\sum_{k\in K}\sum_{m\in M}\sum_{a\in A_k}(\bar{r}_k^m - \hat{C}_{ak})w_k^m(\xi)x_{ak}^m(\xi) - \nu_\xi(x)\Big] - \sum_{i\in H} f_i y_i \tag{5.26}$$

where $\mho = \{(x,y) : (5.2) - (5.6) \text{ are satisfied}\}$, and $\nu_\xi(x)$ is defined as follows:

$$\nu_\xi(x) = \max_{U_r\subseteq K\times M:|U_r|\leq\gamma_r} \sum_{(k,m)\in S_r}\sum_{a\in A_k} \hat{r}_k^m w_k^m(\xi)x_{ak}^m(\xi). \tag{5.27}$$

In the above equation, U_r represents the subset of commodities whose revenue values are subject to variation. The goal of $\nu_\xi(x)$ is to determine the worst case deviation from the total revenue over all possible revenue realizations for a given solution x. Note that in extreme cases when $\gamma_r = 0$ or $\gamma_r = |K| \times |M|$ (alternatively, when $U_r = \emptyset$ or $U_r = K \times M$, respectively), the problem can be reduced to the stochastic model and it has trivial solutions such that for all commodities (k,m), in the former case, $r_k^m = \bar{r}_k^m$, whereas in the latter case, $r_k^m = \bar{r}_k^m - \hat{r}_k^m$, where these cases represent the least and highest levels of conservatism, respectively. In general, a higher value of γ_r leads to a more conservative solution in the expense of a possibly lower profit.

We can reformulate $\nu_\xi(x)$ by introducing a binary variable z_k^m which determines whether or not class $m \in M$ of commodity $k \in K$ is subject to uncertainty; i.e., $z_k^m = 1$ if $(k,m) \in U_r$, and 0 otherwise.

$$\nu_\xi(x) = \quad \max \quad \sum_{k\in K}\sum_{m\in M}\left(\hat{r}_k^m w_k^m(\xi)\sum_{a\in A_k} x_{ak}^m(\xi)\right) z_k^m \tag{5.28}$$

$$\text{s.t.} \qquad \sum_{k\in K}\sum_{m\in M} z_k^m \leq \gamma_r \tag{5.29}$$

$$z_k^m \in \{0,1\} \qquad\qquad k\in K, m\in M. \tag{5.30}$$

Note that since γ_r is integer, $\nu_\xi(x)$ simply sorts the commodities (k,m) in the non-increasing order of $\hat{r}_k^m w_k^m(\xi)\sum_{a\in A_k} x_{ak}^m(\xi)$ and selects the first γ_r of them. Hence, constraint (5.30) can be replaced with its linear relaxation counterpart without losing integrality.

Let $\mu(\xi)$ and $\lambda_k^m(\xi)$ be the dual variables associated with constraints (5.29) and the linear relaxation of (5.30), respectively. The dual of problem (5.28)-(5.30) can be obtained as:

$$\nu_\xi(x) = \quad \min \quad \gamma_r \mu(\xi) + \sum_{k\in K}\sum_{m\in M} \lambda_k^m(\xi) \tag{5.31}$$

$$\text{s.t.} \qquad \mu(\xi) + \lambda_k^m(\xi) \geq \hat{r}_k^m w_k^m(\xi) \sum_{a\in A_k} x_{ak}^m(\xi) \quad k \in K, m \in M \tag{5.32}$$

$$\lambda_k^m(\xi), \mu(\xi) \geq 0 \qquad\qquad k \in K, m \in M. \tag{5.33}$$

With this formulation of $\nu_\xi(x)$, mathematical program (5.26) can be reformulated as the following MILP:

$$\max_{(x,y)\in\mho} \quad E_\xi\Big[\sum_{k\in K}\sum_{m\in M}\sum_{a\in A_k}(\bar{r}_k^m - \hat{C}_{ak}) w_k^m(\xi) x_{ak}^m(\xi) - \gamma_r\mu(\xi) - \sum_{k\in K}\sum_{m\in M}\lambda_k^m(\xi)\Big] - \sum_{i\in H} f_i y_i \tag{5.34}$$

$$\text{s.t.} \quad (5.32), (5.33).$$

5.3.2 Case II: min-max regret criterion

If there exists a set of scenarios describing uncertainty associated with the revenues, one may also use a min-max regret type objective function to model the problem (Alumur et al. [8], Correia and Saldanha-da Gama [40]). Let S_r define the set of scenarios for uncertain revenues and r_k^{ms} denote the amount of revenue obtained from satisfying a unit commodity $k \in K$ of class $m \in M$ under scenario $s \in S_r$.

For a given demand realization $\xi \in \Xi$, the maximum profit that can be achieved under revenue scenario $s \in S_r$, denoted by $Z^s(\xi)$, can be calculated by

$$Z^s(\xi) = \max \sum_{k\in K}\sum_{m\in M}\sum_{a\in A_k}(r_k^{ms} - \hat{C}_{ak})w_k^m(\xi)x_{ak}^m(\xi) - \sum_{i\in H} f_i y_i \tag{5.35}$$

$$\text{s.t.} \quad \sum_{a\in A_k} x_{ak}^m(\xi) \le 1 \qquad k\in K, m\in M \tag{5.36}$$

$$\sum_{a\in A_k: i\in a} x_{ak}^m(\xi) \le y_i \qquad i\in H, k\in K, m\in M \tag{5.37}$$

$$\sum_{k\in K}\sum_{m\in M}\sum_{a\in A_k: i\in a} w_k^m(\xi)x_{ak}^m(\xi) \le \Gamma_i y_i \qquad i\in H \tag{5.38}$$

$$x_{ak}^m(\xi) \ge 0 \qquad k\in K, m\in M, a\in A_k \tag{5.39}$$

$$y_i \in \{0,1\} \qquad i\in H. \tag{5.40}$$

For a given demand realization $\xi \in \Xi$, the regret of a solution $(x(\xi), y)$ under revenue scenario $s \in S_r$ is defined as the difference between the optimal profit that can be achieved under that scenario (i.e. $Z^s(\xi)$) and the total profit associated with $(x(\xi), y)$. With this definition, the *min-max regret stochastic model* can be formulated as follows:

$$\text{RS-II} \quad \min_{(x,y)\in\mho} \; E_\xi\Big[\max_{s\in S_r}\Big\{Z^s(\xi) - (\sum_{k\in K}\sum_{m\in M}\sum_{a\in A_k}(r_k^{ms} - \hat{C}_{ak})w_k^m(\xi)x_{ak}^m(\xi) - \sum_{i\in H} f_i y_i)\Big\}\Big]. \tag{5.41}$$

The inner maximization calculates the maximum regret among all revenue scenarios. Replacing the inner maximization with a continuous variable $V(\xi)$, the above formulation can be linearized as follows:

$$\min_{(x,y)\in\mho} \quad E_\xi[V(\xi)] \tag{5.42}$$

$$\text{s.t.} \quad V(\xi) \ge Z^s(\xi) - (\sum_{k\in K}\sum_{m\in M}\sum_{a\in A_k}(r_k^{ms} - \hat{C}_{ak})w_k^m(\xi)x_{ak}^m(\xi) - \sum_{i\in H} f_i y_i), \quad \xi\in\Xi, s\in S_r. \tag{5.43}$$

Another approach to formulate the min-max regret model would be to maximize the expected regret (Alumur et al. [8]). Here, we model the expectation of the maximum regret. We believe the latter is more realistic, however, results in a larger formulation which is more challenging to solve.

We now define $\bar{V}(\xi) \coloneqq -(V(\xi) - \sum_{i \in H} f_i y_i)$ and for reasons that will become apparent later, we replace $V(\xi)$ with $-(\bar{V}(\xi) - \sum_{i \in H} f_i y_i)$ and reformulate (5.42)-(5.43) in a maximization form as:

$$\max_{(x,y) \in \mho} \quad E_\xi[\bar{V}(\xi)] - \sum_{i \in H} f_i y_i \tag{5.44}$$

$$\text{s.t.} \quad \bar{V}(\xi) - \sum_{k \in K} \sum_{m \in M} \sum_{a \in A_k} (r_k^{ms} - \hat{C}_{ak}) w_k^m(\xi) x_{ak}^m(\xi) \leq -Z^s(\xi) \quad \xi \in \Xi, s \in S_r. \tag{5.45}$$

We now like to compare the min-max regret stochastic model (RS-II) with the robust-stochastic model with max-min criterion (RS-I). Let's first assume that the set of revenue scenarios considered in the min-max regret model (i.e. S_r) complies with the requirements of the uncertainty sets considered in the robust-stochastic model with max-min criterion (i.e. U_r). In other words, let S_r consists of all revenue scenarios involving at most γ_r commodities with an uncertain revenue. For a given solution (x, y), the robust-stochastic model with max-min criterion selects from S_r the scenario that minimizes the total revenue, and maximizes the expectation of this minimal revenue over all possible solutions (x, y). The min-max regret stochastic model, on the other hand, selects from S_r the scenario that maximizes the regret, and minimizes the expectation of this maximal regret over all possible solutions (x, y). Interestingly, as shown in Theorem 1 below, the robust-stochastic version with max-min criterion is actually a special case of the min-max regret stochastic model in which $Z^s(\xi) = \hat{Z}$ for some arbitrary value $\hat{Z}$ (e.g. 0) for each revenue scenario $s \in S_r$ and demand realization $\xi \in \Xi$.

Theorem 1. *Let S_r be the set of revenue scenarios where at most γ_r commodities are subject to revenue uncertainty. Then, the min-max regret stochastic model (5.41), in which*

regrets are calculated with respect to a fixed reference point $\hat{Z}$, is equivalent to the robust-stochastic model with max-min criterion (5.26).

Proof. Let $Z^s(\xi) = \hat{Z}$ for each revenue scenario $s \in S_r$ and demand realization $\xi \in \Xi$. Then, the min-max regret stochastic model (5.41) reads as:

$$\min_{(x,y)\in\mho} \quad E_\xi\Big[\max_{s\in S_r}\Big\{\hat{Z} - (\sum_{k\in K}\sum_{m\in M}\sum_{a\in A_k}(r_k^{ms} - \hat{C}_{ak})w_k^m(\xi)x_{ak}^m(\xi) - \sum_{i\in H} f_i y_i)\Big\}\Big]. \tag{5.46}$$

We now prove that (5.41) is equivalent to (5.46). Since $\hat{Z}$ is constant, it can be taken out from the inner maximization, the expectation, and the minimization, respectively. Hence, (5.46) can be reformulated as:

$$\hat{Z} - \max_{(x,y)\in\mho} \quad E_\xi\Big[\min_{s\in S_r}\Big\{\sum_{k\in K}\sum_{m\in M}\sum_{a\in A_k}(r_k^{ms} - \hat{C}_{ak})w_k^m(\xi)x_{ak}^m(\xi) - \sum_{i\in H} f_i y_i\Big\}\Big]. \tag{5.47}$$

For a given $(x, y) \in \mho$ and for each $\xi \in \Xi$, the inner minimization in (5.47) calculates the worst possible profit associated with (x, y) over all revenue scenarios. Given that each revenue scenario $s \in S_r$ involves at most γ_r commodities with uncertain revenue, we can map each revenue scenario s to a subset of commodities $U_r(s)$ including the commodities with uncertain revenue. That is, $r_k^{ms} = \bar{r}_k^m - \hat{r}_k^m$ if $(k, m) \in U_r(s)$, and $r_k^{ms} = \bar{r}_k^m$, otherwise. Therefore, the inner minimization in (5.47) can be rewritten as:

$$\min_{s\in S_r}\Big\{\sum_{k\in K}\sum_{m\in M}\sum_{a\in A_k}(\bar{r}_k^m - \hat{C}_{ak})w_k^m(\xi)x_{ak}^m(\xi) - \sum_{i\in H} f_i y_i - \sum_{(k,m)\in U_r(s)}\sum_{a\in A_k}(\hat{r}_k^m - \hat{C}_{ak})w_k^m(\xi)x_{ak}^m(\xi)\Big\}, \tag{5.48}$$

Now, since the first two terms of (5.48) are constant with respect to s, we can reformulate (5.48) as:

$$\sum_{k\in K}\sum_{m\in M}\sum_{a\in A_k}(\bar{r}_k^m - \hat{C}_{ak})w_k^m(\xi)x_{ak}^m(\xi) - \sum_{i\in H} f_i y_i - \max_{s\in S_r}\Big\{\sum_{(k,m)\in U_r(s)}\sum_{a\in A_k}(\hat{r}_k^m - \hat{C}_{ak})w_k^m(\xi)x_{ak}^m(\xi)\Big\}, \tag{5.49}$$

Note that the maximization in (5.49) is equivalent to $\nu_\xi(x)$ as defined in (5.27), therefore (5.46) is equivalent to

$$\hat{Z} - \max_{(x,y)\in\mho} \quad E_\xi\Big[\sum_{k\in K}\sum_{m\in M}\sum_{a\in A_k}(\bar{r}_k^m - \hat{C}_{ak})w_k^m(\xi)x_{ak}^m(\xi) - \nu_\xi(x)\Big] - \sum_{i\in H} f_i y_i, \tag{5.50}$$

which is equivalent to the robust-stochastic model with max-min criterion (5.26). □

As a consequence of Theorem 1, the robust-stochastic model with max-min criterion is computationally less challenging as there is no need to compute $Z^s(\xi)$ for each scenario. We empirically analyze the outcome and the level of robustness with both of the models through our computational experiments. In the sequel, we present a solution scheme to solve each of these large mixed-integer stochastic programs.

5.3.3 Solution scheme for the robust-stochastic models

In this section, we present exact algorithms based on BD coupled with SAA to solve the robust-stochastic models with max-min and min-max regret criteria, respectively.

5.3.3.1 Benders decomposition for the robust-stochastic model with max-min criterion

For y set to a specific vector $y := \bar{y}$ and for a given sample $\mathcal{N}$, the *primal subproblem* RSI-PS($\mathcal{N}$) of the SAA counterpart of robust-stochastic model with max-min criterion (5.32)-(5.34) can be formulated as:

$$\text{RS-I-PS}(\mathcal{N}) \quad \max \ \frac{1}{|\mathcal{N}|}[\sum_{n\in\mathcal{N}}\sum_{k\in K}\sum_{m\in M}\sum_{a\in A_k}(\bar{r}_k^m - \hat{C}_{ak})w_k^{mn}x_{ak}^{mn} - (\gamma_r\mu^n + \sum_{n\in\mathcal{N}}\sum_{k\in K}\sum_{m\in M}\lambda_k^{mn})] \tag{5.51}$$

$$\text{s.t.} \quad \hat{r}_k^m w_k^{mn} \sum_{a \in A_k} x_{ak}^{mn} - \mu^n - \lambda_k^{mn} \leq 0 \quad k \in K, m \in M, n \in \mathcal{N} \tag{5.52}$$

$$\sum_{a \in A_k} x_{ak}^{mn} \leq 1 \quad k \in K, m \in M, n \in \mathcal{N} \tag{5.53}$$

$$\sum_{a \in A_k : i \in a} x_{ak}^{mn} \leq \bar{y}_i \quad i \in H, k \in K, m \in M, n \in \mathcal{N} \tag{5.54}$$

$$\sum_{k \in K} \sum_{m \in M} \sum_{a \in A_k : i \in a} w_k^{mn} x_{ak}^{mn} \leq \Gamma_i \bar{y}_i \quad i \in H, n \in \mathcal{N} \tag{5.55}$$

$$x_{ak}^{mn}, \lambda_k^{mn}, \mu^n \geq 0 \quad k \in K, m \in M, a \in A_k, n \in \mathcal{N}. \tag{5.56}$$

Observe that RS-I-PS($\mathcal{N}$) can be decomposed into $|\mathcal{N}|$ independent subproblems, one for each $n \in \mathcal{N}$. Let β_k^{mn}, α_k^{mn}, u_{ik}^{mn}, and b_i^n be the dual variables associated with constraints (5.52)-(5.55), respectively. The *dual subproblem* associated with scenario $n \in \mathcal{N}$ can then be formulated as:

$$\text{RS-I-DS}(\mathcal{N}, n) \quad \min \sum_{k \in K} \sum_{m \in M} \alpha_k^{mn} + \sum_{i \in H} \bar{y}_i \Big(\sum_{k \in K} \sum_{m \in M} u_{ik}^{mn} + \Gamma_i b_i^n \Big) \tag{5.57}$$

$$\begin{aligned} \text{s.t.} \quad & \hat{r}_k^m w_k^{mn} \beta_k^{mn} + \alpha_k^{mn} + u_{ik}^{mn} + u_{jk}^{mn} + w_k^{mn} (b_i^n + b_j^n) \\ & \qquad \geq (\bar{r}_k^m - \hat{C}_{ijk}) w_k^{mn} \qquad k \in K, m \in M, (i,j) \in A_k : i \neq j \end{aligned} \tag{5.58}$$

$$\hat{r}_k^m w_k^{mn} \beta_k^{mn} + \alpha_k^{mn} + u_{ik}^{mn} + w_k^{mn} b_i^n \geq (\bar{r}_k^m - \hat{C}_{iik}) w_k^{mn} \quad k \in K, m \in M, i \in H \tag{5.59}$$

$$\sum_{k \in K} \sum_{m \in M} \beta_k^{mn} \leq \gamma_r \tag{5.60}$$

$$\beta_k^{mn} \leq 1 \quad k \in K, m \in M \tag{5.61}$$

$$\beta_k^{mn}, \alpha_k^{mn}, u_{ik}^{mn}, b_i^n \geq 0 \quad k \in K, m \in M, i \in H. \tag{5.62}$$

Let $P_{\mathcal{N}}^n$ be the set of extreme points of the polyhedron defined by (5.58)-(5.62) for $n \in \mathcal{N}$. Since the subproblem can be decomposed by each scenario $n \in \mathcal{N}$, the Benders cuts can be separated by each $n \in \mathcal{N}$. Hence, the Benders *master problem* RS-I-MP($\mathcal{N}$)

can be reformulated as:

$$\text{RS-I-MP}(\mathcal{N}) \quad \max \quad \frac{1}{|\mathcal{N}|}\sum_{n\in\mathcal{N}}\eta^n - \sum_{i\in H} f_i y_i \tag{5.63}$$

$$\text{s.t.} \quad \eta^n \leq \sum_{k\in K}\sum_{m\in M}\alpha_k^{mn} + \sum_{i\in H} y_i(\Gamma_i b_i^n + \sum_{k\in K}\sum_{m\in M} u_{ik}^{mn}) \quad n\in\mathcal{N}, (\beta^n,\alpha^n,u^n,b^n)\in P_{\mathcal{N}}^n \tag{5.64}$$

$$y_i \in \{0,1\} \qquad i\in H. \tag{5.65}$$

Since RS-I-MP($\mathcal{N}$) contains an exponential number of constraints of the form (5.64), we solve it by employing a cutting-plane method in which RS-I-MP($\mathcal{N}$) is relaxed by considering a limited number of constraints of the form (5.64). The relaxed RS-I-MP($\mathcal{N}$) is iteratively strengthened by generating new cuts of the form (5.64) obtained from solving the dual subproblems on the fly, until the optimal solution to RS-I-MP($\mathcal{N}$) is found. A pseudo-code of the basic BD algorithm is described in Algorithm 3. In this algorithm, UB and LB denote the upper and lower bounds on the optimal value, while Z_{MP}^e and Z_{DS}^{en} stand for the optimal values obtained from the master problem and dual subproblem at iteration e, respectively.

The computational efficiency of the BD algorithm is generally dependent on the number of iterations needed to find an optimal solution and the computational effort required to solve RS-I-MP($\mathcal{N}$) as well as RS-I-DS($\mathcal{N}, n$) at each iteration. To improve the efficiency of the algorithm, we apply variable fixing techniques presented in Chapter 4. In the following section, we describe how the subproblem can be solved efficiently. We also present additional enhancement techniques in this section.

Solving the Benders subproblem. Solving the subproblem is the most challenging part at each step of the BD algorithm. Moreover, the naive implementation of BD is notorious for its slow convergence due to the weakness of the cuts generated at each iteration (see e.g., Rahmaniani et al. [83]). To generate strong cuts, we solve RS-I-DS($\mathcal{N}, n$) for a

Algorithm 3 Benders decomposition for the robust-stochastic model with max-min criterion

$UB \leftarrow +\infty, LB \leftarrow -\infty, e \leftarrow 1$
$P^n_{\mathcal{N}} \leftarrow \emptyset \quad \forall n \in \mathcal{N}$
while $LB < UB$ **do**
    SOLVE RS-I-MP($\mathcal{N}$) and obtain y^e and Z^e_{MP}
    $UB \leftarrow Z^e_{MP}$
    for n in $\mathcal{N}$ **do**
        SOLVE RS-I-DS($\mathcal{N}, n$) with $\bar{y} = y^e$ and obtain $(\beta^n, \alpha^n, u^n, b^n)^e$ and Z^{en}_{DS}
        $P^n_{\mathcal{N}} \leftarrow P^n_{\mathcal{N}} \cup \{(\beta^n, \alpha^n, u^n, b^n)^e\}$
    end for
    $LB \leftarrow \max\{LB, \frac{1}{|\mathcal{N}|} \sum_{n \in \mathcal{N}} Z^{en}_{DS} - \sum_{i \in H} f_i y^e_i\}$
    $e \leftarrow e + 1$
end while

particular $n \in \mathcal{N}$ in two sequential phases based on the set of open/closed hubs as proposed in Section 4.2.3.

Observe that any feasible value of u^{mn}_{ik} and b^n_i associated with the closed hubs are optimal, since their coefficients in the objective function of RS-I-DS($\mathcal{N}, n$) are equal to zero as $\bar{y}_i = 0$. Therefore, these variables and their associated constraints can initially be removed from RS-I-DS($\mathcal{N}, n$) to solve the Phase I subproblem, and appropriate feasible values for these variables can be calculated subsequently in Phase II. In this manner, the optimality of the subproblem is guaranteed in Phase I, while in Phase II, the feasible values of the remaining variables are calculated so as to strengthen the cut.

Let H^e_1 and H^e_0 denote the set of open and closed hubs at iteration e, respectively. In Phase I, we remove the variables u^{mn}_{ik} and b^n_i associated with $i \in H^e_0$ and calculate the values of the remaining variables. Note that when $i \in H^e_1$, constraints (5.53) and (5.55) imply constraints (5.54). Consequently, there exists an optimal solution where the dual values associated with constraints (5.54) (i.e. u^{mn}_{ik}) are equal to 0 for $i \in H^e_1$. Thus, the

Phase I subproblem can be formulated as:

$$\text{RS-I-DS-I}(\mathcal{N}, n) \quad \min \sum_{k\in K}\sum_{m\in M} \alpha_k^{mn} + \sum_{i\in H_1^e} \Gamma_i b_i^n \tag{5.66}$$

$$\text{s.t.} \quad \hat{r}_k^m w_k^{mn}\beta_k^{mn} + \alpha_k^{mn} + w_k^{mn}(b_i^n + b_j^n) \geq (\bar{r}_k^m - \hat{C}_{ijk})w_k^{mn} \quad k \in K, m \in M, (i,j) \in A_{ke}^1 \tag{5.67}$$

$$\hat{r}_k^m w_k^{mn}\beta_k^{mn} + \alpha_k^{mn} + w_k^{mn} b_i^n \geq (\bar{r}_k^m - \hat{C}_{iik})w_k^{mn} \quad k \in K, m \in M, i \in H_1^e \tag{5.68}$$

$$\sum_{k\in K}\sum_{m\in M} \beta_k^{mn} \leq \gamma_r \tag{5.69}$$

$$\beta_k^{mn} \leq 1 \quad k \in K, m \in M \tag{5.70}$$

$$\beta_k^{mn}, \alpha_k^{mn}, b_i^n \geq 0 \quad k \in K, m \in M, i \in H_1^e \tag{5.71}$$

where $A_{ke}^1 = \{(i,j) \in A_k \cap H_1^e \times H_1^e : i \neq j\}$. Given that cardinality of H_1^e is almost certainly small, the Phase I subproblem can be solved using linear programming solvers. Once the optimal values of all the variables in the Phase I subproblem are obtained, the optimal value of the rest of variables will be computed in Phase II.

Observe that if the value of the β_k^{mn} is given for commodity (k,m), then constraints (5.58) and (5.59) associated with this commodity can respectively be rewritten as:

$$\alpha_k^{mn} + u_{ik}^{mn} + u_{jk}^{mn} + w_k^{mn}(b_i^n + b_j^n) \geq (\bar{r}_k^m - \hat{r}_k^m\beta_k^{mn} - \hat{C}_{ijk})w_k^{mn} \quad (i,j) \in A_k : i \neq j \tag{5.72}$$

$$\alpha_k^{mn} + u_{ik}^{mn} + w_k^{mn} b_i^n \geq (\bar{r}_k^m - \hat{r}_k^m\beta_k^{mn} - \hat{C}_{iik})w_k^{mn} \quad i \in H. \tag{5.73}$$

Note that β_k^{mn} expresses the extent to which revenue of commodity (k,m) is subject to uncertainty. Consequently, obtaining the optimal value of the β-variables in Phase I implies resolving the data uncertainty in Phase I. Hence, in Phase II, we work with the realized revenue r_k^m (i.e. $r_k^m = \bar{r}_k^m - \hat{r}_k^m\beta_k^{mn}$) for each commodity (k,m). Thus, the Phase II

subproblem is formulated as

$$\text{RS-I-DS-II}(\mathcal{N}, n) \quad \min \sum_{i \in H_0^e} (\sum_{k \in K} \sum_{m \in M} u_{ik}^{mn} + \Gamma_i b_i^n) \tag{5.74}$$

$$\text{s.t.} \quad u_{ik}^{mn} + u_{jk}^{mn} + w_k^{mn}(b_i^n + b_j^n) \geq \rho_{ijk}^{mn} \quad k \in K, m \in M, (i,j) \in A_{ke}^0 \tag{5.75}$$

$$u_{ik}^{mn} + w_k^{mn} b_i^n \geq \rho_{iik}^{mn} \quad k \in K, m \in M, i \in H_0^e \tag{5.76}$$

$$u_{ik}^{mn}, b_i^n \geq 0 \quad k \in K, m \in M, i \in H_0^e \tag{5.77}$$

where $A_{ke}^0 = \{(i,j) \in A_k \cap H_0^e \times H_0^e : i \neq j\}$, $\rho_{ijk}^{mn} = (r_k^m - \hat{C}_{ijk}) w_k^{mn} - \alpha_k^{mn}$ for $(i,j) \in A_{ke}^0$ and $\rho_{iik}^{mn} = \max\{\max_{j \in H_1^{ei}} \{(r_k^m - \hat{C}_{ijk}) w_k^{mn} - u_{jk}^{mn} - w_k^{mn} b_j^n\}, (r_k^m - \hat{C}_{iik}) w_k^{mn}\} - \alpha_k^{mn}$ for $i \in H_0^e$, in which $H_1^{ei} = \{j \in H_1^e : (i,j) \in A_k \text{ or } (j,i) \in A_k\}$.

To generate strong cuts, we solve RS-I-DS-II$(\mathcal{N}, n)$ as a series of LP-relaxations of knapsack problems as detailed in Section 4.2.3.3.

Acceleration techniques for SAA. We now propose acceleration techniques to reduce the computational time of our SAA algorithm. The acceleration technique for SAA is based on the observation that the cuts generated in solving sample $\hat{\mathcal{N}}$ can be transformed into valid cuts for sample $\mathcal{N}$. More specifically, in solving sample $\mathcal{N}$, we can retrieve feasible solutions for RS-I-DS$(\mathcal{N}, n)$ for scenario n of sample $\mathcal{N}$ from the solutions contained in $P_{\hat{\mathcal{N}}}^{\hat{n}}$ for $\hat{n} \in \hat{\mathcal{N}}$.

Let $(\beta^{\hat{n}}, \alpha^{\hat{n}}, u^{\hat{n}}, b^{\hat{n}}) \in P_{\hat{\mathcal{N}}}^{\hat{n}}$ be a feasible solution for RS-I-DS$(\hat{\mathcal{N}}, \hat{n})$, and $w_k^{m\hat{n}}$ be the demand for commodity $k \in K$ of class $m \in M$ under scenario $\hat{n} \in \hat{\mathcal{N}}$. It can easily be shown that $(\beta^n, \alpha^n, u^n, b^n)$ defined by (5.78)-(5.81) is feasible for RS-I-DS$(\mathcal{N}, n)$:

$$\beta_k^{mn} = \beta_k^{m\hat{n}} \quad k \in K, m \in M \tag{5.78}$$

$$\alpha_k^{mn} = \frac{w_k^{mn}}{w_k^{m\hat{n}}} \alpha_k^{m\hat{n}} \quad k \in K, m \in M \tag{5.79}$$

$$u_{ik}^{mn} = \frac{w_k^{mn}}{w_k^{m\hat{n}}} u_{ik}^{m\hat{n}} \quad k \in K, m \in M, i \in H \tag{5.80}$$

$$b_i^n = b_i^{\hat{n}} \quad i \in H \tag{5.81}$$

Consequently, the solution obtained by (5.78)-(5.81) yields a valid cut for RS-I-MP($\mathcal{N}$). To avoid overloading the master problem with too many cuts, we restrict the algorithm to selecting the best potential cut that is associated with scenario $\hat{n}^* \in \hat{\mathcal{N}}$ obtained via 5.25).

5.3.3.2 Benders decomposition for min-max regret stochastic model

In accordance with the robust-stochastic model with max-min criterion, we again assume that the hub location decisions are handled in the master problem and the rest is left to the subproblem. However as we demonstrate in this section, solving the SAA counterpart of the min-max regret stochastic model (5.44)-(5.45) is more difficult than solving the robust-stochastic model with max-min criterion (5.32)-(5.34).

For a given demand scenario n of sample $\mathcal{N}$ and revenue scenario $s \in S_r$, let $\bar{Z}^{ns}$ be an estimation of the optimal value of (5.35)-(5.40). With y set to a specific vector $y \coloneqq \bar{y}$, the *primal subproblem* RS-II-PS($\mathcal{N}$) reads as:

$$\text{RS-II-PS}(\mathcal{N}) \quad \max \quad \frac{1}{|\mathcal{N}|} \sum_{n \in \mathcal{N}} \bar{V}^n \tag{5.82}$$

$$\text{s.t.} \quad (5.53) - (5.55)$$

$$\bar{V}^n - \sum_{n \in \mathcal{N}} \sum_{k \in K} \sum_{m \in M} \sum_{a \in A_k} (r_k^{ms} - \hat{C}_{ak}) w_k^{mn} x_{ak}^{mn} \leq -\bar{Z}^{ns} \quad n \in \mathcal{N}, s \in S_r \tag{5.83}$$

$$x_{ak}^{mn} \geq 0 \quad k \in K, m \in M, a \in A_k, n \in \mathcal{N}. \tag{5.84}$$

Observe that RS-II-PS($\mathcal{N}$) can be decomposed into $|\mathcal{N}|$ independent subproblems, one for each $n \in \mathcal{N}$. Let α_k^{mn}, u_{ik}^{mn}, b_i^n, and ω^{ns} be the dual variables associated with constraints (5.53)-(5.55) and (5.83), respectively. For a given demand scenario $n \in \mathcal{N}$, the *dual subproblem* RS-II-DS($\mathcal{N}, n$) can then be stated as:

$$\text{RS-II-DS}(\mathcal{N}, n) \quad \min \quad \sum_{k \in K} \sum_{m \in M} \alpha_k^{mn} + \sum_{i \in H} \bar{y}_i (\Gamma_i b_i^n + \sum_{k \in K} \sum_{m \in M} u_{ik}^{mn}) - \sum_{s \in S_r} \bar{Z}^{ns} \omega^{ns} \tag{5.85}$$

$$\text{s.t.} \sum_{s\in S_r} \omega^{ns} = 1 \tag{5.86}$$

$$\alpha_k^{mn} + u_{ik}^{mn} + u_{jk}^{mn} + w_k^{mn}(b_i^n + b_j^n) \geq \sum_{s\in S_r} \omega^{ns}(r_k^{ms} - \hat{C}_{ijk})w_k^{mn} \quad k \in K, m \in M, (i,j) \in A_k : i \neq j \tag{5.87}$$

$$\alpha_k^{mn} + u_{ik}^{mn} + w_k^{mn} b_i^n \geq \sum_{s\in S_r} \omega^{ns}(r_k^{ms} - \hat{C}_{iik})w_k^{mn} \quad k \in K, m \in M, i \in H \tag{5.88}$$

$$\alpha_k^{mn}, u_{ik}^{mn}, b_i^n, \omega^{ns} \geq 0 \quad k \in K, m \in M, i \in H, s \in S_r. \tag{5.89}$$

Define $\bar{P}_{\mathcal{N}}^n$ as the set of extreme points of the feasible region of RS-II-DS$(\mathcal{N}, n)$ for $n \in \mathcal{N}$. Each demand scenario $n \in \mathcal{N}$ can provide a Benders cut; hence, the Benders *master problem* RS-II-MP$(\mathcal{N})$ can be reformulated as below:

$$\text{RS-II-MP}(\mathcal{N}) \quad \max \quad \frac{1}{|\mathcal{N}|}\sum_{n\in\mathcal{N}} \eta^n - \sum_{i\in H} f_i y_i \tag{5.90}$$

$$\text{s.t.} \quad \eta^n \leq \sum_{k\in K}\sum_{m\in M} \alpha_k^{mn} + \sum_{i\in H} y_i(\Gamma_i b_i^n + \sum_{k\in K}\sum_{m\in M} u_{ik}^{mn}) - \sum_{s\in S_r} \bar{Z}^{ns}\omega^{ns} \quad n \in \mathcal{N}, (\alpha^n, u^n, b^n, \omega^n) \in \bar{P}_{\mathcal{N}}^n \tag{5.91}$$

$$y_i \in \{0,1\} \quad i \in H. \tag{5.92}$$

An overview of the BD algorithm for the min-max regret stochastic model is presented in Algorithm 4. As per the robust-stochastic model with max-min criterion, we can enhance the performance of the BD algorithm by employing variable fixing techniques. However, the main difficulty incurred by the min-max regret stochastic model is the need for calculating the optimal values of the deterministic counterparts formulated as (5.35)-(5.40) for each pair of demand and revenue scenario (n, s). More specifically, each replication of the SAA requires computing the $\bar{Z}^{ns}$ values $|\mathcal{N}| \times |S_r|$ times. Hence, cardinality of the sets $\mathcal{N}$ and S_r drastically affect the computational efficiency of solving the min-max regret stochastic problem. In this section, we show how to mitigate this difficulty. We first address how to solve the Benders subproblem RS-II-DS$(\mathcal{N}, n)$ to obtain a lower bound as follows.

Algorithm 4 Benders decomposition for the min-max regret stochastic model

$UB \leftarrow +\infty, LB \leftarrow -\infty, e \leftarrow 1$
$\bar{P}^n_{\mathcal{N}} \leftarrow \emptyset \quad \forall n \in \mathcal{N}$
while $LB < UB$ **do**
  SOLVE RS-II-MP($\mathcal{N}$) and obtain y^e and Z^e_{MP}
  $UB \leftarrow Z^e_{MP}$
  for n in $\mathcal{N}$ **do**
    SOLVE RS-II-DS($\mathcal{N}, n$) with $\bar{y} = y^e$ and obtain $(\alpha^n, u^n, b^n, \omega^n)^e$ and Z^{en}_{DS}
    $\bar{P}^n_{\mathcal{N}} \leftarrow \bar{P}^n_{\mathcal{N}} \cup \{(\alpha^n, u^n, b^n, \omega^n)^e\}$
  end for
  $LB \leftarrow \max\{LB, \frac{1}{|\mathcal{N}|}\sum_{n\in\mathcal{N}} Z^{en}_{DS} - \sum_{i\in H} f_i y^e_i\}$
  $e \leftarrow e + 1$
end while

Solving the Benders subproblem. For a given demand scenario $n \in \mathcal{N}$, we solve RS-II-DS($\mathcal{N}, n$) in two sequential phases based on the set of open/closed hubs. In Phase I, the optimal value of the α- and ω-variables, along with the value of u^{mn}_{ik} and b^n_i for $i \in H^e_1$ are calculated. Similar to the robust-stochastic model with max-min criterion, it can be shown that the optimal value of u^{mn}_{ik} for $i \in H^e_1$ is equal to 0. Hence, the Phase I subproblem can be formulated as

$$\text{RS-II-DS-I}(\mathcal{N}, n) \quad \min \quad \sum_{k\in K}\sum_{m\in M} \alpha^{mn}_k + \sum_{i\in H^e_1} \Gamma_i b^n_i - \sum_{s\in S_r} \bar{Z}^n_s \omega^{ns} \tag{5.93}$$

$$\text{s.t.} \sum_{s\in S_r} \omega^{ns} = 1 \tag{5.94}$$

$$\alpha^{mn}_k + w^{mn}_k (b^n_i + b^n_j) \geq \sum_{s\in S_r} \omega^{ns}(r^{ms}_k - \hat{C}_{ijk}) w^{mn}_k \quad k \in K, m \in M, (i,j) \in A^1_{ke} \tag{5.95}$$

$$\alpha^{mn}_k + w^{mn}_k b^n_i \geq \sum_{s\in S_r} \omega^{ns}(r^{ms}_k - \hat{C}_{iik}) w^{mn}_k \quad k \in K, m \in M, i \in H^e_1 \tag{5.96}$$

$$\alpha^{mn}_k, b^n_i, \omega^{ns} \geq 0 \quad k \in K, m \in M, i \in H^e_1, s \in S_r. \tag{5.97}$$

Upon computing the optimal value of the Phase I variables, we obtain the optimal value of the rest of variables (i.e. u_{ik}^{mn} and b_i^n for $i \in H_0^e$) in Phase II. As per the robust-stochastic version with max-min criterion, in Phase II, we work with the adjusted revenue (i.e. $r_k^m = \sum_{s \in S_r} \omega^s r_k^{ms}$) for each commodity (k, m). Therefore, for a given $n \in \mathcal{N}$, the Phase II subproblem can be formulated as the linear program (5.74)-(5.77) given for the Phase II subproblem of the robust-stochastic version with max-min criterion, which can be solved as a series of LP-relaxations of knapsack problems using the same sequential procedure.

Acceleration techniques. The SAA counterpart of the min-max regret stochastic model exhibits a more repetitive structure than the SAA counterpart of the (max-min) stochastic model, in that solving the min-max regret stochastic problem for each sample $\mathcal{N}$ requires obtaining the $\bar{Z}^{ns}$ values for each demand scenario $n \in \mathcal{N}$ and each revenue scenario $s \in S_r$. Although this additional step requires extra computational effort, if treated carefully, its repetitive structure can be efficiently exploited for speeding up the SAA algorithm.

For each demand scenario $n \in \mathcal{N}$ and each revenue scenario $s \in S_r$, $\bar{Z}^{ns}$ can be obtained by solving the deterministic formulation (5.35)-(5.40) using a BD algorithm as detailed in Section 4.2.3, where for y set to a specific vector $y := \bar{y}$, the *dual subproblem* $\mathrm{DS}(\mathcal{N}, n, s)$ is formulated as:

$$\mathrm{DS}(\mathcal{N}, n, s) \quad \min \quad \sum_{k \in K} \sum_{m \in M} \alpha_k^m + \sum_{i \in H} \bar{y}_i (\Gamma_i b_i + \sum_{k \in K} \sum_{m \in M} u_{ik}^m) \tag{5.98}$$

$$\text{s.t.} \quad \alpha_k^m + u_{ik}^m + u_{jk}^m + w_k^{mn}(b_i + b_j) \geq (r_k^{ms} - \hat{C}_{ijk}) w_k^{mn} \qquad k \in K, m \in M, (i,j) \in A_k : i \neq j \tag{5.99}$$

$$\alpha_k^m + u_{ik}^m + w_k^{mn} b_i \geq (r_k^{ms} - \hat{C}_{iik}) w_k^{mn} \qquad k \in K, m \in M, i \in H \tag{5.100}$$

$$\alpha_k^m, u_{ik}^m, b_i \geq 0 \qquad k \in K, m \in M, i \in H. \tag{5.101}$$

Our proposed acceleration technique for the min-max regret stochastic model is four-fold: (i) generating valid cuts for solving scenario pair (n, s) from the cuts generated for

solving scenario pair $(\hat{n}, s)$, (ii) generating valid cuts for solving scenario pair (n, s) from the cuts generated for solving scenario pair $(n, \hat{s})$, (iii) approximating the $\bar{Z}^{ns}$ values, and (iv) generating valid cuts for solving the min-max regret stochastic problem from the cuts generated for obtaining the $\bar{Z}^{ns}$ values. We introduce the following proposition for step (i):

Proposition 5. *Let $(\alpha^{\hat{n}s}, u^{\hat{n}s}, b^{\hat{n}s})$ be a feasible solution for DS$(\hat{\mathcal{N}}, \hat{n}, s)$, and $w_k^{m\hat{n}}$ be the demand for commodity $k \in K$ of class $m \in M$ under scenario $\hat{n} \in \hat{\mathcal{N}}$. $(\alpha^{ns}, u^{ns}, b^{ns})$ defined by (5.102)-(5.104) is feasible for DS$(\mathcal{N}, n, s)$:*

$$b_i^{ns} = b_i^{\hat{n}s} \qquad i \in H \tag{5.102}$$

$$\alpha_k^{mns} = \frac{w_k^{mn}}{w_k^{m\hat{n}}} \alpha_k^{m\hat{n}s} \qquad k \in K, m \in M \tag{5.103}$$

$$u_{ik}^{mns} = \frac{w_k^{mn}}{w_k^{m\hat{n}}} u_{ik}^{m\hat{n}s} \qquad k \in K, m \in M, i \in H \tag{5.104}$$

Proof. From (5.103) and (5.104), we obtain $\alpha_k^{m\hat{n}s} = \frac{w_k^{m\hat{n}}}{w_k^{mn}} \alpha_k^{mns}$ and $u_{ik}^{m\hat{n}s} = \frac{w_k^{m\hat{n}}}{w_k^{mn}} u_{ik}^{mns}$, respectively. Feasibility of $(\alpha^{ns}, u^{ns}, b^{ns})$ for DS$(\mathcal{N}, n, s)$ can easily be verified by replacing $b_i^{\hat{n}s}$, $\alpha_k^{m\hat{n}s}$, and $u_{ik}^{m\hat{n}s}$ respectively with b_i, $\frac{w_k^{m\hat{n}}}{w_k^{mn}} \alpha_k^{mns}$, and $\frac{w_k^{m\hat{n}}}{w_k^{mn}} u_{ik}^{mns}$, in constraints (5.99)-(5.101) associated with DS$(\hat{\mathcal{N}}, \hat{n}, s)$. □

Consequently, the feasible solution obtained for DS$(\mathcal{N}, n, s)$ defined by (5.102)-(5.104) provides a valid cut for solving the demand scenario $n \in \mathcal{N}$ and revenue scenario $s \in S_r$. Note that the same proposition holds when $\hat{\mathcal{N}} = \mathcal{N}$. Similarly, Proposition 6 shows how step (ii) can be achieved by generating feasible solutions for DS$(\mathcal{N}, n, s)$ from the feasible solutions of DS$(\mathcal{N}, n, \hat{s})$.

Proposition 6. *Let $(\alpha^{n\hat{s}}, u^{n\hat{s}}, b^{n\hat{s}})$ be a feasible solution for DS$(\mathcal{N}, n, \hat{s})$, then $(\alpha^{ns}, u^{ns}, b^{ns})$ defined by (5.105)-(5.107) is feasible for DS$(\mathcal{N}, n, s)$:*

$$b_i^{ns} = b_i^{n\hat{s}} \qquad i \in H \tag{5.105}$$

$$\alpha_k^{mns} = \max\{0, \alpha_k^{mn\hat{s}} + w_k^{mn}(r_k^{ms} - r_k^{m\hat{s}})\} \qquad k \in K, m \in M \tag{5.106}$$

$$u_{ik}^{mns} = u_{ik}^{mn\hat{s}} \qquad k \in K, m \in M, i \in H \tag{5.107}$$

Proof. Replacing $b_i^{n\hat{s}}$ and $u_{ik}^{mn\hat{s}}$ respectively with b_i^{ns} and u_{ik}^{mns} in constraints (5.99) and (5.100) of DS$(\mathcal{N}, n, \hat{s})$, and adding $w_k^{mn}(r_k^{ms} - r_k^{m\hat{s}})$ to both sides of these constraints yields

$$\alpha_k^{mn\hat{s}} + w_k^{mn}(r_k^{ms} - r_k^{m\hat{s}}) + u_{ik}^{mns} + u_{jk}^{mns} + w_k^{mn}(b_i^{ns} + b_j^{ns}) \geq (r_k^{ms} - \hat{C}_{ijk})w_k^{mn}$$
$$\alpha_k^{mn\hat{s}} + w_k^{mn}(r_k^{ms} - r_k^{m\hat{s}}) + u_{ik}^{mns} + w_k^{mn}b_i^{ns} \geq (r_k^{ms} - \hat{C}_{iik})w_k^{mn}.$$

Hence, any $\alpha_k^{mns} \geq 0$ satisfying $\alpha_k^{mns} \geq \alpha_k^{mn\hat{s}} + w_k^{mn}(r_k^{ms} - r_k^{m\hat{s}})$ provides a feasible solution to DS$(\mathcal{N}, n, s)$. □

The valid cuts obtained by these propositions accelerate the BD algorithm for calculating the $\bar{Z}^{ns}$ values; however, computing the optimal values for all scenario pairs in all replications is computationally burdensome and also unnecessary. Note that sufficiently close demand scenarios are likely to result in the same optimal hub locations. Therefore, we only calculate the optimal $\bar{Z}^{ns}$ values for the first replication of the SAA algorithm, and approximate the $\bar{Z}^{ns}$ values (step (iii)) for the subsequent replications as follows.

Let $\mathcal{N}_t$ denote the realized demand sample $\mathcal{N}$ at replication t of the SAA algorithm, for $t = 1, \ldots, \mathcal{M}$. At replication $t > 1$, for a given demand scenario $n \in \mathcal{N}_t$, let $\hat{n}$ be the closest demand scenario to n among the demand scenarios in the first replication as selected via (5.25). We estimate $\bar{Z}^{ns}$ by fixing y at $\hat{y}^{\hat{n}s}$, where $\hat{y}^{\hat{n}s}$ is the optimal location of the hubs under the scenario pair $(\hat{n}, s)$ for $\hat{n} \in \mathcal{N}_1$ and $s \in S_r$. Once the $\bar{Z}^{ns}$ values are obtained, we generate valid cuts for the min-max regret stochastic problem using the following proposition (step (iv)):

Proposition 7. *Let $(\alpha^{n\hat{s}}, u^{n\hat{s}}, b^{n\hat{s}})$ be a feasible solution for DS$(\mathcal{N}, n, \hat{s})$ for some particular $\hat{s} \in S_r$, then $(\alpha^n, u^n, b^n, \omega^n)$ is feasible for RS-II-DS$(\mathcal{N}, n)$, where $(\alpha^n, u^n, b^n) = (\alpha^{n\hat{s}}, u^{n\hat{s}}, b^{n\hat{s}})$ and*

$$\omega^{ns} = 1 \text{ if } s = \hat{s} \text{ and } \omega^{ns} = 0 \text{ if } s \neq \hat{s} \qquad\qquad s \in S_r.$$

Proof. The proof can be easily verified by noting that the feasible region of DS$(\mathcal{N}, n, \hat{s})$ is equivalent to the feasible region of RS-II-DS$(\mathcal{N}, n)$ when $\omega^{n\hat{s}}$ is set to 1. □

Algorithm 5 Accelerated SAA for the min-max regret stochastic model

for t in $1, \ldots, \mathcal{M}$ **do**
  if $t = 1$ **then**
    for $s \in S_r$ **do**
      $P_1^s \leftarrow \emptyset$
      for $n \in \mathcal{N}_1$ **do**
        $\bar{P}_1^{ns} \leftarrow \emptyset$
        if $n = 1$ **then**
          if $s > 1$ **then**
            Convert the solutions contained in $P_1^{\hat{s}}$ for each $\hat{s} < s$ to feasible solutions for $\text{DS}(\mathcal{N}_1, n, s)$ using Proposition 6 and add them to P_1^s.
          end if
          Calculate $\bar{Z}^{ns}$ using the initial cuts associated with P_1^s.
          Store the obtained dual solutions in P_1^s.
          $\bar{P}_1^{ns} \leftarrow P_1^s$
        else
          Convert the solutions contained in P_1^s to feasible solutions for $\text{DS}(\mathcal{N}_1, n, s)$ using Proposition 5 and store the obtained solutions in $\bar{P}_1^{ns}$.
          Generate initial cuts for (n, s) using the solutions contained in $\bar{P}_1^{ns}$.
          Calculate $\bar{Z}^{ns}$ using the generated initial cuts.
        end if
      end for
    end for
  else
    for $n \in \mathcal{N}_t$ **do**
      Let $\hat{n}$ be the closest demand scenario in $\mathcal{N}_1$ to n obtained via 5.25.
      for $s \in S_r$ **do**
        Approximate $\bar{Z}^{ns}$ using $\hat{y}^{\hat{n}s}$.
        Convert the solutions contained in P_1^s to feasible solutions for $\text{DS}(\mathcal{N}_t, n, s)$ using Proposition 5 and store the obtained solutions in $\bar{P}_t^{ns}$.
      end for
    end for
  end if
  Obtain initial cuts for the min-max regret stochastic model associated with $\mathcal{N}_t$ using the solutions contained in $\bar{P}_t^{ns}$ using Proposition 7.
  SOLVE the min-max regret stochastic model using Algorithm 4.
end for

Note that, if we eliminate a set of hubs through variable fixing techniques, the dual variables associated with those hubs will not be computed in the subproblem. Hence, for the dual solutions obtained by a scenario pair (n, s) to be usable for another scenario pair (or for the min-max regret stochastic problem), we cannot employ the variable fixing techniques. Therefore, we sacrifice the first demand scenario of the first replication and obtain the complete dual solutions for each revenue scenario without fixing any variables. These solutions are then used for the other scenario pairs (within current replication or subsequent replications) using Propositions 5 and 6 as well as for the min-max regret problems using Proposition 7.

The proposed accelerated SAA algorithm is detailed in Algorithm 5. We refer each demand scenario by an integer n and each revenue scenario by an integer s. Moreover, P_1^s denotes the set of dual solutions obtained in solving the first demand scenario of the first replication under the revenue scenario $s \in S_r$. At replication t, $\bar{P}_t^{ns}$ consists of feasible solutions for scenario pair $(n, s) \in \mathcal{N}_t \times S_r$ obtained by converting the solutions contained in P_1^s.

5.3.4 Computational experiments and comparisons

We use the same setting as detailed in Sections 4.3 and 5.2.2 to perform computational experiments for the robust-stochastic models. In the first part of the computational experiments, we analyze our results obtained with the robust-stochastic model with max-min criterion. The second part of the experiments is devoted to the results obtained with the min-max regret stochastic model. In the last section, we compare the quality of the solutions as well as the optimal hub networks obtained from stochastic and robust-stochastic models.

5.3.4.1 Computational results with the robust-stochastic model with max-min criterion

For the analysis with max-min model, we take $\hat{r}_k^m \sim U[0, \varphi\bar{r}_k^m]$ to generate intervals of uncertainty, where φ is the maximum possible deviation from the nominal value of revenue. We first evaluate the effect of the uncertainty budget (γ_r) on total profit. We select two instances of the AP dataset on 20 and 25 nodes with $\varphi = 0.5$, and test the model using $\gamma_r \in \{0, 5\%, 10\%, \ldots, 100\%\}$. For simplicity, we use percentage to represent the budget of uncertainty which corresponds to the percentage of the revenue parameters under uncertainty.

Figures 5.3a and 5.3b plot the percentage of decrease from the nominal profit for different values of γ_r for the AP20TL and AP25LT instances, respectively. Let Z_{γ_r} denote the optimal profit obtained from the robust-stochastic model with max-min criterion when budget of uncertainty is γ_r and Z_0 denote the objective function value with the nominal profit that can be obtained from the stochastic model. The percentage of decrease from the nominal profit can then be calculated as $\frac{Z_0 - Z_{\gamma_r}}{Z_0}$ for any γ_r.

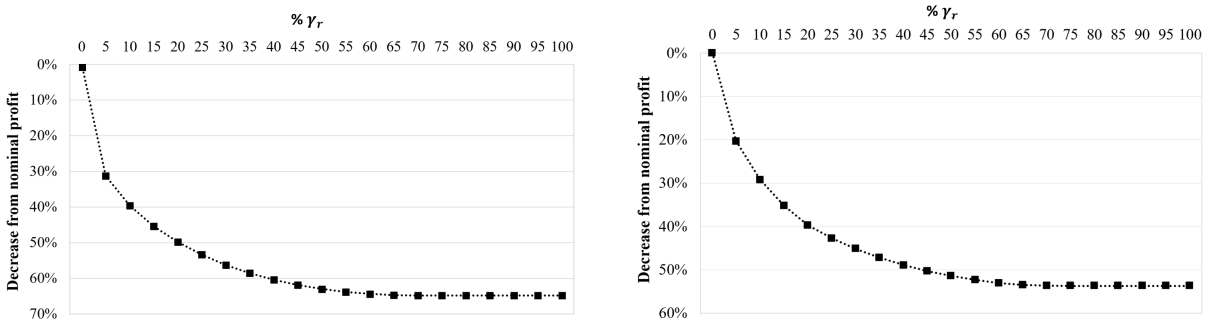

(a) AP20TL (b) AP25LT

Figure 5.3: Effect of the uncertainty budget.

It is clear that a higher value of γ_r leads to a more conservative solution with a lower Z_{γ_r}. Moreover, as shown in Bertsimas and Sim [18], Z_{γ_r} is a concave function of γ_r. Consequently, as noted from the Figures 5.3a and 5.3b, for smaller values of γ_r, percentage

of decrease from the nominal profit drops faster compared to higher values of the budget of uncertainty. In particular, when we select our budget of uncertainty with $\gamma_r \geq 55\%$, then observe from both of the figures that there is not much deviation in the optimal profits. This observation indicates that small and moderate values of γ_r provide better insights for evaluating the effects of the uncertainty budget on the solutions. For this reason, we use $\gamma_r \in \{15\%, 25\%, 50\%\}$ during the rest of our computational analysis.

We now analyze the results obtained from the max-min model for larger size instances with up to 75 nodes from the AP dataset. For each instance, we consider two values to represent the amount of deviation from the nominal value of revenues; $\varphi \in \{0.5, 1\}$. The computational results are summarized in Table 5.3. The first two columns provide the size and name of the instances and the amount of deviation, respectively. The columns labeled "Profit", "Avg. iter.", and "Time (sec)" indicate the optimal expected profit, the average number of iterations required for the convergence of the BD algorithm at each replication of SAA, and the computation time of the instances (in seconds) obtained from solving the model, respectively. The columns labeled "Open hubs" show the locations of the hub nodes. Table 5.3 is split into three parts to represent the results for $\gamma_r = 15\%$, $\gamma_r = 25\%$, and $\gamma_r = 50\%$, respectively.

All of the instances presented in Table 5.3 are solved to optimality. We observe that the computation times and average number of iterations do not vary significantly by varying γ_r values. This can be attributed to the fact that the number of dual variables associated with the intervals of uncertainty is independent from the value of γ_r. This characteristic enables the algorithm to solve instances with up to 16,875 commodities containing stochastic demand and uncertain revenue. The averages of the computational times reported in Table 5.3 for the $\gamma_r = 15\%$, 25%, and 50% instances are 3.8, 3.4, and 2.8 hours, respectively. These results clearly confirm the efficiency of the proposed algorithm for the robust-stochastic model with max-min criterion.

The profits obtained from the max-min model represent the lowest profit that can be expected, as long as the revenues comply with the model of uncertainty. This profit

Table 5.3: Computational results for the robust-stochastic model with the max-min criterion with 48 instances of the AP dataset.

Instance		$\gamma_r = 15\%$				$\gamma_r = 25\%$				$\gamma_r = 50\%$			
$\|N\|$	φ	Profit	Avg. iter.	Time (sec)	Open hubs	Profit	Avg. iter.	Time (sec)	Open hubs	Profit	Avg. iter.	Time (sec)	Open hubs
10LL	0.5	11,051	2.01	16	5,9	10,629	2.01	16	5,9	10,129	2.01	19	5,9
	1	10,057	2.01	21	5,9	9,536	2.01	19	5,9	9,336	2.01	78	5,9
10LT	0.5	2,799	2.01	14	5	2,522	2.01	13	5	2,222	2.01	13	5
	1	2,370	2.01	18	5	1,973	2.01	14	5	1,773	2.01	12	5
10TL	0.5	10,805	2.01	15	5,9	10,384	2.01	15	5,9	9,784	2.01	19	5,9
	1	9,720	2.01	21	5,9	9,098	2.01	17	5,9	9,088	2.01	77	5,9
10TT	0.5	2,409	2.01	13	5	2,349	2.01	13	5	2,049	2.01	13	5
	1	2,378	2.01	17	5	2,185	2.01	14	5	1,685	2.01	13	5
20LL	0.5	71,687	13.26	2,342	7,9,10,19	67,929	13.05	1,948	7,9,10,19	55,471	13.36	2,402	7,9,10,19
	1	49,394	9.71	1,526	7,10,19	43,784	9.5	2,257	7,10,19	26,496	7.83	2,130	10,19
20LT	0.5	33,992	8.03	2,265	5,10,12,14	31,514	7.82	1,099	5,10,12,14	24,129	6.10	1,383	5,10,12,14
	1	20,639	6.09	1,802	5,10,12,14	16,736	5.81	2,022	10,12,14	12,166	4.06	285	10,14
20TL	0.5	28,963	3.02	347	7,10	26,602	2.74	154	7,10	19,612	3.07	143	7,10
	1	16,662	3.01	311	7,10	12,667	3.17	194	7,10	9,168	3.08	105	10
20TT	0.5	5,416	2.01	78	10	4,911	2.01	71	10	4,565	2.01	57	10
	1	1,558	2.01	139	10	527	2.01	79	10	436	2.01	60	10
25LL	0.5	95,864	18.53	6,567	7,14,17,23	91,273	18.32	1,783	7,14,17,23	76,665	18.73	5,300	7,14,17,23
	1	67,639	12.63	2,028	7,14,17	60,669	12.42	3,848	7,14,17	38,708	17.63	2,035	9,17
25LT	0.5	59,640	8.02	2,413	6,9,10,12,14,25	55,493	7.91	1,555	6,9,10,12,25	44,722	9.64	2,607	6,9,10,12,25
	1	41,798	6.60	1,886	6,9,12,14,25	36,685	6.39	2,186	9,12,14,25	23,167	6.60	1,762	12,14,25
25TL	0.5	49,639	8.07	1,966	6,9,14	46,153	7.86	1,586	6,9,14	35,093	7.20	1,638	6,9,14
	1	33,417	7.20	1,118	6,9,14	27,273	6.99	2,078	6,9,14	16,152	6.06	860	14
25TT	0.5	17,306	8.03	1,933	6,10,14	15,481	7.82	1,067	10,14	12,515	8.03	1,219	10,14
	1	10,282	7.02	1,329	10,14	8,632	6.81	1,632	14	8,205	2.01	321	14
40LL	0.5	61,336	26.03	21,631	12,22,26,29	58,575	25.82	16,324	12,22,26,29	53,575	24.01	19,324	12,22,26,29
	1	42,520	25.54	20,749	17,26,35	38,203	25.33	19,017	17,26,35	31,203	23.18	18,017	17,26,35
40LT	0.5	48,425	22.13	21,852	10,14,26,30,38	46,080	21.92	18,448	10,14,26,30,38	42,080	17.42	18,448	10,14,26,38
	1	29,070	19.09	20,318	10,17,26, 38	27,736	18.88	21,547	10,26, 38	22,736	15.75	16,547	10,26, 38
40TL	0.5	42,569	16.83	8,116	14,19,29	40,477	16.12	6,903	14,19,29	35,185	10.09	71,032	14,29
	1	25,900	10.96	6,401	14,29	22,730	10.75	9,165	14,29	14,752	8.16	3,367	14,29
40TT	0.5	32,427	10.03	10,331	14,19,25,38	30,583	9.82	7,523	14,19,25,38	26,691	7.55	3,027	14,19,38
	1	20,168	8.43	8,252	14,19,38	17,523	8.22	10,048	14,19,38	11,809	4.24	948	14,38
50LL	0.5	59,282	22.71	14,393	15,28,33,35	57,541	22.5	12,143	15,28,33,35	54,541	16.94	12,143	15,28,33,35
	1	39,066	20.08	16,141	15,28,33,35	36,174	17.27	16,732	15,28,35	31,174	14.18	10,732	15,28,35
50LT	0.5	55,565	19.23	15,057	26,32,46	54,186	16.02	10,436	26,32,46	52,186	13.07	13,436	26,32,46
	1	39,119	17.08	13,326	26,32,46	35,992	9.87	14,681	26,46	30,992	8.74	8,681	26,46
50TL	0.5	34,324	9.13	9,645	26,45	32,431	8.92	5,912	26,45	27,449	8.23	6,113	26,45
	1	17,729	7.73	7,912	24	15,340	4.52	9,448	24	9,882	3.23	2,436	24
50TT	0.5	29,183	4.06	7,299	26,48	27,727	3.85	4,479	26,48	24,434	3.01	4,125	26,48
	1	16,113	3.81	6,729	26,48	13,639	3.6	8,759	26	9,800	3.02	2,403	26
75LL	0.5	93,115	47.37	68,749	14,26,35,38,56	81,343	47.16	65,231	14,26,35,38,56	55,318	41.82	63,194	14,26,38,56
	1	64,054	45.29	64,184	14,26,35,38,56	53,172	41.23	57,418	14,26,38,56	32,719	23.08	56,319	14,38,56
75LT	0.5	74,926	43.16	59,317	25,32,35,38,59	57,343	42.95	53,568	25,35,38,59	41,663	24.76	43,717	25,38,59
	1	40,963	45.83	61,732	25,32,35,38,59	31,568	40.26	55,619	25,35,38,59	24,428	19.80	21,368	25,38
75TL	0.5	52,219	11.76	47,273	14,35,37	39,618	11.21	45,236	14,35,37	25,763	9.96	20,813	14,37
	1	27,165	10.74	45,613	14,35,37	21,308	5.91	34,192	14,37	19,233	2.21	12,341	37
75TT	0.5	42,708	11.63	45,763	26,32,38,59	30,784	11.42	30,118	26,38	20,619	9.59	21,679	26,38
	1	28,816	8.89	31,573	26,38,59	17,193	8.28	29,918	26,38	14,672	2.20	11,972	38

provides a valuable information, in particular to a conservative decision maker, since the profit associated with this solution will never fall below the obtained value.

Next, we analyze the effects of variability in uncertain revenues on the optimal solutions presented in Table 5.3. When the level of uncertainty (i.e., φ and γ_r) increases, the net profit value and the number of open hubs in the optimal solutions decrease. It can also be observed that the set of open hubs with a high level of uncertainty (e.g., $\gamma_r = 50\%$ and $\varphi = 1$) is a subset of the open hubs, when the level of uncertainty is low (e.g., $\gamma_r = 15\%$ and $\varphi = 0.5$). For example, in the optimal solution of 20LL with $\gamma_r = 50\%$ and $\varphi = 1$, hubs are located at nodes 10 and 19. While, by decreasing γ_r to 15% and φ to 0.5, hubs are located at nodes 7, 9, 10, and 19.

Table 5.4: Percentage of demand satisfied for each demand class with the max-min model.

Instance type	φ	$\gamma_r = 15\%$				$\gamma_r = 25\%$				$\gamma_r = 50\%$			
		Demand Class (%)			Avg.	Demand Class (%)			Avg.	Demand Class (%)			Avg.
		m=1	m=2	m=3		m=1	m=2	m=3		m=1	m=2	m=3	
LL	0.5	97.56	84.19	69.38	83.71	87.50	74.75	58.42	73.56	74.89	62.81	44.81	60.84
	1	87.80	75.94	50.83	71.52	78.42	67.10	41.85	62.45	66.58	55.96	31.07	51.20
LT	0.5	91.13	78.44	57.69	75.75	84.29	69.84	48.88	67.67	72.92	57.68	37.97	56.19
	1	83.40	68.46	39.14	63.67	73.65	59.34	30.87	54.62	62.90	49.21	19.89	44.00
TL	0.5	93.69	82.34	61.56	79.20	86.66	71.72	51.08	69.82	75.66	58.29	38.05	57.33
	1	85.69	71.10	40.62	65.80	77.27	66.41	32.07	58.58	65.54	56.78	20.81	47.71
TT	0.5	83.62	72.19	42.38	66.06	76.43	65.68	32.75	58.29	65.53	54.48	21.89	47.30
	1	73.73	63.00	26.98	54.57	64.45	53.98	18.14	45.52	53.02	41.70	8.62	34.45

Table 5.4 presents the percentages of satisfied demand from different market segments. For a given (φ, γ_r) pair, the averages for each demand class are calculated over instances from Table 5.3 with the same type of installation costs and capacities. The average percentages of total satisfied demand are provided in the last columns corresponding to each γ_r value. When φ or γ_r value increases, the percentage of satisfied demand for all three market segments decreases as expected. For a given (φ, γ_r) pair, in the instances with

the same configuration of hub installation costs and capacities, the first class is the one with the highest percentages of satisfied demand, while the third demand class has the least. This is because serving the first and third classes result the highest and lowest revenues, respectively. On average, instances with loose capacities (LL and TL) yield higher percentages compared to the instances with tight capacities (LT and TT).

5.3.4.2 Computational results with the min-max regret stochastic model

We now analyze the results obtained with the min-max regret stochastic model. We use instances with up to 75 nodes from the AP dataset. For each instance, we perform two sets of experiments each involving five different scenarios with uncertain revenues (i.e., $|S_r| = 5$). In the first set, revenue scenarios are randomly generated from the interval $[0.75\bar{r}_k^m, \bar{r}_k^m]$, while in the second set, revenue scenarios are drawn from the interval $[0.5\bar{r}_k^m, \bar{r}_k^m]$, where $\bar{r}_k^m$ is the nominal revenue of commodity k of class m.

The computational results are summarized in Table 5.5, which is split into two parts to represent the results for $r_k^{ms} \in [0.75\bar{r}_k^m, \bar{r}_k^m]$ and $r_k^{ms} \in [0.5\bar{r}_k^m, \bar{r}_k^m]$, respectively. In this table, the column "Regret" indicates the optimal regret of the problem and "Avg. profit" represents the average anticipated profits, which are computed by taking the average profits over 50 demand and 5 revenue scenarios in 60 replications. The rest of the columns report the same as in Table 5.3.

All of the instances in Table 5.5 are solved to optimality. The CPU times and average number of iterations required for solving the instances to optimality indicate the efficiency and robustness of the algorithm and also the acceleration techniques proposed for the min-max regret stochastic model. As can be observed from Table 5.5, different revenue intervals have no significant impact on the performance of the algorithm. In particular, the averages of the computational time for $r_k^{ms} \in [0.75\bar{r}_k^m, \bar{r}_k^m]$ and $r_k^{ms} \in [0.5\bar{r}_k^m, \bar{r}_k^m]$ are 3.8 and 3.7 hours, respectively.

The regret values reported in Table 5.5 indicate the maximum amount of profit that can be lost under this data uncertainty; implying that if the decision maker employs the

Table 5.5: Computational results for the min-max regret stochastic model with 24 instances of the AP dataset.

Instance	$r_k^{ms} \in [0.75\bar{r}_k^m, \bar{r}_k^m]$					$r_k^{ms} \in [0.5\bar{r}_k^m, \bar{r}_k^m]$				
$\|H\|$	Regret	Avg. profit	Avg. iter.	Time (sec)	Open hubs	Regret	Avg. profit	Avg. iter.	Time (sec)	Open hubs
10LL	139	13,642	2.00	39	5,9	678	8,379	2.00	40	5,9
10LT	565	4,700	2.00	31	5	1,296	1,692	2.00	39	5
10TL	137	11,023	2.00	32	5,9	975	7,942	2.00	31	5,9
10TT	561	3,560	2.00	26	5	1,368	1,799	2.00	31	5
20LL	550	73,309	5.70	2,237	7,9,10,19	2,323	40,839	7.20	1,820	7,10,19
20LT	902	35,684	3.04	1,946	5,10,12,14	1,994	23,234	6.00	1,241	5,10,14
20TL	1,027	29,181	2.03	104	7,10	2,137	21,532	3.00	144	7,10
20TT	1,074	7,231	2.00	91	10	1,799	5,712	2.00	102	10
25LL	145	94,318	2.10	4,563	7,14,17,23	781	70,435	3.84	4,548	7,14,17,23
25LT	383	59,317	2.00	5,394	6,9,10,12,14,25	1,203	41,059	5.03	5,637	6,9,12,14,25
25TL	760	48,941	2.90	2,572	6,9,14	1,094	31,520	4.00	2,776	6,9,14
25TT	979	17,593	4.00	1,774	10,14	1,872	11,451	3.00	457	14
40LL	219	65,561	6.07	22,437	12,22,26,29	935	49,338	6.79	18,717	12,26,29
40LT	189	56,402	4.70	20,214	12,14,26,29,30,38	869	37,804	4.03	15,749	14,26,29,38
40TL	127	48,637	2.00	4,426	14,19,29	929	34,389	2.21	2,616	14,29
40TT	397	37,614	4.01	9,180	14,19,25,38	1,170	25,789	2.16	4,736	14,19,38
50LL	126	64,073	4.09	14,718	15,28,33,35	489	35,848	5.12	15,134	15,28,33,35
50LT	148	60,578	2.00	7,625	6,26,32,46	577	35,812	4.07	7,526	6,26,32,46
50TL	233	37,516	3.00	4,712	26,45	780	15,456	4.40	4,495	26,45
50TT	363	31,974	2.00	5,021	26,48	1,083	13,384	2.00	5,549	26,48
75LL	368	100,106	5.86	72,163	14,23,35,38,56	954	59,933	6.14	74,318	14,23,35,38,56
75LT	464	80,243	4.91	67,335	14,25,32,38,59	1,063	37,002	5.08	67,660	14,25,32,38,59
75TL	534	55,236	4.79	43,307	14,35,37	1,187	24,537	4.36	47,208	14,35,37
75TT	599	46,406	4.15	37,639	26,32,38	1,608	25,810	4.09	41,314	26,32,38

obtained solution, the anticipated loss in profit is guaranteed to be less than this value. Moreover, the average profits provide an insight on the expected profit.

We now analyze the effect of the lower bound of the interval from which revenue scenarios are generated on the optimal solutions. For a given instance, when the lower bound decreases from 0.75 to 0.5, that is, when the range of fluctuations in revenue values increases, the regret of the solution increases, while the average profit and the optimal number of open hubs decrease. This is because with a wider range of fluctuations in the data, we would expect lower revenues. Accordingly, the installation cost of fewer hubs can be justified by the expected revenue. It is worthwhile to also note that the set of open hubs, when $r_k^{ms} \in [0.5\bar{r}_k^m, \bar{r}_k^m]$, turned out to be a subset of the open hubs, when $r_k^{ms} \in [0.75\bar{r}_k^m, \bar{r}_k^m]$ in all the instances in Table 5.5.

Table 5.6: Percentage of demand satisfied for each demand class with min-max regret model.

Instance type	$r_k^{ms} \in [0.75\bar{r}_k^m, \bar{r}_k^m]$				$r_k^{ms} \in [0.5\bar{r}_k^m, \bar{r}_k^m]$			
	Demand Class (%)			Avg.	Demand Class (%)			Avg.
	m=1	m=2	m=3		m=1	m=2	m=3	
LL	97.19	83.34	48.67	76.40	93.21	74.66	37.56	68.48
LT	89.90	70.80	36.68	65.79	84.02	58.25	26.97	56.41
TL	92.21	71.38	38.35	67.31	88.07	62.51	28.05	59.55
TT	76.90	47.51	17.96	47.46	66.09	32.70	12.56	37.12

Table 5.6 presents the percentages of satisfied demand from different market segments for $r_k^{ms} \in [0.75\bar{r}_k^m, \bar{r}_k^m]$ and $[0.5\bar{r}_k^m, \bar{r}_k^m]$. When the lower bound of the interval decreases, the percentage of satisfied demand for all three market segments also decreases. Similar to our observations with Table 5.4, in the instances with the same configuration, the first and third classes result in the highest and lowest percentages of satisfied demand, respectively. For a given revenue interval, the percentage of satisfied demand in the instances with loose capacities, on average, is higher than that of the instances with tight capacities.

5.3.4.3 Comparison of stochastic and robust-stochastic solutions

In this section, we compare the solutions obtained from the stochastic and the two robust-stochastic models to analyze the effect of uncertain revenues. For the stochastic model, we use the nominal revenues (i.e., $\bar{r}_k^m$). For the robust-stochastic models, the set of revenue scenarios considered in the min-max regret model (i.e., S_r) should comply with the requirements of the uncertainty sets considered in the max-min model (i.e., φ and γ_r). Recall that in the max-min version, we use φ to determine the variability in uncertain revenue, such that $\hat{r}_k^m \sim U[0, \varphi\bar{r}_k^m]$ and the interval of uncertainty for revenue is $[\bar{r}_k^m - \hat{r}_k^m, \bar{r}_k^m]$. These intervals are used to satisfy the budget of uncertainty constraint (5.29). For the min-max regret stochastic model, we generate ten revenue scenarios (i.e., $|S_r| = 10$) using the same intervals as in the max-min version (i.e., $r_k^{ms} \in [\bar{r}_k^m - \hat{r}_k^m, \bar{r}_k^m]$ for each $s \in S_r$) and implicitly satisfy the budget of uncertainty constraint (5.29) by ensuring that $\sum_k \sum_m \frac{\bar{r}_k^m - r_k^{ms}}{\hat{r}_k^m} \leq \gamma_r$, for each scenario $s \in S_r$.

Note that each model optimizes a different metric, hence, we cannot compare the quality of the solutions based on the individual objective function values. However, we can compare the hub networks obtained from each of the models. We suggest evaluating the quality of the solutions under two metrics: the profit that can be expected from each solution, and the frequency at which each solution attains the highest profit among other solutions.

For the first metric, let $(\tilde{x}, \tilde{y})$ denote the optimal solution obtained from any of the stochastic or robust-stochastic models. For revenue $r_k^m \in [\bar{r}_k^m - \hat{r}_k^m, \bar{r}_k^m]$, the total profit associated with a solution $(\tilde{x}, \tilde{y})$ is calculated as:

$$\begin{aligned} Z(\tilde{x}, \tilde{y}) &= E_\xi[\sum_{k\in K}\sum_{m\in M}\sum_{a\in A_k}(r_k^m - \hat{C}_{ak})w_k^m(\xi)\tilde{x}_{ak}^m(\xi)] - \sum_{i\in H}\tilde{y}_i f_i \\ &= \sum_{k\in K}\sum_{m\in M} r_k^m \tilde{X}_k^m - \tilde{C} \end{aligned} \tag{5.108}$$

where

$$\tilde{X}_k^m = E_\xi[\sum_{a\in A_k} w_k^m(\xi)\tilde{x}_{ak}^m(\xi)] \text{ and } \tilde{C} = E_\xi[\sum_{k\in K}\sum_{m\in M}\sum_{a\in A_k}\hat{C}_{ak}w_k^m(\xi)\tilde{x}_{ak}^m(\xi)] + \sum_{i\in H}\tilde{y}_i f_i.$$

Recall that r_k^m is a random variable (with unknown distribution); therefore, $Z(\tilde{x}, \tilde{y})$ is also a random variable with the expected value

$$E_r[Z(\tilde{x}, \tilde{y})] = \sum_{k \in K} \sum_{m \in M} E[r_m^k] \tilde{X}_k^m - \tilde{C}. \tag{5.109}$$

In our experiments, we adapt the SAA scheme and use $|\mathcal{N}| = 50$ demand scenarios. Moreover, we assume that $r_k^m \sim U[\bar{r}_k^m - \hat{r}_k^m, \bar{r}_k^m]$; therefore, $E_r[Z(\tilde{x}, \tilde{y})]$ can easily be computed by setting $E[r_m^k] = \bar{r}_k^m - 0.5\hat{r}_k^m$.

The second metric estimates the percentage that a solution outperforms the other two solutions in terms of the profit that can be obtained under different revenue realizations. To compute these percentages, we generate a large sample of revenue scenarios (e.g. of size 1,000) and estimate the percentages by counting the realizations under which each model outperforms the others.

We performed the above analysis using four instances from the AP dataset: 20LL, 25LT, 40TL, and 50LL. For each instance, we consider five levels of variability for the revenue intervals, $\varphi \in \{0.2, 0.4, 0.6, 0.8, 1\}$, and two values for the budget of uncertainty with $\gamma_r \in \{25\%, 50\%\}$. Computational results are reported in Table 5.7. Columns under the heading of "Expected profit" represent the expected profit obtained from the stochastic, robust-stochastic model with max-min criterion, and min-max regret stochastic model, respectively. Columns under the heading "Frequency of attaining the highest expected profit (%)", on the other hand, provide the percentage that each model yields the highest profit among the three models under 1000 scenarios. The bold entries in Table 5.7 highlight the highest expected profit for each instance.

The solutions obtained from both of the robust-stochastic models outperform the solutions obtained from the stochastic model based on the nominal revenues, in general. On average, the robust-stochastic models yield significantly higher expected profits compared to the stochastic model. More specifically, in our experiments, there is a 97% chance that at least one of the robust-stochastic models dominates the nominal case. The robustness of the solutions obtained from the robust-stochastic models increases as the uncertainty in

the revenues (i.e. φ) increases. These observations underline the robustness of the solutions obtained from the robust-stochastic models over the stochastic model and justify the need for incorporating both sources of uncertainty in decision making.

Table 5.7: Profit comparison with stochastic and robust-stochastic models.

Instance		$\gamma_r = 25\%$						$\gamma_r = 50\%$					
		Expected profit			Frequency of attaining the highest expected profit (%)			Expected profit			Frequency of attaining the highest expected profit (%)		
$\|N\|$	φ	Nominal revenue	Max-min criterion	Min-max regret	Nominal revenue	Max-min criterion	Min-max regret	Nominal revenue	Max-min criterion	Min-max regret	Nominal revenue	Max-min criterion	Min-max regret
20LL	0.2	42,746	**42,791**	42,748	22.7	54.5	22.8	42,746	42,899	**43,063**	0.1	8.0	91.9
	0.4	32,896	34,671	**36,210**	0.0	0.0	100.0	32,896	35,232	**36,396**	0.0	0.0	100.0
	0.6	23,047	26,225	**29,678**	0.0	0.0	100.0	23,047	27,950	**29,879**	0.0	0.0	100.0
	0.8	13,197	18,720	**23,180**	0.0	0.0	100.0	13,197	18,985	**23,602**	0.0	0.0	100.0
	1	3,348	14,087	**16,769**	0.0	2.4	97.6	3,348	16,298	**17,595**	0.0	12.9	87.1
25LT	0.2	80,587	80,373	**80,609**	23.3	0.0	76.7	80,587	80,425	**80,655**	4.8	0.0	95.2
	0.4	69,063	67,812	**69,225**	9.1	0.0	90.9	69,063	65,583	**69,324**	2.4	0.0	97.6
	0.6	57,539	53,817	**57,988**	1.9	0.0	98.1	57,539	52,355	**58,038**	17.9	0.0	82.1
	0.8	46,015	42,143	**46,948**	0.4	0.0	99.6	46,015	40,420	**49,117**	0.0	0.0	100.0
	1	34,491	34,108	**36,131**	0.2	3.5	96.3	34,491	34,634	**41,383**	0.0	0.0	100.0
40TL	0.2	52,727	52,659	52,830	0.0	0.0	100.0	52,727	52,666	**52,839**	0.0	0.0	100.0
	0.4	45,753	45,488	45,935	0.0	0.0	100.0	45,753	45,363	**45,950**	0.0	0.0	100.0
	0.6	38,779	**40,131**	39,142	0.0	100.0	0.0	38,779	**39,864**	39,541	0.0	95.6	4.4
	0.8	31,805	31,531	**32,664**	0.0	0.0	100.0	31,805	31,905	**36,304**	0.0	0.0	100.0
	1	24,831	23,562	**26,216**	0.0	0.0	100.0	24,831	24,353	**30,462**	0.0	0.0	100.0
50LL	0.2	54,568	**54,692**	54,681	0.0	83.6	16.4	54,568	54,684	**54,705**	0.0	0.6	99.4
	0.4	47,232	47,354	**47,449**	0.0	3.3	96.7	47,232	47,485	**47,519**	0.0	27.1	72.9
	0.6	39,897	**40,279**	40,181	0.0	77.4	22.6	39,897	**42,151**	40,762	0.0	100.0	0.0
	0.8	32,562	**37,606**	33,286	0.0	100.0	0.0	32,562	**38,646**	36,247	0.0	100.0	0.0
	1	25,226	**28,177**	26,323	0.0	100.0	0.0	25,226	**31,280**	29,937	0.0	99.9	0.1
Avg.		39815	40811	**41910**	2.9	26.2	70.9	39815	41159	**43166**	1.3	22.2	76.5

When the two robust-stochastic models are compared with each other, the min-max regret model turned out to be likely to yield the highest profit. In particular, the min-max regret model attained the highest profit in 71% of the instances whereas the max-min model attained the highest profit only in 22%. It can also be observed from the results reported in Table 5.7 that increasing the budget of uncertainty from $\gamma_r = 25\%$ to 50% results in a higher expected profit for the robust-stochastic models, on average. This suggests a positive effect of increasing the level of conservatism on the quality of the solutions obtained from

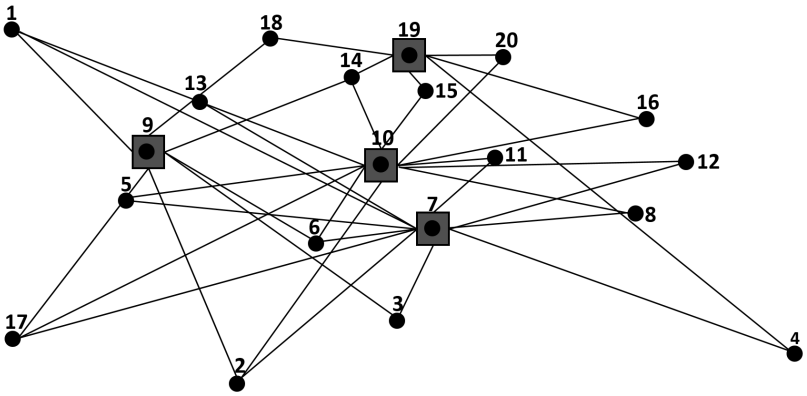

(a) Stochastic solution with nominal revenue

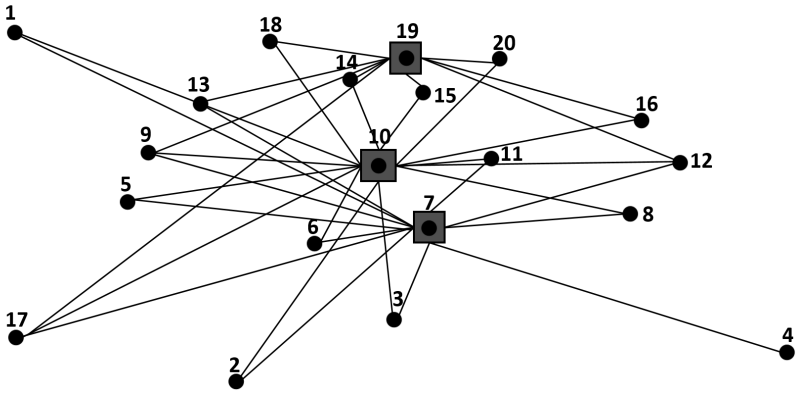

(b) Robust-stochastic solution with max-min criterion

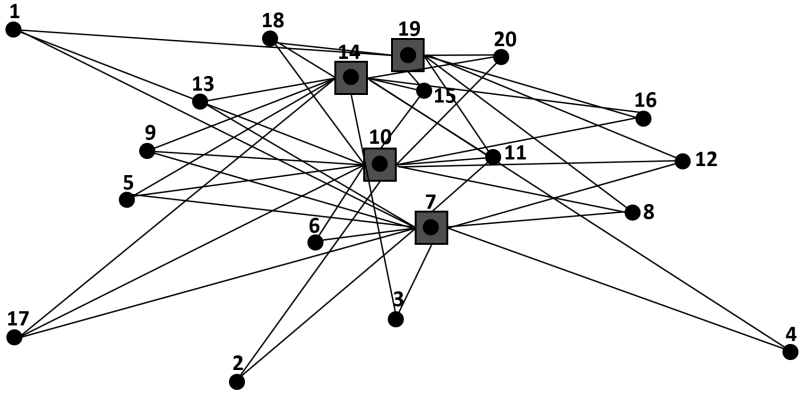

(c) Min-max regret stochastic solution

Figure 5.4: Hub networks of stochastic and robust-stochastic models for 20LL from AP dataset with $\varphi = 0.6$ and $\gamma_r = 0.5$.

the robust-stochastic models. Increasing the level of conservatism plays a role in favour, in particular, of the min-max regret model, as it not only increases the expected profit, but also increases the percentage that this model yields the highest profit among the three models.

We now depict the differences between the optimal hub networks obtained with stochastic and robust-stochastic models on the 20LL instance from the AP dataset with $\varphi = 0.6$ and $\gamma_r = 0.5$. Figures 5.4a, 5.4b, and 5.4c show the optimal hub networks from stochastic, max-min, and min-max regret models, respectively. In these figures, squares represent the established hubs and the thin lines the allocation connections. To provide a better representation, we omitted the inter-hub links in these figures. Note that each model selects a different set of hub locations. The least number of hubs are opened in Figure 5.4b, which corresponds to the conservative attitude of the max-min criterion.

Apart from the locations of the hubs, another difference can be observed on the number of allocation links. When there is uncertainty in revenues (Figures 5.4b and 5.4c), more access network connections are built compared with the nominal revenue setting in the stochastic model (Figure 5.4a). Note that the commodities with higher nominal revenues are more prone to revenue loss, in general. This is because deviation from the nominal revenue is a fraction of the nominal value. Accordingly, due to limited capacities for hubs, when revenues are uncertain, the commodities with lower revenues may also become desirable to be satisfied. This results in building denser hub networks with more allocation connections.

5.4 Conclusion

In this chapter, we first addressed demand uncertainty and proposed a two-stage stochastic program for the profit maximizing hub location problems with capacity allocation. We then developed robust-stochastic models for the problem in which two different types of uncertainty including stochastic demand and uncertain revenue were simultaneously in-

corporated into the problem. To incorporate uncertain revenues into the problem, we employed robust optimization techniques and considered two particular cases including interval representation with a max-min criterion and discrete scenarios using a min-max regret objective. We proposed mixed integer programming formulations for each of these cases and showed that the robust-stochastic version with max-min criterion is a special case of the min-max regret stochastic model.

We developed exact algorithms based on Benders decomposition coupled with sample average approximation scheme to solve the proposed models. We additionally developed novel acceleration techniques to enhance the performance of the algorithms enabling them to solve large-scale intractable instances of the stochastic and robust-stochastic problems. The implementation of these acceleration techniques resulted in up to five times improvement in CPU times with the stochastic model. We performed extensive computational experiments on the well-known AP dataset to evaluate the efficiency of the algorithms and also to analyze the effects of uncertainty under different settings. The results show that our algorithms were able to optimally solve instances involving up to 75 nodes and 16,875 commodities of different demand classes, confirming the efficiency of the algorithms.

The results obtained from the stochastic and robust-stochastic models provided several observations, which can be used as a guideline in the design of optimal hub networks to maximize profit. For example, in the stochastic model, the amount of net profit is very sensitive to the variance of the stochastic demand. However, it was observed that the long-term location decisions do not change significantly under these variations. In the robust-stochastic models, on the other hand, the net profit and the number of open hubs in the optimal solutions decrease significantly by increasing level of uncertainty associated with the revenues.

We also compared the quality of the solutions obtained from the stochastic and robust-stochastic models. The expected profit obtained from both of the robust-stochastic models is significantly higher than that of the stochastic model. We additionally observe that the uncertainty associated with revenues results in building denser hub networks with a higher

number of allocation connections.

Chapter 6

Conclusions and Future Work

This chapter provides a summary and states the contributions of the thesis as well as future research directions.

6.1 Summary and Contributions

In this thesis, we incorporated revenue and profit within hub location problems and relaxed the assumption of forcing all demand to be served while determining the optimal hub locations, allocations, and network flows.

In Chapter 3, we introduced new problems and developed mathematical models determining the locations of hubs, designing the hub networks, and routing the demand in order to maximize profit. We proposed novel mathematical formulations considering the single and multiple as well as the r-allocation patterns. For each allocation pattern, we also modeled the versions in which direct connections between non-hub nodes are allowed. The proposed models design hub networks in the most profitable way considering all possibilities for shipments. To test and evaluate the performances of the models, we used two well-known data sets from the literature. We analyzed the resulting hub networks under

various parameter settings. Furthermore, the effect of the economies of scale discount on total profit was also analyzed and the trade-off between different allocation strategies as well as the impact of allowing for direct connections were explored.

The results provided insights on where to locate hubs, how to design hub networks, what portion of the demand to serve, and how to route flows. The best net profit values were obtained with the multiple allocation model allowing for direct connections, whereas the lowest profits were obtained with the single allocation model when direct connections are not allowed. The results also showed that the decision maker can obtain significantly more profit when the discount on transportation costs due to economies of scale is higher.

In Chapter 4, we considered revenue management decisions within hub location problems and determined how to allocate available capacities of hubs to demand of commodities from different market segments. We proposed a strong MILP formulation of the problem and developed two exact algorithms based on a Benders reformulation to solve large-size instances of the problem. We introduced a new methodology to strengthen the Benders optimality cuts by decomposing the subproblem in a two-phase fashion and proposed two algorithms. The first algorithm is based on solving the subproblem as a set of LP-relaxations of maximum weighted matching problems, while the second solves the subproblem as a series of LP-relaxations of knapsack problems. The algorithms were enhanced by the integration of improved variable fixing techniques.

The major contribution of this chapter was the methodology. We developed a new two-phase methodology for solving the subproblem to strengthen the Benders optimality cuts, and proposed two new Benders-based algorithms to optimally solve large-scale instances of the profit maximizing hub location problems with capacity allocation. We showed that both algorithms result in generating very strong cuts that outperform the best known cuts from the literature (Pareto-optimal cuts; Magnanti and Wong 61) in terms of both quality and computational efficiency. We also proposed several variable fixing techniques improving the convergence. The decomposition methodology for solving the Benders subproblem as well as the improved variable fixing proposed in this thesis can be used to solve several

classes of transportation and network optimization problems, including, but not limited to, other facility location and network design problems.

The efficiency and robustness of the algorithms were evaluated through extensive computational experiments. To date, the largest capacitated hub location instances that could be solved optimally contained 300 nodes (Contreras et al. 37). Our computational results showed that large-scale instances with up to 500 nodes can be solved to optimality with our methodology, while considering an even more difficult problem setting with generic capacity constraints, multiple demand segments, and a profit maximizing objective function.

In Chapter 5, we first proposed a two-stage stochastic program for profit maximizing hub location problems with capacity allocation by considering uncertainty associated with the demand. We then extended the model by investigating robust-stochastic formulations for the problem in which two different types of uncertainty including stochastic demand and uncertain revenue were simultaneously incorporated into the problem. To incorporate uncertain revenues into the problem, we employed robust optimization techniques and considered two particular cases including interval representation with a max-min robustness criterion and discrete scenarios using a min-max regret objective. We proposed mixed integer programming formulations for each of theses cases and developed Benders-based algorithms coupled with sample average approximation scheme to obtain solutions to problems with large number of scenarios. We additionally proposed novel acceleration techniques to improve the convergence of the algorithms.

The main contribution of this chapter from a modeling perspective was that we developed novel robust-stochastic programming approaches to simultaneously model two different types of uncertainty, in particular, stochastic demand and uncertain revenues. Moreover, we proved that the robust-stochastic version with max-min criterion can be viewed as a special case of the min-max regret stochastic model. To the best of our knowledge, this is the first study that compares two robust approaches under a stochastic setting. The proposed modeling techniques can be used to formulate uncertainty in other types of optimization problems.

From a methodological point of view, our contribution was to extend the two-phase methodology introduced in Chapter 4 for strengthening the Benders optimality cuts in order to optimally solve stochastic and robust-stochastic versions of the profit maximizing hub location problems with capacity allocation. Furthermore, we developed a general technique for accelerating Benders decomposition coupled with SAA capable of reusing the cuts generated during the SAA process. We showed that implementation of this acceleration technique can result in up to five times improvement in CPU times. Moreover, the effectiveness of this technique was highlighted especially for the min-max regret stochastic model, enabling our algorithm to solve large-scale intractable instances of this problem. We performed considerable computational analysis and were able to solve instances with up to 75 nodes and 16,875 commodities of multiple demand classes, which are the largest set of instances that have been solved in the literature for any type of stochastic hub location problems.

We compared the quality of the solutions obtained from the stochastic and robust-stochastic models. The results provided several important insights in the design of optimal hub networks to maximize profit. For example, the expected profit obtained from both of the robust-stochastic models are significantly higher than that of the stochastic model. In the design of hub networks, the uncertainty associated with the revenues results in building denser hub networks with a higher number of allocation connections. These observations justify the need for embedding both sources of uncertainty to design robust hub networks.

6.2 Future Research Directions

Revenue can be considered in hub location models either in the objective function or as a constraint. Profit maximizing hub location problems that were studied throughout this thesis consider revenue only in the objective function where the total profit is calculated by subtracting total cost from the total revenue. Another way of modeling revenue in HLPs is by maximizing total revenue (not profit), subject to a given budget. These type

of formulations are referred as orienteering problems in vehicle routing literature (see, e.g.,Vansteenwegen et al. [97] and Gunawan et al. [53]). Unlike maximizing profit, in orienteering problems, costs are excluded from the objective function, but, constrained by a predetermined amount of budget. In orienteering HLPs, the aim can be to decide which set of or what proportion of origin-destination pairs to serve to maximize total revenue without exceeding the given budget.

Another future direction would be to incorporate pricing decisions within hub location problems. In this setting, revenues are considered as decision variables rather than input parameters. To model these problems, in addition to the main decisions considered in hub location problems (e.g., the locations of hubs, the allocations of demand nodes to the hubs, and the routes of flows through the network), the price setting decisions also need to be determined to maximize profit.

From the cost point of view, the problems introduced in this thesis obey the classical assumption in hub location studies, where the economies of scale is exploited between hubs. Different approaches can be considered to incorporate economies of scale into the proposed models, including flow dependent discounts for inter-hub links using non-linear cost functions (Bryan [20], Klincewicz [58], and de Camargo et al. [43]), hub arc location models (Campbell et al. [31] and Campbell et al. [32]), incomplete inter-hub network designs (Alumur et al. [6] and Contreras et al. [38]), models with fixed and variable cost components such as modeling fixed and variable costs of vehicles (Kimms [56] and Serper and Alumur [89]), and considering economies of scale with flow thresholds (Podnar et al. [82]).

References

[1] Adulyasak, Y., Cordeau, J.-F., Jans, R., 2015. Benders decomposition for production routing under demand uncertainty. Operations Research 63 (4), 851–867.

[2] Aissi, H., Bazgan, C., Vanderpooten, D., 2009. Min–max and min–max regret versions of combinatorial optimization problems: A survey. European Journal of Operational Research 197 (2), 427–438.

[3] Alibeyg, A., Contreras, I., Fernández, E., 2016. Hub network design problems with profits. Transportation Research Part E: Logistics and Transportation Review 96, 40–59.

[4] Alibeyg, A., Contreras, I., Fernández, E., 2018. Exact solution of hub network design problems with profits. European Journal of Operational Research 266 (1), 57–71.

[5] Alumur, S. A., Kara, B. Y., 2008. Network hub location problems: The state of the art. European Journal of Operational Research 190 (1), 1–21.

[6] Alumur, S. A., Kara, B. Y., Karasan, O. E., 2009. The design of single allocation incomplete hub networks. Transportation Research Part B: Methodological 43 (10), 936–951.

[7] Alumur, S. A., Kara, B. Y., Karasan, O. E., 2012. Multimodal hub location and hub network design. Omega 40 (6), 927–939.

[8] Alumur, S. A., Nickel, S., Saldanha-da Gama, F., 2012. Hub location under uncertainty. Transportation Research Part B: Methodological 46 (4), 529–543.

[9] Alumur, S. A., Yaman, H., Kara, B. Y., 2012. Hierarchical multimodal hub location problem with time-definite deliveries. Transportation Research Part E 48, 1107–1120.

[10] Álvarez-Miranda, E., Ljubić, I., Toth, P., 2013. Exact approaches for solving robust prize-collecting steiner tree problems. European Journal of Operational Research 229 (3), 599–612.

[11] Aykin, T., 1994. Lagrangian relaxation based approaches to capacitated hub-and-spoke network design problem. European Journal of Operational Research 79 (3), 501–523.

[12] Aykin, T., 1995. Networking policies for hub-and-spoke systems with application to the air transportation system. Transportation Science 29 (3), 201–221.

[13] Balas, E., 2007. The prize collecting traveling salesman problem and its applications. In: The traveling salesman problem and its variations. Springer, pp. 663–695.

[14] Balas, E., Zemel, E., 1980. An algorithm for large zero-one knapsack problems. Operations Research 28 (5), 1130–1154.

[15] Beasley, J. E., 1990. OR Library: Hub location. http://people.brunel.ac.uk/mastjjb/jeb/ orlib/phubinfo.html.

[16] Ben-Tal, A., Goryashko, A., Guslitzer, E., Nemirovski, A., 2004. Adjustable robust solutions of uncertain linear programs. Mathematical Programming 99 (2), 351–376.

[17] Bertsimas, D., Brown, D. B., Caramanis, C., 2011. Theory and applications of robust optimization. SIAM review 53 (3), 464–501.

[18] Bertsimas, D., Sim, M., 2003. Robust discrete optimization and network flows. Mathematical Programming 98 (1-3), 49–71.

[19] Boland, N., Krishnamoorthy, M., Ernst, A. T., Ebery, J., 2004. Preprocessing and cutting for multiple allocation hub location problems. European Journal of Operational Research 155 (3), 638–653.

[20] Bryan, D., 1998. Extensions to the hub location problem: Formulations and numerical examples. Geographical Analysis 30 (4), 315–330.

[21] Burkard, R. E., Dell'Amico, M., Martello, S., 2009. Assignment problems. Vol. 125. SIAM.

[22] Camargo, R. S., de Miranda Jr, G., 2012. Single allocation hub location problem under congestion: Network owner and user perspectives. Expert Systems with Applications 39 (3), 3385–3391.

[23] Camargo, R. S., de Miranda Jr, G., Ferreira, R. P., 2011. A hybrid outer-approximation/Benders decomposition algorithm for the single allocation hub location problem under congestion. Operations Research Letters 39 (5), 329–337.

[24] Camargo, R. S., de Miranda Jr, G., Løkketangen, A., 2013. A new formulation and an exact approach for the many-to-many hub location-routing problem. Applied Mathematical Modelling 37 (12-13), 7465–7480.

[25] Camargo, R. S., de Miranda Jr, G., Luna, H., 2008. Benders decomposition for the uncapacitated multiple allocation hub location problem. Computers & Operations Research 35 (4), 1047–1064.

[26] Camargo, R. S., de Miranda Jr, G., Luna, H. P. L., 2009. Benders decomposition for hub location problems with economies of scale. Transportation Science 43 (1), 86–97.

[27] Camargo, R. S., de Miranda Jr, G., O'Kelly, M. E., Campbell, J. F., 2017. Formulations and decomposition methods for the incomplete hub location network design problem with and without hop-constraints. Applied Mathematical Modelling 51, 274–301.

[28] Campbell, J. F., 1992. Location and allocation for distribution systems with transshipments and transportion economies of scale. Annals of Operations Research 40 (1), 77–99.

[29] Campbell, J. F., 1994. Integer programming formulations of discrete hub location problems. European Journal of Operational Research 72 (2), 387–405.

[30] Campbell, J. F., Ernst, A. T., Krishnamoorthy, M., 2002. Hub location problems. Facility Location: Applications and Theory, 373–407.

[31] Campbell, J. F., Ernst, A. T., Krishnamoorthy, M., 2005. Hub arc location problems: Part I - Introduction and Results. Management Science 51 (10), 1540–1555.

[32] Campbell, J. F., Ernst, A. T., Krishnamoorthy, M., 2005b. Hub arc location problems: Part II - Formulations and Optimal Algorithms. Management Science 51 (10), 1556–1571.

[33] Campbell, J. F., O'Kelly, M. E., 2012. Twenty-five years of hub location research. Transportation Science 46 (2), 153–169.

[34] Contreras, I., 2015. Hub location problems. In: Location Science. Springer, pp. 311–344.

[35] Contreras, I., Cordeau, J.-F., Laporte, G., 2011. Benders decomposition for large-scale uncapacitated hub location. Operations Research 59 (6), 1477–1490.

[36] Contreras, I., Cordeau, J.-F., Laporte, G., 2011. Stochastic uncapacitated hub location. European Journal of Operational Research 212 (3), 518–528.

[37] Contreras, I., Cordeau, J.-F., Laporte, G., 2012. Exact solution of large-scale hub location problems with multiple capacity levels. Transportation Science 46 (4), 439–459.

[38] Contreras, I., Fernández, E., Marín, A., 2010. The tree of hubs location problem. European Journal of Operational Research 202 (2), 390–400.

[39] Contreras, I., Tanash, M., Vidyarthi, N., 2013. The cycle hub location problem. Technical Report CIRRELT 59.

[40] Correia, I., Saldanha-da Gama, F., 2015. Facility location under uncertainty. In: Location Science. Springer, pp. 177–203.

[41] Crainic, T. G., 2000. Service network design in freight transportation. European Journal of Operational Research 122 (2), 272–288.

[42] Dantzig, G. B., 1957. Discrete-variable extremum problems. Operations Research 5 (2), 266–288.

[43] de Camargo, R. S., Miranda Jr, G., Luna, H. P. L., 2009. Benders decomposition for hub location problems with economies of scale. Transportation Science 43 (1), 86–97.

[44] Ebery, J., Krishnamoorthy, M., Ernst, A., Boland, N., 2000. The capacitated multiple allocation hub location problem: Formulations and algorithms. European Journal of Operational Research 120 (3), 614–631.

[45] Eiselt, H. A., Marianov, V., 2009. A conditional p-hub location problem with attraction functions. Computers & Operations Research 36 (12), 3128–3135.

[46] Ernst, A. T., Krishnamoorthy, M., 1996. Efficient algorithms for the uncapacitated single allocation p-hub median problem. Location Science 4 (3), 139–154.

[47] Ernst, A. T., Krishnamoorthy, M., 1998a. Exact and heuristic algorithms for the uncapacitated multiple allocation p-hub median problem. European Journal of Operational Research 104 (1), 100–112.

[48] Gabrel, V., Murat, C., Thiele, A., 2014. Recent advances in robust optimization: An overview. European Journal of Operational Research 235 (3), 471–483.

[49] Galil, Z., 1986. Efficient algorithms for finding maximum matching in graphs. ACM Computing Surveys (CSUR) 18 (1), 23–38.

[50] Gelareh, S., Nickel, S., 2011. Hub location problems in transportation networks. Transportation Research Part E: Logistics and Transportation Review 47 (6), 1092–1111.

[51] Gelareh, S., Nickel, S., Pisinger, D., 2010. Liner shipping hub network design in a competitive environment. Transportation Research Part E: Logistics and Transportation Review 46 (6), 991–1004.

[52] Ghaffarinasab, N., 2018. An efficient matheuristic for the robust multiple allocation p-hub median problem under polyhedral demand uncertainty. Computers & Operations Research 97, 31–47.

[53] Gunawan, A., Lau, H. C., Vansteenwegen, P., 2016. Orienteering problem: A survey of recent variants, solution approaches and applications. European Journal of Operational Research 255 (2), 315–332.

[54] Horner, M. W., O'Kelly, M. E., 2001. Embedding economies of scale concepts for hub network design. Journal of Transport Geography 9 (4), 255–265.

[55] Hwang, Y. H., Lee, Y. H., 2012. Uncapacitated single allocation p-hub maximal covering problem. Computers & Industrial Engineering 63 (2), 382–389.

[56] Kimms, A., 2006. Economies of scale in hub & spoke network design models: We have it all wrong. In: Perspectives on Operations Research. Springer, pp. 293–317.

[57] Kleywegt, A. J., Shapiro, A., Homem-de Mello, T., 2002. The sample average approximation method for stochastic discrete optimization. SIAM Journal on Optimization 12 (2), 479–502.

[58] Klincewicz, J. G., 2002. Enumeration and search procedures for a hub location problem with economies of scale. Annals of Operations Research 110 (1-4), 107–122.

[59] Lin, C.-C., Lee, S.-C., 2018. Hub network design problem with profit optimization for time-definite LTL freight transportation. Transportation Research Part E: Logistics and Transportation Review 114, 104–120.

[60] Lüer-Villagra, A., Marianov, V., 2013. A competitive hub location and pricing problem. European Journal of Operational Research 231 (3), 734–744.

[61] Magnanti, T. L., Wong, R. T., 1981. Accelerating Benders decomposition: Algorithmic enhancement and model selection criteria. Operations Research 29 (3), 464–484.

[62] Mahmutoğulları, A. İ., Kara, B. Y., 2015. Hub location problem with allowed routing between nonhub nodes. Geographical Analysis 47 (4), 410–430.

[63] Mak, W.-K., Morton, D. P., Wood, R. K., 1999. Monte Carlo bounding techniques for determining solution quality in stochastic programs. Operations Research Letters 24 (1-2), 47–56.

[64] Marianov, V., Serra, D., 2003. Location models for airline hubs behaving as M/D/c queues. Computers & Operations Research 30 (7), 983–1003.

[65] Marianov, V., Serra, D., ReVelle, C., 1999. Location of hubs in a competitive environment. European Journal of Operational Research 114 (2), 363–371.

[66] Marín, A., 2005. Formulating and solving splittable capacitated multiple allocation hub location problems. Computers & Operations Research 32 (12), 3093–3109.

[67] Marin, A., Cánovas, L., Landete, M., 2006. New formulations for the uncapacitated multiple allocation hub location problem. European Journal of Operational Research 172 (1), 274–292.

[68] Martins de Sá, E., Camargo, R. S., de Miranda Jr, G., 2013. An improved Benders decomposition algorithm for the tree of hubs location problem. European Journal of Operational Research 226 (2), 185–202.

[69] Martins de Sá, E., Contreras, I., Cordeau, J.-F., Saraiva de Camargo, R., de Miranda Jr, G., 2015. The hub line location problem. Transportation Science 49 (3), 500–518.

[70] Martins de Sá, E. M., Morabito, R., de Camargo, R. S., 2018. Benders decomposition applied to a robust multiple allocation incomplete hub location problem. Computers & Operations Research 89, 31–50.

[71] Meraklı, M., Yaman, H., 2016. Robust intermodal hub location under polyhedral demand uncertainty. Transportation Research Part B: Methodological 86, 66–85.

[72] Meraklı, M., Yaman, H., 2017. A capacitated hub location problem under hose demand uncertainty. Computers & Operations Research 88, 58–70.

[73] Nickel, S., Schöbel, A., Sonneborn, T., 2001. Hub location problems in urban traffic networks. In: Mathematical Methods on Optimization in Transportation Systems. Springer, pp. 95–107.

[74] O'Kelly, M. E., 1986. The location of interacting hub facilities. Transportation Science 20 (2), 92–106.

[75] O'Kelly, M. E., 1987. A quadratic integer program for the location of interacting hub facilities. European Journal of Operational Research 32 (3), 393–404.

[76] O'Kelly, M. E., 1992. Hub facility location with fixed costs. Papers in Regional Science 71 (3), 293–306.

[77] O'Kelly, M. E., Bryan, D., 1998. Hub location with flow economies of scale. Transportation Research Part B: Methodological 32 (8), 605–616.

[78] O'Kelly, M. E., Bryan, D., Skorin-Kapov, D., Skorin-Kapov, J., 1996. Hub network design with single and multiple allocation: A computational study. Location Science 4 (3), 125–138.

[79] O'Kelly, M. E., Campbell, J. F., Camargo, R. S., de Miranda Jr, G., 2015. Multiple allocation hub location model with fixed arc costs. Geographical Analysis 47 (1), 73–96.

[80] Peker, M., Kara, B. Y., 2015. The p-hub maximal covering problem and extensions for gradual decay functions. Omega 54, 158–172.

[81] Pirkul, H., Schilling, D. A., 1998. An efficient procedure for designing single allocation hub and spoke systems. Management Science 44 (12-part-2), S235–S242.

[82] Podnar, H., Skorin-Kapov, J., Skorin-Kapov, D., 2002. Network cost minimization using threshold-based discounting. European Journal of Operational Research 137 (2), 371–386.

[83] Rahmaniani, R., Crainic, T. G., Gendreau, M., Rei, W., 2017. The Benders decomposition algorithm: A literature review. European Journal of Operational Research 259 (3), 801–817.

[84] Rodriguez-Martin, I., Salazar-Gonzalez, J. J., 2008. Solving a capacitated hub location problem. European Journal of Operational Research 184 (2), 468–479.

[85] Santoso, T., Ahmed, S., Goetschalckx, M., Shapiro, A., 2005. A stochastic programming approach for supply chain network design under uncertainty. European Journal of Operational Research 167 (1), 96–115.

[86] Sasaki, M., Campbell, J. F., Krishnamoorthy, M., Ernst, A. T., 2014. A stackelberg hub arc location model for a competitive environment. Computers & Operations Research 47, 27–41.

[87] Sasaki, M., Fukushima, M., 2001. Stackelberg hub location problem. Journal of the Operations Research Society of Japan 44 (4), 390–402.

[88] Schütz, P., Tomasgard, A., Ahmed, S., 2009. Supply chain design under uncertainty using sample average approximation and dual decomposition. European Journal of Operational Research 199 (2), 409–419.

[89] Serper, E. Z., Alumur, S. A., 2016. The design of capacitated intermodal hub networks with different vehicle types. Transportation Research Part B: Methodological 86, 51–65.

[90] Shapiro, A., Homem-de Mello, T., 1998. A simulation-based approach to two-stage stochastic programming with recourse. Mathematical Programming 81 (3), 301–325.

[91] Sim, T., Lowe, T. J., Thomas, B. W., 2009. The stochastic p-hub center problem with service-level constraints. Computers & Operations Research 36 (12), 3166–3177.

[92] Skorin-Kapov, D., Skorin-Kapov, J., O'Kelly, M., 1996. Tight linear programming relaxations of uncapacitated p-hub median problems. European Journal of Operational Research 94 (3), 582–593.

[93] Sung, C., Jin, H., 2001. Dual-based approach for a hub network design problem under non-restrictive policy. European Journal of Operational Research 132 (1), 88–105.

[94] Taherkhani, G., Alumur, S. A., 2019. Profit maximizing hub location problems. Omega 86, 1–15.

[95] Taherkhani, G., Alumur, S. A., Hosseini, M., 2019. Benders decomposition for profit maximizing hub location problems with capacity allocation. Technical Report.

[96] Taherkhani, G., Alumur, S. A., Hosseini, M., 2019. Robust-stochastic models for profit maximizing hub location problems. Technical Report.

[97] Vansteenwegen, P., Souffriau, W., Van Oudheusden, D., 2011. The orienteering problem: A survey. European Journal of Operational Research 209 (1), 1–10.

[98] Wagner, B., 2007. An exact solution procedure for a cluster hub location problem. European Journal of Operational Research 178 (2), 391–401.

[99] Wieberneit, N., 2008. Service network design for freight transportation: A review. OR Spectrum 30 (1), 77–112.

[100] Yaman, H., 2009. The hierarchical hub median problem with single assignment. Transportation Research Part B: Methodological 43 (6), 643–658.

[101] Yaman, H., 2011. Allocation strategies in hub networks. European Journal of Operational Research 211 (3), 442–451.

[102] Yaman, H., Elloumi, S., 2012. Star p-hub center problem and star p-hub median problem with bounded path lengths. Computers & Operations Research 39 (11), 2725–2732.

[103] Yang, T.-H., 2009. Stochastic air freight hub location and flight routes planning. Applied Mathematical Modelling 33 (12), 4424–4430.

[104] Zetina, C. A., Contreras, I., Cordeau, J.-F., Nikbakhsh, E., 2017. Robust uncapacitated hub location. Transportation Research Part B: Methodological 106, 393–410.

Appendix A

A.1 Hybrid MWM-Knapsack Method

We show how proper values of $(b_i)_{i \in H_0^e}$ can be found via a relaxation of DS-II (4.25)-(4.28). Observe that by relaxing constraints (4.26), relaxed DS-II can be decomposed into $|H_0^e|$ independent smaller subproblems for each $i \in H_0^e$:

$$\text{(Relaxed DS-II}(i)\text{)} \quad \text{Minimize} \quad \Gamma_i b_i + \sum_{k \in K} \sum_{m \in M} u_{ik}^m \tag{A.1}$$

$$u_{ik}^m + w_k^m b_i \geq \rho_{ii}^{km} \qquad (k,m) \in K \times M \tag{A.2}$$

$$u_{ik}^m, b_i \geq 0 \qquad (k,m) \in K \times M \tag{A.3}$$

Similar to problem (4.58)-(4.60), this problem is the dual of the LP-relaxation of a knapsack problem with knapsack capacity Γ_i, and items $(k,m) \in K \times M$ with weight w_k^m and profit ρ_{ii}^{km}, and can be solved in the same fashion. As explained in Section 4.2.3.3, b_i is the profit-to-weight ratio of the break item $(\bar{k}, \bar{m})$

$$b_i = \rho_{ii}^{\bar{k}\bar{m}} / w_{\bar{k}}^{\bar{m}}. \tag{A.4}$$

Note that even though problem (4.58)-(4.60) has a formulation similar to problem (A.1)-(A.3), they are inherently different: problem (4.58)-(4.60) is a restriction of DS-II, whereas problem (A.1)-(A.3) is a relaxation of DS-II, hence the solution obtained by (A.1)-(A.3)

may not be feasible to DS-II. Therefore, once the value of $(b_i)_{i \in H_0^e}$ is calculated, to obtain a complete feasible solution we calculate the value of u using the MWM algorithm.

It is worth mentioning that the major computational effort required for solving this problem is due to calculating ρ_{ii}^{km} values, while the time required for solving the knapsack problem itself is almost negligible even for the largest instances. On the other hand, note that we need to calculate ρ_{ii}^{km} as part of preparing DS-II (4.25)-(4.28), no matter what the value of b is. This means using this hybrid MWM-Knapsack method, we can find promising values of b for the MWM problems (hence stronger cuts) without incurring additional computational cost.

A.2 Supplementary Numerical Results

To determine the best values to use for the parameters p_Q (proportion of hubs that are less likely to be open in the optimal solution) and n_Q (number of subsets into which Q is partitioned) in our variable fixing tests in Chapter 4, we selected medium- and large-size instances with 40-100 nodes from the AP dataset and took runs under different p_Q and n_Q values. For each instance, we performed computational tests with $p_Q \in \{50\%, 75\%, 100\%\}$ and $n_Q \in \{1, 2, \ldots, 10\}$, respectively. (The $p_Q = 100\%$ and $n_Q = 1$ combination corresponds to the tests introduced in Contreras et al. 35.) The computational results are summarized in Table A.1.

The first two columns of Table A.1 report the instance size and the number of hub elimination subsets (n_Q) used, respectively. The columns labeled "Average time" and "Average % hubs elim." report the average computational times in seconds and the average percentage of the total candidate hubs that were eliminated under the three different p_Q values. The averages are calculated over four same-size instances with different installation costs and capacities.

When the values presented in Table A.1 are averaged, the combination $p_Q = 75\%$ and $n_Q = 6$ provides the best results in terms of average computational time and average

Table A.1: Computational results for different p_Q and n_Q values with 16 instances of the AP dataset.

Instance		$p_Q = 100\%$		$p_Q = 75\%$		$p_Q = 50\%$	
$\|H\|$	n_Q	Average time	Average % hubs elim.	Average time	Average % hubs elim.	Average time	Average % hubs elim.
40	1	19.60	70.63	19.66	79.38	19.45	81.88
	2	19.77	82.50	19.47	84.38	19.45	83.13
	3	20.05	81.88	19.90	84.38	19.53	83.13
	4	20.19	85.00	19.99	85.00	19.93	80.63
	5	20.35	85.63	20.48	83.75	20.20	80.00
	6	21.05	85.63	20.55	83.13	20.65	76.25
	7	20.83	85.63	21.22	79.38	20.36	74.38
	8	21.35	85.00	21.38	79.38	20.72	68.13
	9	21.41	81.25	21.22	76.25	20.91	66.25
	10	21.58	80.63	21.46	74.38	20.74	63.75
50	1	21.39	83.50	20.36	85.50	20.98	86.50
	2	20.77	86.00	20.02	85.00	20.15	86.50
	3	20.26	89.50	19.83	88.50	20.58	86.50
	4	20.28	90.00	20.03	88.00	20.25	83.50
	5	19.78	90.00	20.03	87.00	20.08	83.00
	6	19.86	90.00	20.28	86.00	21.04	83.50
	7	19.88	89.00	20.04	85.00	20.58	78.00
	8	20.46	89.00	20.11	84.50	20.83	77.00
	9	20.86	88.00	20.56	82.00	21.04	75.00
	10	20.25	84.00	20.97	78.00	20.54	70.50
75	1	148.00	86.00	152.76	89.33	148.11	89.00
	2	149.38	89.33	148.21	92.00	150.00	90.00
	3	146.08	92.33	146.32	91.33	144.23	90.33
	4	144.27	92.00	145.04	91.33	144.91	87.00
	5	149.96	92.00	145.80	91.00	142.15	88.67
	6	151.31	92.67	144.93	90.67	146.04	88.00
	7	159.46	92.00	146.52	88.67	149.52	85.00
	8	156.55	90.67	146.69	89.67	150.75	84.67
	9	149.52	91.00	146.40	88.00	145.76	83.33
	10	157.78	90.67	145.13	86.00	146.11	81.67
100	1	489.43	85.50	483.90	88.50	481.12	89.75
	2	441.71	92.25	430.57	92.00	441.58	92.25
	3	422.44	93.75	427.37	93.75	424.23	92.25
	4	421.21	94.25	407.14	93.25	412.89	91.75
	5	405.94	94.25	407.84	93.50	407.36	91.00
	6	419.81	94.50	394.60	93.50	413.73	89.75
	7	414.71	94.00	397.70	91.00	424.58	88.50
	8	415.16	93.00	401.41	90.75	424.00	86.00
	9	411.12	92.50	397.78	90.75	417.26	85.25
	10	407.30	91.25	405.67	89.50	420.62	84.25

percentage of hubs eliminated in the optimal solution. Hence, we used the aforementioned values for the corresponding parameters in our computational experiments.